Cosmological Implications of Extended Massive Gravity Theories

PhD Thesis

By

MICHAEL KENNA-ALLISON

Institute of Cosmology and Gravitation
UNIVERSITY OF PORTSMOUTH

The thesis is submitted in partial fulfilment of the requirements for the award of the degree of DOCTOR OF PHILOSOPHY of the University of Portsmouth.

"WEDNESDAY 31ST MARCH 2021"

Abstract

The origin of the late-time acceleration of the universe is one of the biggest questions in cosmology. We give the name *dark energy* to the substance which is responsible for this, highlighting our ignorance on its origin. The most widely accepted explanation is that of the cosmological constant. However the naturalness of the cosmological constant, and the theoretical inconsistency with the value expected from quantum field theory, poses a question over whether this is the true explanation of the late-time acceleration. In this thesis, we investigate models of massive gravity, which arise from modifying Einstein's theory of General Relativity, to tackle the late-time acceleration problem in a more natural way than the cosmological constant. The theories we will study are the bigravity and generalised massive gravity theories.

In this work we are principally concerned with both the theoretical consistency and phenomenological implications of the aforementioned theories. To study the theoretical consistency we study cosmological perturbations and derive the stability conditions, whilst for the phenomenological study we investigate the background evolution and the effects on the large scale structure of the universe. We also investigate the screening mechanisms, which are important to allow the recovery of General Relativity on local, well tested, scales.

The first part of the thesis is dedicated to the history of massive gravity. The timeline of the development of dRGT (de-Rham, Gabadadze, Tolley) massive gravity is discussed in detail in chapter 2. The second part of chapter 2 discusses the cosmological solutions in massive gravity, and the requirement to study extensions of the theory to find stable cosmologies. We also introduce other models of massive gravity which could explain the late-time acceleration.

In chapter 3 we study the low energy limit model of bigravity. We study the linear scalar perturbations and investigate the modified Poisson's equation. To determine the details of the screening, we derive the non-linear equations and identify the Vainshtein radius. We conclude by discussing the viability of bigravity theories for dark energy.

In chapter 4 we introduce the generalised massive gravity and study its stability at the level of the quadratic action for cosmological perturbations. To do so, we derive the stability conditions as a function of the model parameters. Imposing that we require late-time acceleration and the absence of instabilities, we identify a region of parameter space in which the theory is stable. Building upon the analysis in chapter 4, we study generalised massive gravity in more detail in chapter 5. We perform a full background analysis, identifying the expansion history and equation of state of dark energy for a

concrete model. Later on in chapter 5 we study the linear scalar perturbations, focusing on the effects of generalised massive gravity on large scale structure. We finish the chapter by investigating the propagation of gravitational waves and conclude the thesis with future directions and open questions in the field.

DEDICATION AND ACKNOWLEDGEMENTS

I would like to thank many people for making this thesis possible. First and foremost my supervisors Emir Gumrukcuoglu and Kazuya Koyama, whose invaluable advice and guidance supported me throughout the years. A special mention for Emir, whose door was always open if I needed help and who dedicated many hours in reading this thesis. I could not ask for more from a supervisory team. Also I would like to thank my VIVA examiners Clare Burrage and Rob Crittenden for a great discussion.

A large majority of the work in this thesis utilised the xPand [1] package. Special thanks to Obinna Umeh for helping with xPand and answering all my questions.

The next people I want to thank are my office mates. Everyone who I shared with in 3.12 throughout the years, thank you for making it an enjoyable experience. Special mention to Ben, Rob, Paul and Matt who indoctrinated me to the pub life. I look forward for the time when we can go to the pub in person again! Thank you to all the great friends I made over years, Chris, Jacob, Bill, Natalie, Mike, Andrius and Guilherme Brando de Oliveira.

I cannot fail to mention the ICG Intergálacticos, it took a pandemic to stop us from dominating the staff league. A big thank you to all for playing. Special mention for Steve and Sam, the regulars at Friday football, and everyone else who I played football with in Portsmouth, especially those who participated in the games against the undergraduates[1]. We shall have to play again one day! Thank you to Plymouth Argyle for being a very average, frustrating to watch, football team. Saturday's at 3pm would not be the same. Special mention for Ryan Lowe for finally going 2 up front.

Thank you to my family for all your love and support, especially Bonnie and Clyde for proof-reading the thesis. Thank you for letting us stay in Grandmas's house the last few months.

Finally, thank you to Laura for always being there for me and supporting me in the last few months. I am very grateful. We made some great memories in the last year which I will never forget.

I would like to dedicate this thesis to Grandma.

[1] We won the series 3-1, just putting it out there.

Author's declaration

Whilst registered as a candidate for the above degree, I have not been registered for any other research award. The results and conclusions embodied in this thesis are the work of the named candidate and have not been submitted for any other academic award

TABLE OF CONTENTS

List of Tables

Table **Page**

List of Figures

Figure **Page**

CHAPTER 1

INTRODUCTION

Cosmology is the study of the time evolution of the universe from the big bang all the way through to the present day. The question we as cosmologists ask is what is at the origin of the observations that we see. Curiosities like this have intrigued astronomers for thousands of years, from scientists and philosophers working on the first cosmological model, which was introduced by Plato and placed the earth at the centre of the universe, to the era of precision cosmology we are now in. We have in our armoury many experiments which probe all areas of the universe to unprecedented precision. Planck [2] provides a wealth of information about the Cosmic Microwave Background (CMB), shedding light on the early universe. The Laser Interferometer Gravitational-Wave Observatory (LIGO) [3] has detected many different sources of gravitational waves, which provide insight to gravitational interactions in the strong field regime. The Sloan Digital Sky Survey (SSDS) [4] is a spectroscopic redshift survey which has detailed over one quarter of the night sky and EUCLID [5] is a futuristic experiment which will attempt to map the geometry of the universe by measuring the shape of galaxies at different redshifts, to understand the nature of dark energy. Combining all these probes points us towards the standard model of cosmology, the *Lambda Cold Dark Matter* model, or ΛCDM. ΛCDM is a remarkable achievement of the scientific community, but it is not a complete model of the universe. We do not know how the universe came into existence, but we know to remarkable precision what happened after its birth all the way up until the present day, thanks to developments in theory and to the aforementioned observations. By uniting the observational data from all these experiments with the

predictions from theoretical models, we can continue to understand the physics of the universe.

In the next few paragraphs we very briefly summarise the timeline of the universe from the big bang up until the present day, see the following textbooks for a more detailed summary [6–8].

Our understanding of the evolution of the universe starts with inflation. Shortly after the big bang, which assuming ΛCDM happened around 13.7 billion years ago, there was a period when the universe underwent a rapid accelerated expansion [9], which is given the name inflation. In the simplest models, inflation is driven by a scalar field (the inflaton) slowing rolling down its potential, and ends with the inflaton decaying into standard model particles and the radiation which we observe today via the process of reheating [10]. The end of inflation also marks the beginning of the radiation dominated era. As the universe expanded and the plasma cooled, the temperature dropped to a point marking the electroweak phase transition, around $T_{ew} \sim 246\text{GeV}$, which corresponds to the vacuum expectation value of the Higgs field. This broke $SU(2) \times U(1)$ symmetry of the electroweak force into the $U(1)$ of electromagnetism, separating electromagnetism from the weak interaction. The electroweak phase transition marks the beginning of the quark epoch. After the QCD phase transition, where quarks and gluons were confined within hadrons, the universe was a hot dense plasma containing only hadrons, mesons, leptons and photons. Neutrinos then decoupled, electrons and positrons annihilated each other and the universe continued to cool until protons and neutrons are bound into atomic nuclei in a process called big bang nucelosynthesis (BBN). After BBN the universe entered the matter dominated epoch, the majority of which is made up of dark matter whose origin is still unknown. The first neutral atoms were produced in recombination, in which electrons bound to protons to form neutral Hydrogen atoms. Once the neutral atoms had formed, baryonic matter decoupled from the photons allowing the photons to free steam away and form the CMB which we observe today.

After more expansion and cooling the first stars were formed, around 200 million years after the big bang. Galaxies and galaxy clusters formed and the energy density of matter dropped as the universe continued to expand. The universe then reached a pivotal point. Around the time of the formation of the solar system, around 9 billion years after the big bang, the energy density of matter dropped below that of the vacuum energy. The universe then entered the dark energy dominated era in which the expansion of the universe started to accelerate again. This observation was confirmed by measuring the luminosities of high redshift, type Ia supernovae [11, 12]. It was discovered that

the luminosities of the supernovae sample were dimmer than they would be in the case of the universe undergoing a decelerated expansion. In the framework of ΛCDM, the accelerated expansion of the universe is due to Λ, the cosmological constant. The cosmological constant is a constant energy density which exists throughout the universe. It exerts a negative pressure which drives the accelerated expansion. However, as we shall see, the cosmological constant is what calls the ΛCDM model into question regarding the nature of dark energy.

In this thesis, we motivate the study of alternative sources of the accelerated expansion of the universe by modifying Einstein's theory of General Relativity. In the rest of chapter 1 we outline the theory of general relativity and the problems associated with the ΛCDM model. We discuss the famous *Lovelock's theorem*, which protects GR and how to bypass it when considering modifications of gravity. We then discuss potential problems that arise in the form of theoretical inconsistencies and the failure to reproduce observational tests when one goes beyond GR. Finally, at the end of the chapter we discuss mechanisms which allow modified theories of gravity to bypass tight observational constraints on local scales, but allow for order one deviations on cosmological scales which can drive the accelerated expansion of the universe.

1.1 General Relativity

For well over a century now, Einstein's theory of General Relativity (GR) [13] has passed a plethora of observational tests [14]. From predicting the deflection angle of light rays around massive objects, which is given the name gravitational lensing, to predicting the peculiar feature of the perihelion precession of Mercury's orbit, to even sub-millimetre laboratory tests [14]. Einstein's intuition at the time was extraordinary, from the equivalence principle and coordinate invariance to a fully non-linear theory of gravity describing the dynamics of spacetime itself. The discovery of GR was years ahead of its time, and decades later through the development of field theory [7] and particle physics, GR was found to be the *unique* theory of an interacting, massless spin-2 field.

To understand the phenomenology of GR, we first have to understand the theoretical foundations, therefore we begin with the Einstein-Hilbert action

$$S = \frac{1}{16\pi G}\int d^4x\sqrt{-g}(R-2\Lambda) + \int d^4x\sqrt{-g}\,\mathscr{L}_m[g_{\mu\nu},\Psi^i], \tag{1.1}$$

where G is Newton's gravitational constant which can be written in terms of the reduced

Planck mass via,

$$M_p = \frac{1}{\sqrt{8\pi G}} \sim 2.4 \times 10^{18}\text{GeV}. \tag{1.2}$$

Here $g_{\mu\nu}$ is the metric tensor, R is the Ricci scalar, Λ is the cosmological constant, $d^4x\sqrt{-g}$ is the volume element written in terms of the determinant of the metric $g_{\mu\nu}$ and $\mathscr{L}_m[g_{\mu\nu}, \Psi^i]$ is the matter Lagrangian describing the motion of matter fields Ψ^i. The Ricci scalar is the simplest curvature invariant one can write down and is constructed from the trace of the Ricci tensor using the inverse metric $g^{\mu\nu}$,

$$R = g^{\mu\nu}R_{\mu\nu}, \tag{1.3}$$

which in itself can be written as a contraction over the Riemann tensor,

$$R_{\mu\nu} = R^{\rho}{}_{\mu\rho\nu}. \tag{1.4}$$

The Riemann tensor quantifies how much curvature is present in the 4D spacetime manifold and is written in terms of derivatives of the metric tensor,

$$R^{\rho}{}_{\sigma\mu\nu} = \partial_\mu\Gamma^{\rho}_{\sigma\nu} - \partial_\nu\Gamma^{\rho}_{\sigma\mu} + \Gamma^{\rho}_{\lambda\mu}\Gamma^{\lambda}_{\sigma\nu} - \Gamma^{\rho}_{\lambda\nu}\Gamma^{\lambda}_{\sigma\mu}, \tag{1.5}$$

making use of the Christoffel symbols $\Gamma^{\mu}_{\nu\rho}$,

$$\Gamma^{\sigma}_{\mu\nu} = \frac{1}{2}g^{\sigma\lambda}\left(\partial_\mu g_{\lambda\nu} + \partial_\nu g_{\lambda\mu} - \partial_\lambda g_{\mu\nu}\right). \tag{1.6}$$

Here, $\partial_\mu \equiv \frac{\partial}{\partial x^\mu}$ and indices are raised and lowered with $g^{\mu\nu}$. To obtain the Einstein equations, we apply the principle of least action to (1.1). Introducing a small perturbation to the metric g as $g^{\mu\nu} \to g^{\mu\nu} + \delta g^{\mu\nu}$, the action (1.1) becomes,

$$\delta S = \int d^4x \left[\frac{1}{16\pi G}\left(\frac{\delta R}{\delta g^{\mu\nu}} + \frac{(R-2\Lambda)}{\sqrt{-g}}\frac{\delta\sqrt{-g}}{\delta g^{\mu\nu}}\right) + \frac{1}{\sqrt{-g}}\frac{\delta(\sqrt{-g}\,\mathscr{L}_m)}{\delta g^{\mu\nu}}\right]\sqrt{-g}\,\delta g^{\mu\nu}. \tag{1.7}$$

Using the fact that the variation of the metric determinant can be written as,

$$\delta\sqrt{-g} = -\frac{1}{2}\sqrt{-g}\,g_{\mu\nu}\delta g^{\mu\nu}, \tag{1.8}$$

and imposing the metric variation $\delta g^{\mu\nu}$ smoothly vanishes in the limit of reaching the boundary of the spacetime, along with the tensor identities in [15, 16], we arrive at the Einstein field equations,

$$G_{\mu\nu} \equiv R_{\mu\nu} - \frac{1}{2}Rg_{\mu\nu} + \Lambda g_{\mu\nu} = 8\pi G T_{\mu\nu}. \tag{1.9}$$

In (1.9) the energy-momentum tensor $T_{\mu\nu}$ is defined as

$$T_{\mu\nu} \equiv \frac{-2}{\sqrt{-g}} \frac{\delta(\sqrt{-g}\mathscr{L}_m[g_{\mu\nu}, \Psi^i])}{\delta g^{\mu\nu}}. \tag{1.10}$$

The Einstein field equations (1.9) exemplify the famous quote from John Wheeler: "*Space tells matter how to move, matter tells space how to curve*", which was the essence of Einstein's intuition. Due to the diffeomorphism invariance of GR, the Einstein tensor obeys the following conservation law known as the *Bianchi identity*,

$$\nabla_\mu G^{\mu\nu} = 0, \tag{1.11}$$

where ∇^μ is the covariant derivative associated with the metric $g_{\mu\nu}$. From the Einstein field equations (1.9), the Bianchi identity implies the following relation for the energy-momentum tensor,

$$\nabla_\mu T^{\mu\nu} = 0, \tag{1.12}$$

which results in the local conservation of energy-momentum. Written in terms of the ordinary 4-derivative and Christoffel symbols (1.12) is,

$$\nabla_\mu T^{\mu\nu} \equiv \partial_\mu T^{\mu\nu} + \Gamma^\nu_{\mu\rho} T^{\mu\rho} + \Gamma^\mu_{\mu\rho} T^{\rho\nu} = 0. \tag{1.13}$$

To study the motion of particles, we derive the equation of motion which comes from the variation of the action with respect to the coordinates for a point particle. The separation between two events in spacetime is measured using the line element,

$$ds^2 = g_{\mu\nu} dx^\mu dx^\nu. \tag{1.14}$$

The proper time is defined by $d\tau^2 = -ds^2$. The particle will follow the path which extremizes the proper time, or the shortest path in curved space. Using this, we can construct the action for a point particle with mass m parameterised by the worldline $x^\mu = x^\mu(\tau)$,

$$S = m \int \sqrt{-g_{\mu\nu} \frac{dx^\mu}{d\tau} \frac{dx^\nu}{d\tau}}\, d\tau. \tag{1.15}$$

Upon variation we obtain the following,

$$g_{\mu\gamma} \frac{d^2 x^\mu}{d\tau^2} = \frac{1}{2} \left[\frac{\partial g_{\mu\gamma}}{\partial x^\nu} + \frac{\partial g_{\gamma\nu}}{\partial x^\mu} - \frac{\partial g_{\mu\nu}}{\partial x^\gamma} \right] \frac{dx^\mu}{d\tau} \frac{dx^\nu}{d\tau}, \tag{1.16}$$

which can be written in the more familiar form,

$$\frac{d^2x^\mu}{d\tau^2} = -\Gamma^\mu_{\nu\gamma}\frac{dx^\gamma}{d\tau}\frac{dx^\nu}{d\tau}. \tag{1.17}$$

Equation (1.17) is known as the *geodesic* equation and by specifying the geometry of spacetime (the metric tensor), one can obtain the particle trajectory x^μ. Taking the weak field limit of the geodesic equation, we can recover an analogue of Newton's second law which relates the acceleration felt by a test mass to the local gravitational potential Φ

$$\vec{a} = -\nabla\Phi. \tag{1.18}$$

1.2 Standard Model of Cosmology

Before we detail the standard model of cosmology, the ΛCDM model, we must first outline the two main assumptions which form the foundation for the most successful model of our universe to date.

- **Cosmological Principle**: The cosmological principle is based on two key observations, the first being that the universe appears to be isotropic in all directions. This means that every direction we survey, the universe looks the same. The second key observation is that the universe is homogeneous at every point in space, which states the universe is the same at every point. Observations of the temperature of CMB photons today

  $$T_{z=0} = 2.73 \pm \delta T\ K, \tag{1.19}$$

  with fluctuations of the order,

  $$\frac{\delta T}{T_{z=0}} \approx 10^{-5}, \tag{1.20}$$

  allow us to estimate the temperature of the universe at the time the CMB was formed [17],

  $$T_{z=1100} = T_{z=0}\frac{a_{z=0}}{a_{z=1100}} \approx 3000K, \tag{1.21}$$

  where $z = 1100$ is the redshift corresponding to the time of recombination. The smallness of the temperature fluctuations of the early universe implies the early universe was isotropic. The observation which supports homogeneity is that of

galaxy redshift distributions, such as the two degree field galaxy redshift survey [18] or the BOSS galaxy sample [19] that found that on large scales the distribution of galaxies is homogeneous. This implies that, locally at least, the universe appears to be homogeneous.

- **The laws of gravity are described by GR:** The second assumption is that gravity on all scales is described GR. It is this assumption which we are going to break in this thesis, for reasons we shall see later on in this chapter.

1.2.1 Friedmann-Lemaître-Robertson-Walker metric

Mathematically we can describe the dynamics of spacetime through the Friedmann-Lemaître-Robertson-Walker (FLRW) metric, which is the metric describing a homogeneous, isotropic and expanding universe in 4 dimensions. The line element can be written as,

$$ds^2 = -dt^2 + a(t)^2 \left[\frac{dr^2}{1-Kr^2} + r^2 d\Omega^2 \right], \tag{1.22}$$

where $d\Omega^2 = d\theta^2 + \sin^2\theta d\phi^2$ is the line element on the 2-sphere, $a(t)$ is the scale factor, r is the comoving radial coordinate and K represents the curvature parameter which can take values $\{K < 0, K = 0, K > 0\}$. Geometrically, the aforementioned values of K represent an open (hyperbolic), flat (euclidean) and closed (spherical) universe respectively.

The scale factor, albeit dimensionless, is a very important quantity in the ΛCDM model. It determines whether the universe is expanding or contracting, and is used to determine physical distances from $R = a(t)r$. Throughout this work, we set $a(t_0) = 1$, where a subscript 0 means the quantity in question is evaluated today. From the scale factor, we can define the *Hubble parameter* as $H = \frac{\dot{a}}{a}$, where a dot identifies a time derivative, which quantifies how much the universe is expanding. The value of the Hubble parameter today, i.e. H_0, is the cause of a lot of investigation for cosmologists as there is a tension [20] between early time and late time measurements. The CMB predicts $H_0 = 67.44 \pm 0.58$ km s^{-1} Mpc^{-1} [2], whilst late time cepheid measurements from the SH0ES collaboration infer $H_0 = 74.03 \pm 1.42$ km s^{-1} Mpc^{-1} [21–23]. The CMB result is obtained from assuming a flat ΛCDM cosmology whilst the SH0ES result is independent of the cosmological model, so the SH0ES result could be hinting at physics beyond ΛCDM [24].

1.2.2 Cosmological Distances

The measurement of the supernovae in the SH0ES collaboration relies on our knowledge of understanding how light travels in an expanding universe. Light travels on null geodesics, that is $ds^2 = 0$, and applying that in (1.22) and considering only light travelling in the radial direction gives,

$$\frac{dt}{a(t)} = \pm \frac{dr}{\sqrt{1-Kr^2}}. \tag{1.23}$$

Consider a burst of light travelling towards us from a distant galaxy emitted at $t = t_e$ and $r = r_e$ and is observed by us on earth at $t = t_0$ and $r = 0$. The signal we observe is determined by solving the following integral equation,

$$\int_{t_e}^{t_0} \frac{dt}{a(t)} = -\int_{r_e}^{0} \frac{dr}{\sqrt{1-Kr^2}} = \int_0^{r_e} \frac{dr}{\sqrt{1-Kr^2}}, \tag{1.24}$$

where we chose the minus sign in (1.23) as the light from the galaxy is travelling towards us. Now the galaxy emits another burst of light at a time $t_e + \delta t_e$ and is observed by us on earth at $t_0 + \delta t_0$. As we are in comoving coordinates the right hand side of the integral is independent of when the signal was emitted, hence

$$\int_{t_e}^{t_0} \frac{dt}{a(t)} - \int_{t_e+\delta t_e}^{t_0+\delta t_o} \frac{dt}{a(t)} = 0, \tag{1.25}$$

$$\implies \int_{t_e}^{t_e+\delta t_e} \frac{dt}{a(t)} = \int_{t_0}^{t_0+\delta t_0} \frac{dt}{a(t)}, \tag{1.26}$$

$$\implies \frac{\delta t_e}{a(t_e)} = \frac{\delta t_0}{a(t_0)}. \tag{1.27}$$

We can re-write (1.27) in terms of the wavelengths of the emitted light rays,

$$\frac{1}{a(t_e)} = \frac{\lambda_0}{\lambda_e}. \tag{1.28}$$

The fractional change of the emitted and observed wavelengths is defined as the *redshift* of the source, i.e. $z = (\lambda_0 - \lambda_e)/\lambda_e$. Using this, we can derive a simple relation between the scale factor and the redshift,

$$a(t_e) = \frac{1}{1+z}. \tag{1.29}$$

Essentially, redshift explains why the wavelengths of photons travelling to us from far away galaxies are stretched as the universe expands. It is this knowledge of how photons

travel in an expanding universe that led astronomers to understand that the universe was expanding faster than predicted. They observed that the luminosities of type Ia supernovae were dimmer than predicted by a non-accelerating universe. To understand this, the distance to the supernovae must have been known.

Let's consider a flat FLRW background, where a light ray is again travelling in the radial direction. The line element reduces to,

$$ds^2 = -dt^2 + a^2 dr^2. \tag{1.30}$$

Now consider a supernovae at $r = r_e, t = t_e$ which emits a light ray measured on earth at $r = 0, t = t_0$. Integrating (1.30) becomes,

$$d_c \equiv r_e = -\int_{t_0}^{t_e} \frac{dt}{a(t)} = \int_0^z \frac{dz'}{H(z')}, \tag{1.31}$$

where d_c is defined to be the comoving distance to the supernovae and we used the definition of redshift (1.29) to convert from the time coordinate to redshift. The flux $\mathscr{F}$ observed on earth from the supernovae with luminosity L_0 is defined as the energy observed, per unit time per unit area,

$$\mathscr{F} = \frac{L_0}{4\pi d_c^2}. \tag{1.32}$$

The *luminosity distance* is defined by,

$$d_L^2 = \frac{L_s}{4\pi \mathscr{F}}, \tag{1.33}$$

where L_s is the absolute luminosity of the source. Combining the above equations yields,

$$d_L^2 = d_c^2 \left(\frac{L_s}{L_0}\right). \tag{1.34}$$

We can re-write the relation above by considering the following: the change in the energy of light ΔE_s being emitted by the supernovae in a time Δt_s, which is measured here on earth as energy ΔE_0 in a time Δt_0. Therefore (1.34) becomes,

$$d_L^2 = d_c^2 \left(\frac{\Delta E_s}{\Delta E_0}\frac{\Delta t_0}{\Delta t_s}\right). \tag{1.35}$$

As the energy of a photon is proportional to the inverse of its wavelength we can write,

$$d_L^2 = d_c^2 \left(\frac{\lambda_0}{\lambda_s}\frac{\Delta t_0}{\Delta t_s}\right), \tag{1.36}$$

which using the results in (1.27,1.29,1.28) and taking the square root reduces to,

$$d_L = d_c(1+z), \tag{1.37}$$

which is the luminosity distance of the source. As almost every type Ia supernovae has the same intrinsic brightness, i.e. a standard candle, we can use the observed brightness to measure the distance to them and compare against the redshift.

1.2.3 Dynamics of FLRW metric

Before describing the dynamics of the FLRW metric, we have to specify the matter content of the universe. We consider n perfect fluids, which are described by the energy-momentum tensor

$$T^{(n)}_{\mu\nu} = (\rho_n + P_n)u^n_\mu u^n_\nu + P_n g_{\mu\nu}, \tag{1.38}$$

where u^n_μ is the 4-velocity, ρ_n is the density of each fluid species and P_n is the pressure. To achieve homogeneity and isotropy, both are assumed to be independent of the spatial coordinates. Requiring that the expansion is in the rest frame of the fluid, the 4-velocity takes the simple form $u_\mu = (-1, \vec{0})$ which yields a simpler form for $T^\mu{}_\nu$ [1],

$$T^\mu{}_\nu = \begin{pmatrix} -\rho & 0 & 0 & 0 \\ 0 & P & 0 & 0 \\ 0 & 0 & P & 0 \\ 0 & 0 & 0 & P \end{pmatrix}. \tag{1.39}$$

Substituting (1.38) and (1.22) into the Einstein equations (1.9) yields, for the time-time component, the first of the *Friedmann* equations,

$$3\left(\frac{\dot{a}^2}{a^2} + \frac{K}{a^2}\right) = 8\pi G \sum_n \rho_n + \Lambda. \tag{1.40}$$

By using the definition of the Hubble parameter we can rewrite the relation above,

$$H^2 = \frac{8\pi G}{3}\sum_n \rho_n - \frac{K}{a^2} + \frac{\Lambda}{3}. \tag{1.41}$$

It is useful to write (1.41) in terms of the dimensionless energy density parameters. To do this we first define the *critical energy density* ρ_c, which is the minimum amount of energy density which keeps the universe spatially flat in the absence of the cosmological constant.

$$H^2 = \frac{8\pi G\rho}{3} \implies \rho_c = \frac{3H^2}{8\pi G}. \tag{1.42}$$

Defining the dimensionless energy-density parameters as follows,

$$\Omega_n = \frac{\rho_n}{\rho_c},\ \Omega_K = \frac{-K}{(aH)^2},\ \Omega_\Lambda = \frac{\Lambda}{3H^2}, \tag{1.43}$$

[1] Here we briefly drop the n index for ease of notation and from here on, we work with $T^\mu{}_\nu \equiv g^{\mu\sigma}T_{\nu\sigma}$

allows us to rewrite (1.41) as,

$$1 = \sum_n \Omega_n + \Omega_K + \Omega_\Lambda. \tag{1.44}$$

The trace of the spatial component of the Einstein equations yields the second Friedmann equation,

$$3H^2 + 2\dot{H} = 8\pi G \sum_n P_n - \frac{K}{a^2} + \Lambda. \tag{1.45}$$

Combining the two Friedmann equations, (1.41) and (1.45) yields the acceleration equation,

$$\frac{\ddot{a}}{a} = -\frac{4\pi G}{3} \sum_n \left(P_n + 3\rho_n\right) + \frac{\Lambda}{3}. \tag{1.46}$$

From equation (1.46) we can see how the dynamics of the expansion of the universe is affected by the matter content. If the dominant matter species in the universe obeys

$$\rho_n + 3P_n < 0, \tag{1.47}$$

then the expansion of the universe accelerates due to the right hand side of (1.46) being manifestly positive. We can re-write (1.47) using the *equation of state* parameter,

$$w_n \equiv P_n/\rho_n \tag{1.48}$$

which yields the simple relation for (1.47) $w_n < -1/3$. Hence, if any fluid with an equation of state $w_n < -1/3$ is the dominant species in the universe, the expansion of the universe accelerates.

Mathematically, the conservation of energy-momentum is represented by the vanishing of the divergence of the energy-momentum tensor $\nabla^\mu T^{(n)}_{\mu\nu} = 0$. This yields the following matter equation of motion, which is named the *continuity equation*,

$$\dot{\rho_n} + 3H(\rho_n + P_n) = 0. \tag{1.49}$$

Here each species satisfies its own continuity equation independently and are not coupled to each other. For fluids with a constant equation of state, equation (1.49) has a simple solution,

$$\rho_n(a) = \rho_{0(n)} \left(\frac{a_{0(n)}}{a_n}\right)^{3(1+w_n)} \tag{1.50}$$

Fluid type	Equation of State	$\rho(a)$
Cold matter	$w = 0$	$\propto a^{-3}$
Radiation	$w = 1/3$	$\propto a^{-4}$
Cosmological constant	$w = -1$	$\propto const$
Curvature	$w = -1/3$	$\propto a^{-2}$

Table 1.1: Table showing how the energy density scales with the scale factor for varying components of the universe.

where a subscript zero means the quantity in question is evaluated today and we choose to normalise $a(t_0) = 1$. We can also define the total energy density as the sum of the individual components,

$$\rho_{tot} = \sum_n \rho_n(a). \tag{1.51}$$

We are now in a position to see how different fluids affect the expansion history of the universe. Table 1 shows how the energy density scales for various components of the universe. Using (1.50) and the definition of cosmological redshift, we can rewrite (1.44) as,

$$H^2(z) = H_0^2 \left[\Omega_{r,0}(1+z)^4 + \Omega_{m,0}(1+z)^3 + \Omega_{K,0}(1+z)^2 + \Omega_{\Lambda,0}\right], \tag{1.52}$$

The parameters $(\Omega_{m,0}, \Omega_{r,0}, \Omega_{\Lambda,0}, \Omega_{K,0}, H_0)$ are determined via observations. See [2] for their exact values, including the error bars and how they are experimentally determined, but here we briefly comment on each value and its significance.

1.2.4 Cosmological Parameters

Matter

We split $\Omega_{m,0}$ into two components: one for baryonic matter $\Omega_{BM,0}$ and one for cold dark matter $\Omega_{CDM,0}$. Baryonic matter is made up of all the baryons in the universe, i.e. protons and neutrons [2]. However, despite baryonic matter making up all the matter we observe, $\Omega_{BM,0} \sim 0.05$, which is a tiny fraction of the total energy budget of the universe. On the other hand $\Omega_{CDM,0} \sim 0.26$ which constitutes a large portion of the matter in the universe which we cannot directly observe [3]. Such a large contribution is required to explain the rotation curves of galaxies, and more recently the formation and evolution of galaxy clusters as well as the large scale structure (LSS) of the universe [25].

[2] Which in turn consist of three quarks.

[3] Here 'dark' refers to the fact that whatever substance constitutes dark matter does not interact with electromagnetism, or if it does, it does so very weakly.

Radiation

From (1.52) we see that radiation dilutes much faster than matter as the universe expands, hence the small value $\Omega_{r,0} \sim 9 \times 10^{-5}$. Relic photons from the CMB make up most of the energy density of radiation in the present epoch.

Curvature

Current experiments [2] show no direct detection of curvature in the universe and all observations point to the universe being spatially flat, with the curvature density parameter being $\Omega_{K,0} \sim 10^{-3}$. However, as we shall see later in this thesis, keeping a non-zero value for the curvature, but still within observational bounds, can lead to interesting phenomenology.

Cosmological Constant

The final piece of the cosmological puzzle is the energy density which arises from the cosmological constant. The value $\Omega_{\Lambda,0} \sim 0.7$ shows that the cosmological constant (or dark energy) makes up 70% of the energy budget of the universe and it is required to explain the accelerated expansion of the universe. Inspecting the form of (1.52) shows that the cosmological constant is unaffected by the cosmological expansion, hence when the cosmological constant is the dominant species then the expansion of the universe accelerates.

Using (1.52) and the definition of redshift we can make predictions in the ΛCDM model, for example we can numerically compute the age of the universe,

$$\int_0^{t_0} dt = \int_0^{\infty} \frac{dz}{H(z)(1+z)} \tag{1.53}$$

$$\implies t_0 = H_0^{-1} \int_0^{\infty} \frac{dz}{H(z)(1+z)} \sim 13 \text{ billion years.} \tag{1.54}$$

Under the assumption of ΛCDM, the age of the universe is approximately 13 billion years. Despite the success of the ΛCDM model in describing many of the cosmological observations, the standard model of cosmology is not without problems, seeking many researchers to study alternative cosmological models.

1.3 Questioning ΛCDM

The remarkable success of ΛCDM perhaps leads us to ask the question, what is the problem? However, there are still many mysteries regarding the nature of dark energy and dark matter which have yet to be resolved. It is by considering alternative models and ideas that we learn more about the composition and structure of the universe, as history has proved.

In the 19th century peculiarities in Mercury's orbit were hypothesised to be caused by the presence of a dark planet 'Vulcan', by the French astronomer Urbain le Verrier. The discovery of Vulcan was confirmed by amateur astronomer Edmon Lescarbault shortly after, although no direct observation had been made. Both won the prestigious Legion d'honneur award. Note here that Newtonian gravity was the accepted theory of gravity at the time. Einstein then published the theory of General Relativity around 50 years later, and explained perfectly the peculiarities in Mercury's orbit without the need of a planet Vulcan. Newtonian gravity was then realised to be the weak field limit of GR. Who is to say that GR is not the limit of some more complex theory of gravity which introduces beyond ΛCDM physics? If we place ourselves in Le Verrier's position now, we have not detected dark matter directly or a cosmological constant but we *hypothesise* what they are, and until we detect them and understand their origins, it is critical to seek alternative cosmologies beyond ΛCDM as that is where the true answer could lie.

1.3.1 Old Cosmological Constant Problem

The biggest challenge facing the ΛCDM model is that of the old cosmological constant problem. Simply put, the observed value for the vacuum energy is far below that of the value predicted for the vacuum energy from quantum field theory (QFT). To outline the problem we calculate the vacuum energy density arising from the cosmological constant in ΛCDM. The relation we find is

$$\rho_\Lambda = \rho_c \left(\frac{\Lambda}{3H^2}\right) = \left(\frac{3H_0^2}{8\pi G}\right)\Omega_{\Lambda,0}. \tag{1.55}$$

Plugging in numbers yields the following observed value for the vacuum energy,

$$\rho_\Lambda^{\text{obs}} \sim (10^{-3}\text{eV})^4. \tag{1.56}$$

To compare this with the vacuum energy predicted from QFT we follow a similar argument to [26]. A naive calculation of the vacuum energy yields,

$$\rho_\Lambda^{\text{vac}} \approx \int_0^\infty dk k^2 \sqrt{k^2+m^2}. \tag{1.57}$$

However, the above integral has a quartic divergence in k, so to circumvent this we introduce a cut-off scale $k_{\max}$ which corresponds to the energy scale up to which we can trust the standard model of particle physics. The value of the vacuum energy therefore becomes,

$$\rho_\Lambda^{\text{vac}} \sim \int_0^{k_{\max}} dk k^2 k_{\max} \sqrt{k^2 + m^2} \sim k_{\max}^4. \tag{1.58}$$

Finally, we are agnostic about the scale involved and consider the highest energy scale which would give rise to the highest value for the vacuum energy, which is given by the Planck scale. Therefore, the approximate value for the vacuum energy is

$$\rho_\Lambda^{\text{vac}} \sim \text{Mp}^4 = 10^{121} \rho_\Lambda^{\text{obs}}, \tag{1.59}$$

which is a striking mismatch between the theoretical prediction and the observed value. In fact, regardless of where we choose the cut-off the discrepancy remains at $\mathcal{O}(> 45)$ orders of magnitude. Such is the discrepancy between $\rho_\Lambda^{\text{obs}}$ and $\rho_\Lambda^{\text{vac}}$, that a fine-tuning of 121 decimal places is required to bring the large contribution from the theoretical prediction down to the observed value. Renormalisation can improve the amount of fine-tuning required, see [27] for a discussion, but even after renormalisation there still persists a fine-tuning problem.

Suppose we have our fine-tuned bare vacuum energy such that,

$$\rho_\Lambda^{\text{bare}} = \frac{\Lambda_{\text{bare}}}{8\pi G} = \rho_\Lambda^{\text{obs}} - \rho_\Lambda^{\text{vac}}. \tag{1.60}$$

We can write the Einstein-Hilbert action in terms of this new Λ_{bare}

$$S = \frac{1}{16\pi G} \int d^4x \sqrt{-g} (R - 2\Lambda_{\text{bare}}). \tag{1.61}$$

However, the tuning in (1.60) is sensitive to the UV physics and is unstable under radiative corrections [28]. This means at each loop order one has to re-tune the vacuum energy down to match the observed value, which poses a question regarding the naturalness of the cosmological constant. In this thesis we study different approaches to the problem of the late-time acceleration of the universe, which don't suffer from the naturalness issue that the cosmological constant suffers from.

There is also another problem associated with the cosmological constant, which we don't aim to solve in this thesis but are mentioning for completeness, and it is the *why now?* question. That is to say, why in the epoch of human observation the value of $\Omega_{m,0}$ and $\Omega_{\Lambda,0}$ are the same order of magnitude. There is a debate as to whether this is actually a problem, but models exist which solve this problem via the means of a interaction between dark matter and dark energy [29, 30].

1.4 Modified Gravity

We know that vacuum energy exists due to the experimental evidence in Casimir effect experiments [31]. The question of whether the vacuum energy is simply a cosmological constant, or something more exotic, has really gained momentum this millennium. This is due to the development of phenomenologically interesting models combined with the power of a large number of state of the art observations, which can rule out and constrain alternative models of gravity and dark energy. In order to find alternatives to the cosmological constant and to investigate cosmologies which go beyond ΛCDM, we have to go back to the assumptions which form the basis of the ΛCDM model and reconsider if they are actually valid assumptions. That is to say, we shall not break the assumption of homogeneity and isotropy in this thesis, although there are models which break these assumptions. Such models are the Lemaître-Tolman-Bondi models [32–34], but these models come into tension with LSS data.

1.4.1 How to modify GR

In this work, we are principally concerned with breaking the 2nd assumption of the ΛCDM model: that GR is valid on all scales. How to break and modify GR, however, is non-trivial as it is protected by the famous *Lovelock's theorem* (1971) which states: In 4 dimensions GR, plus a cosmological constant, is the unique gravitational theory describing a massless spin-2 field which yields second order equations of motion [35, 36]. Therefore, to modify GR we must have one (or more) of the following:

· **1.** The equations of motion are *emergent*, or in other words, they do not arise from an action. One example of such a theory is emergent gravity [37] which can be used as an alternative model to cold dark matter [38].

· **2.** Lorentz invariance is broken. Breaking of Lorentz invariance can lead to a UV complete theory of gravity, an example being Hořava gravity [39]. However, due to the recent binary neutron star merger [40], detected by the LIGO-VIRGO collaboration, and the detection of an optical counterpart [41], this has put tight constraints on this class of gravitational theory [42].

· **3.** Non-locality. A non-local theory of gravity contains operators in the Lagrangian such as,

$$L_{NL} \supseteq R\frac{1}{\Box^2}R, \tag{1.62}$$

where $\Box = \nabla^\mu \nabla_\mu$. Here, the non local term produces an effective dark energy with a phantom equation of state ($w < -1$), negating the need for a cosmological constant [43].

· **4.** Extra dimensions. Higher dimensional theories of gravity such as DGP (Dvali-Gabadadze-Porati) [44] and braneworld gravity [45] are string theory inspired constructions whereby at low energies gravity is localised on the brane and GR is recovered, whilst at high energies gravity leaks into the bulk spacetime resulting in interesting consequences for cosmology and high energy astrophysics.

· **5.** Higher derivatives in the action. One of Lovelock's assumptions is that the equations of motion for the metric tensor are second order. Theories such as Stelle's classical gravity [46] includes higher derivatives of the metric in the action, which lead to fourth order equations of motion.

· **6.** Extra fields. Adding extra field content to GR is another way of introducing modifications. The Horndeski class of theory [47] is the most general scalar-tensor theory which leads to second order equations of motion, thus avoiding the Ostragradski ghost instability [48], even though the action contains higher derivative interactions. The covariant action for the Horndeski class takes the following form,

$$\mathscr{L}_H = \sum_{i=2}^{5} \mathscr{L}_i, \tag{1.63}$$

where $\mathscr{L}_i$ are covariantisations of the galileon interactions [49] and take the form,

$$\begin{aligned}
&\mathscr{L}_2 = K(\phi, X), \\
&\mathscr{L}_3 = -G_3(\phi, X)\Box\phi, \\
&\mathscr{L}_4 = G_4(\phi, X)R + G_{4,X}(\phi, X)\left[(\Box\phi)^2 - (\nabla_\mu\nabla_\nu\phi)^2\right], \\
&\mathscr{L}_5 = G_5(\phi, X)G^{\mu\nu}\nabla_\mu\nabla_\nu\phi \\
&\quad -\frac{1}{6}G_{5,X}(\phi, X)\left[(\Box\phi)^3 - 3\Box\phi(\nabla_\mu\nabla_\nu\phi)^2 + 2(\nabla_\mu\nabla_\nu\phi)^3\right].
\end{aligned} \tag{1.64}$$

In (1.64) (K, G_3, G_4, G_5) are free functions of a scalar field ϕ and its corresponding kinetic term $X = -g^{\mu\nu}\partial_\mu\partial_\nu\phi$, a comma represents a derivative and $G^{\mu\nu}$ is the Einstein tensor. Not every theory which can be derived from the Horndeski action introduces an extra scalar field, i.e. setting $G_5 = 0$, $G_4 = 1$, $G_3 = 0$, $K = -2\Lambda$ recovers the GR action (1.1) which is simply a metric gravitational theory. However, the Horndeski theory is primarily used in the context of scalar-tensor theories

whereby the extra scalar field introduced via the terms in (1.64) can be chosen in such a way to drive the accelerated expansion of the universe without the need of a cosmological constant and is a compelling candidate for dark energy. However, as with the case with Hořava gravity, the detection of the binary neutron star merger with optical counterpart has constrained the space of viable Horndeski theories [50]. The problem being a large subset of the Horndeski class predict a speed of gravitational waves different from the speed of light $c_T \neq c$ [4]. There is however, a caveat which the reader should be aware of. It was shown that the cut-off scale of the Horndeski theory lies very close to the energy scale of the LIGO observations [51]. Furthermore, at energies close to the UV cut-off, it was shown that a toy model of the Horndeski theory with a partial UV completion can predict $c_T = c$ at LIGO energy scales but have $c_T < c$ at lower energies. The upshot of this result is that in order to describe physics and compare with data close to or around the cut-off of the EFT, knowing the UV completion of the theory is important and one can not necessarily draw conclusions about the predictions of the theory around the cut-off of the EFT without knowing the UV completion.

As seen in the case of Horndeski theory, an extra scalar field can be introduced which has interesting phenomenological properties. But why stop there? Vector fields [52, 53] can be introduced which have self-accelerating properties or extra tensor fields like in bigravity [54].

There are many other theories of modified gravity which fit into one or more of these categories, which have interesting implications for cosmology and high energy physics. For more information see the reviews [26, 55, 56] and references therein. In this thesis, we shall focus on working with extra tensor fields which give rise to interesting cosmology, which to the most part fall into point 6.

1.4.2 Consequences of modifying GR

Now we have introduced how to modify GR, we have to face the consequences of modifying the most successful theory of gravity to date. Introducing a wanted effect, such as obtaining a solution for dark energy[5] without introducing a cosmological constant, nearly always brings about unwanted effects. Such pathologies can include the violation of solar

[4] One should note, however, that GR exists as a theory within the Horndeski framework, so one should be careful when making comments regarding the validity of the entire Horndeski class.

[5] We will refer to these solutions as self-accelerating solutions.

system and laboratory tests, which are the most successful predictions of GR, or the emergence of theoretical inconsistencies within the construction of the theory. Different classes of theories will have different problems and also different phenomenological consequences, and in this section we briefly discuss the consequences of modifying GR and what problems it can lead to.

The basic principle is this: extra fields mediate extra forces, and on the face of it, the lack of a detection of any "fifth" forces in nature is a thorn in the side of many theories of modified gravity. See [14] for a review on tests of gravity conducted from laboratory to galactic scales. In addition, it was also shown that recently no deviation from GR has been found at extra-galactic scales [57], but the scales we are extrapolating GR to, in terms of cosmology, are way beyond any scale that GR has been tested to date. We also know that GR is not a UV complete theory, and requires modification in the UV due to GR being non-renormalisable below the Planck scale. Therefore there is good motivation to seek modifications in both the IR and UV regime.

Theoretical considerations must also be taken into account when discussing the viability of an extended theory of gravity [55, 58]. These concepts will be important throughout this thesis. To illustrate the different theoretical issues one could have, we consider a simple scalar field toy model described by the action,

$$S^{\phi} = \int dt d^3x \left(\mathcal{K}\dot{\phi}^2 - \mathcal{G}\partial_i\phi\partial^i\phi - m^2\phi^2 \right). \tag{1.65}$$

A *tachyonic* instability arises if the scalar field has a negative mass squared $m^2 < 0$. However this can be a mild instability if the mass of the field is small, as the time the instability takes to develop is described by $t_I \sim m^{-1}$. This means for small masses the instability can be pushed to arbitrarily large times.

A *gradient* instability arises if the coefficient of the gradient term has the wrong sign, which for our toy model means $\mathcal{G} < 0$. This type of instability is dangerous as the timescale of the instability depends on the wavenumber of the mode, so for smaller scales the timescale of the instability shortens.

Finally, a *ghost* instability arises if the kinetic term has the wrong sign, so $\mathcal{K} < 0$. This is also a dangerous instability [58, 59]. The consequence of a ghost mode is that the vacuum breaks down due to the hamiltonian of the theory being unbounded, which results in the theory instantly becoming unstable [60]. Particles are produced out of the vacuum at a very high rate, which is un-physical. Another way of generating a ghost is to have higher derivatives in the Lagrangian. These type of ghosts are given the name *Ostrogradsky ghosts* [48], named after Mikhail Ostrogradsky. A toy Lagrangian with

higher derivatives takes the form [58],

$$\mathscr{L}^{ghost} = -\frac{1}{2}(\partial\phi)^2 + \frac{1}{2\Lambda}(\Box\phi)^2 - V(\phi), \tag{1.66}$$

where Λ is the cutoff of the effective theory. At first glance, this appears to be a healthy Lagrangian. To expose the ghost pathology we introduce an equivalent formulation of (1.66) [58],

$$\mathscr{L}^{ghost} = -\frac{1}{2}(\partial\phi)^2 + \chi\Box\phi - \frac{\Lambda^2}{2}\chi^2 - V(\phi), \tag{1.67}$$

where χ is an auxiliary field. Integrating out χ, i.e solving its equation of motion, and substituting back into (1.67) we recover the original ghostly Lagrangian (1.66). We are allowed to integrate out massive fields when the cut-off of the effective field theory is equal to or below the mass of the field. Diagonalising (1.67) utilising the field redefinition $\phi = \psi - \chi$ and integrating by parts we obtain the equivalent formulation of (1.66)

$$\mathscr{L}^{ghost} = -\frac{1}{2}(\partial\psi)^2 + \frac{1}{2}(\partial\chi)^2 - \frac{\Lambda^2}{2}\chi^2 - V(\psi,\chi). \tag{1.68}$$

Here the nature of the ghost is apparent. We have transformed a theory with higher derivatives into a theory with two scalar fields, where the field χ has the wrong sign kinetic term, signalling the presence of a ghost.

To be a healthy and successful modified gravity theory, the theory must pass all observational tests to date and be theoretically consistent. Once these hurdles have been passed, then the phenomenological implications can be studied. However, there is a caveat regarding the lack of a fifth force detection. Many theories of modified gravity have *screening mechanisms* which hide the effect of the force due to the extra degrees of freedom on local scales, such as the solar system, and on cosmological scales the fifth force activates and drives the accelerated expansion of the universe. In the next section, we briefly discuss a variety of screening mechanisms present in modified theories of gravity.

1.4.3 Screening Mechanisms

To illustrate the screening mechanisms which are present in modified theories of gravity, let's consider a generalisation of the scalar field Lagrangian (1.65) [55, 58, 61] minimally coupled to an external source,

$$\mathscr{L}^{\phi} = -\frac{1}{2}Z(\phi)^2 g^{\mu\nu}\partial_\mu\phi\partial_\nu\phi - V(\phi) + \tilde{g}(\phi)T^{\mu}_{\mu}. \tag{1.69}$$

Here $Z(\phi)$ is the kinetic function and is dependent on the background field value $\bar{\phi}$ only, $V(\phi)$ is the potential, $\tilde{g}(\phi)$ is a coupling function and T^{μ}_{μ} is the trace of the energy-momentum tensor, which we assume to be non-relativistic matter $T^{\mu}_{\mu} = -\rho$. Expanding (1.69) to second order in the field fluctuation $\delta\phi$, introduced via $\phi = \bar{\phi} + \delta\phi$ yields,

$$\mathscr{L}^{\phi} \supseteq -\frac{1}{2}Z(\bar{\phi})^2\partial_{\mu}\delta\phi\partial^{\mu}\delta\phi - m(\bar{\phi})^2\delta\phi^2 - g(\bar{\phi})\delta\phi M\delta^3(\vec{x}) + ... \tag{1.70}$$

where we considered a static point mass in 3 dimensions, $\rho = M\delta^3(\vec{x})$, and

$$g(\phi) \equiv \frac{d\tilde{g}}{d\phi}. \tag{1.71}$$

The behaviour of the scalar field fluctuations $\delta\phi$ around the background value $\bar{\phi}$ depends on 3 functions: the mass $m(\bar{\phi})^2 \equiv 2\partial^2 V/\partial\bar{\phi}^2$, the coupling function which quantifies how the scalar field couples to matter $g(\bar{\phi})$ and the kinetic function $Z(\bar{\phi})$. Each 3 of these functions can screen the scalar field in different ways, and we briefly describe each one of them in turn.

Large Mass If the mass of the field $m(\bar{\phi})$ is large enough in areas of high density, such as the solar system, then the scalar field does not propagate above the Compton wavelength. On the other hand, if the mass is low in low density environments, such as the cosmological background, then the scalar field mediates a fifth force which modifies gravity on large scales. A typical model which realises this type of screening is chameleon gravity [62, 63], however these models have been heavily constrained by observations [64] and to act as dark energy require a cosmological constant [65] to achieve self acceleration.

Small Coupling Alternatively, one could have $g(\bar{\phi})$ being small enough in dense environments, so again the fifth force is screened. But on cosmological scales, the coupling can be order 1 so the fifth force contributes the same order of magnitude as the Newtonian force. The symmetron [61] and dilaton [66] realise this method of screening.

Large kinetic term Having a large kinetic function $Z(\bar{\phi})$ results in an interesting class of screening mechanism which depends on the derivatives of the scalar. There are two options: screening by the first derivative $\partial\phi$ becoming large, as in k-mouflage (k-essence theories [67]), or by the second derivative $\partial^2\phi$ becoming large. The latter is associated with the *Vainshtein mechanism*, which will be discussed in detail in

chapter 2 and has an important role to play when studying theories of massive gravity. Having a large $Z(\bar{\phi})$ results in the normalisation of the kinetic term being no longer unity, so upon canonical normalisation (1.70) schematically contains,

$$\mathscr{L} \supseteq -\frac{1}{2}\partial_\mu \delta\tilde{\phi}\partial^\mu \delta\tilde{\phi} - \frac{g(\bar{\phi})}{Z(\bar{\phi})}\delta\tilde{\phi}M\delta^3(\vec{x}). \tag{1.72}$$

From (1.72) it is clear to see that a large $Z(\bar{\phi})$ in dense environments will suppress the coupling to matter, again screening the effect of the fifth force.

1.5 Cosmological Perturbations

We conclude this chapter with a brief introduction into cosmological perturbations. See [68, 69] for comprehensive reviews on the subject. Cosmological perturbations are a very useful tool for quantifying small deviations from the standard cosmological background. Given an FLRW background described by the $\bar{g}_{\mu\nu}$, fluctuations on top of this background are described by the metric perturbation $\delta g_{\mu\nu}$, which is spacetime dependent and contains scalar, vector and tensor perturbations. In general, there are two approaches for studying cosmological perturbations in the context of modified gravity theories. The first is to work with an explicit model, and use the predictions from the model to constrain the model parameters directly. The second is to work in a general framework for parameterising deviations away from GR, such as the PPF (Parameterised post-Friedmann) [70–72] or PPN (Parameterised post-Newtonian) [73]. In this thesis we will work with the first approach, but see the above references for details on the alternative approach.

To mathematically describe how to perform perturbations, we begin with the curved background FLRW metric,

$$ds^2 = \bar{g}_{\mu\nu}dx^\mu dx^\nu = -dt^2 + a^2\Omega_{ij}dx^i dx^j, \tag{1.73}$$

where Ω_{ij} is the metric on the constant time hypersurfaces,

$$\Omega_{ij} = \delta_{ij} + \frac{K\delta_{il}\delta_{jm}x^l x^m}{1 - K\delta_{lm}x^l x^m}. \tag{1.74}$$

For matter we consider the following energy momentum tensor,

$$T^\mu_\nu = \left(\bar{\rho} + \bar{P}\right)u^\mu u_\nu + \bar{P}\delta^\mu_\nu. \tag{1.75}$$

In (1.75) $\bar{u}^\mu$ is the background 4-velocity which satisfies $\bar{u}^\mu\bar{u}_\nu = -1$, $\bar{\rho}$ and $\bar{P}$ are the background values for the energy density and pressure respectively.

The standard analysis of cosmological perturbations revolves around deriving the equations of motion governing the perturbations, then substituting the fields in terms of their harmonics in curved space [74, 75]. The harmonic expansion for a scalar quantity is

$$\phi = \int d^3k \phi_{|\vec{k}|} Y(\vec{k},\vec{x}), \tag{1.76}$$

where k is the comoving wavenumber of the length scale $\lambda = 2\pi/k$, $\phi_{|\vec{k}|}$ is the mode function and the harmonics satisfy the relation

$$D^i D_i Y(\vec{k},\vec{x}) = -k^2 Y(\vec{k},\vec{x}). \tag{1.77}$$

In (1.77) D^i is the covariant derivative associated with the metric Ω_{ij}.

In general there are three different regimes when studying perturbations: the large k regime corresponding to modes with wavenumbers smaller than the horizon, ie: $k << aH$. In this regime motion is relativistic and requires a full relativistic treatment. The linear quasi-static regime is described by modes with $k >> aH$, in this regime linear theory is sufficient and the motion is non-relativistic. The final regime is the small scale, non-linear regime where perturbation theory is no longer applicable and is the most difficult regime to describe. Density perturbations are no longer small and may couple to additional fields present in modified gravity theories, which makes this regime tricky to quantitatively analyse, however this regime can be the most interesting for detecting modified gravity signatures. In the linear regime, each Fourier mode evolves independently which is not the case in the non-linear regime. N-body simulations are required to study particle motions in this regime which can be computationally expensive [76, 77] and which typically show deviations from the linear theory around $k \sim 0.1\text{Mpc}^{-1}$.

Introducing a perturbation to the metric tensor as,

$$g_{\mu\nu} = \bar{g}_{\mu\nu} + \delta g_{\mu\nu}, \tag{1.78}$$

with components,

$$\delta g_{\mu\nu} = \begin{pmatrix} \delta g_{00} & a\delta g_{0i} \\ a\delta g_{i0} & a^2 \delta g_{ij} \end{pmatrix}, \tag{1.79}$$

the full line element becomes,

$$ds^2 = -(1-\delta g_{00})dt^2 + 2a\delta g_{0i} dx^i dt + a^2(\Omega_{ij} + \delta g_{ij}) dx^i dx^j. \tag{1.80}$$

We can further decompose the metric perturbations as [58, 69],

$$\begin{aligned} \delta g_{00} &= -2\phi \\ \delta g_{0i} &= D_i B^S + B_i^V \\ \delta g_{ij} &= 2\psi\Omega_{ij} + D_i D_j S^S + D_i F_j^V + D_j F_i^V + \gamma_{ij}, \end{aligned} \tag{1.81}$$

where the vectors are divergence free $D^i B_i^V = D^i F_i^V = 0$ and the tensor γ_{ij} is divergence free and traceless $D^i \gamma_{ij} = \Omega^{ij}\gamma_{ij} = 0$.

For the matter sector, in the case of a pressure-less perfect fluid, the perturbed energy-momentum tensor takes the form

$$\delta T^\mu_\nu = \delta\rho \bar{u}^\mu \bar{u}_\nu + \bar{\rho}(\delta u^\mu \bar{u}_\nu + \bar{u}^\mu \delta u_\nu). \tag{1.82}$$

Using $g_{\mu\nu}u^\mu u^\nu = -1$ and introducing a perturbation to the spatial component of the 4-velocity $v^i = D^i v$ we deduce that,

$$u^\mu = (1-\phi, D^i v), \quad u_\mu = (-1-\phi, a^2 D_i v). \tag{1.83}$$

Which leads to the following form for T^μ_ν

$$\begin{aligned} T^0_0 &= -(\bar{\rho} + \delta\rho) \\ T^i_0 &= -\bar{\rho} D^i v \\ T^0_i &= a^2 \bar{\rho} D_i v \\ T^i_j &= 0. \end{aligned} \tag{1.84}$$

Note that in the presence of pressure, the spatial components of the energy-momentum tensor are non-vanishing. We will use these results in the subsequent chapters to analyse perturbations in massive gravity cosmology.

1.6 Gauge transformations

We now discuss the effect on the metric perturbation under a general coordinate transformation. A diffeomorphism is a spacetime transformation of the form,

$$x^\mu \to x'^\mu = x^\mu + \xi^\mu(x), \tag{1.85}$$

where ξ^μ is the spacetime dependent gauge parameter which is assumed to be small. Under this transformation, different quantities will transform according to their rank. Due to the diffeomorphism invariance of GR, the following relationship holds between the line elements ds^2 and ds'^2,

$$g_{\mu\nu} dx^\mu dx^\nu = g'_{\mu\nu} dx'^\mu dx'^\nu. \tag{1.86}$$

Using this, we obtain how the metric transforms under a diffeomorphism (1.85),

$$g'_{\mu\nu}(x') = g_{\alpha\beta}(x) \frac{\partial x^\alpha}{\partial x'^\mu} \frac{\partial x^\beta}{\partial x'^\nu}. \tag{1.87}$$

We can re-write the left hand side of (1.87) by Taylor expanding,

$$\text{LHS} = \bar{g}_{\mu\nu}(x) + \xi^{\alpha}\partial_{\alpha}\bar{g}_{\mu\nu}(x) + \delta g'_{\mu\nu}, \tag{1.88}$$

and similarly for the right hand side,

$$\text{RHS} = \bar{g}_{\mu\nu}(x) + \delta g_{\mu\nu} - \partial_{\mu}\xi^{\rho}\bar{g}_{\rho\nu} - \partial_{\nu}\xi^{\rho}\bar{g}_{\mu\rho}. \tag{1.89}$$

Equating the two results above, we obtain how the metric perturbation transforms

$$\Delta\delta g_{\mu\nu} \equiv \delta g'_{\mu\nu} - \delta g_{\mu\nu} = -\partial_{\mu}\xi^{\rho}\bar{g}_{\rho\nu} - \partial_{\nu}\xi^{\rho}\bar{g}_{\mu\rho} - \xi^{\alpha}\partial_{\alpha}\bar{g}_{\mu\nu}(x). \tag{1.90}$$

The diffeomorphism ξ^{μ} can be chosen in a certain way to render some of the metric perturbations in (1.81) zero, which is particularly useful to simplify computations. This will have no effect on observable quantities however, as they are gauge invariant. One particular choice corresponds to setting $B^S = S^S = 0$, which is known as the Newtonian gauge. In this gauge, the line element simplifies to,

$$ds^2 = -(1+2\phi)dt^2 + a^2(1+2\psi)\Omega_{ij}dx^i dx^j, \tag{1.91}$$

where we have omitted the vector and tensor components as they decouple at linear order due to the rotational symmetry of the background [78]. When analysing the stability of generalised massive gravity in chapter 4 we will re-introduce the vector and tensor modes, but for this discussion it is convenient to omit them. The benefit of this choice means that, in the case of zero spatial curvature and Cartesian coordinates, the metric is now diagonal meaning it is easier to perform computations, and in this thesis we discuss density perturbations which are scalar quantities

Sometimes it is useful to work with gauge invariant variables. One particular choice is known as the Bardeen variables [79]. In terms of the metric perturbations they are,

$$\Phi_B = \phi - \frac{d}{dt}\left[a^2\left(\frac{\dot{S^S}}{2} - \frac{B^S}{a}\right)\right]; \Psi_B = \psi - a^2 H\left(\frac{\dot{S^S}}{2} - \frac{B^S}{a}\right). \tag{1.92}$$

1.7 Conclusions

In this section we have introduced the foundations of General Relativity which is the underlying theory of gravity behind the standard model of cosmology. We discussed problems associated with ΛCDM, namely the cosmological constant problem, and discussed possible solutions via modifications of gravity. We then introduced modified gravity and

gave a brief tour of the zoo of models which can, or cannot, account for the late time acceleration of the universe, without so far pledging allegiance to a particular model. We then discussed possible issues with modifying gravity such as the violation of solar system and observational tests, which can be resolved by screening mechanisms, or the generation of theoretical inconsistencies.

It is at this point we choose our particular class of theory to study, which is massive gravity. We shall see how postulating the presence of a graviton mass has been a very popular avenue of research over the last decade. In chapter 2 we shall describe the history of massive gravity, from linear Fierz-Pauli in the early 20th century to the current status today, focusing on the problems and the subsequent resolutions bought about by developments in the field. In the subsequent chapters, we study bigravity and generalised massive gravity as extensions to dRGT as possible dark energy models.

CHAPTER 2

MASSIVE GRAVITY

Introduction

A theory of massive gravity is a gravitational theory which propagates a massive spin-2 particle, and from the equation which counts the degrees of freedom for massive particles [1], we know that the theory must have 5 degrees of freedom. From particle physics experiments we have experimentally detected massive spin-0 and massive spin-1 particles [80, 81], in the form of the Higgs and W, Z bosons respectively. So to postulate that the graviton has a non-zero mass is quite a natural one from the point of view of particle physics.

To motivate why adding mass to the graviton could yield a solution to the dark energy conundrum, we consider the simpler case of adding mass to a scalar field. Starting from the Klein-Gordon equation for a massive scalar field sourced by a point source located at the origin,

$$(-\nabla^2 + m^2)\phi = \delta(\vec{x}), \tag{2.1}$$

we get the solution,

$$\phi(\vec{x}) = \frac{1}{4\pi r} e^{-mr}. \tag{2.2}$$

[1] dof = 2S + 1 where S is the spin of a massive particle. This is related to the Poincare representations of massive spinning particles around Minkowski, i.e. these are the number of degrees of freedom we expect from a massive spin S particle around Minkowski.

Equation (2.2) tells us that the field profile drops off exponentially quickly as $r \to \frac{1}{m}$, or in other words, on scales larger than the Compton wavelength of the particle, $\lambda = \frac{1}{m}$. The result of this is that the force exerted by a massive particle has a finite range. Assuming the field profile for a massive graviton follows that of (2.2) and taking $m \sim H_0$ yields that the force drops off on distances $r \sim H_0^{-1}$, which corresponds to the Hubble radius. Therefore, postulating that the graviton has a mass of the order of the Hubble parameter could lead to a decay of the gravitational force on cosmological distances and drive the accelerated expansion of the universe. This is the essence of what modified gravity theories aspire to achieve.

Endowing the graviton with a non-zero mass was first considered in 1939 by Fierz and Pauli [82], who wrote down the linear theory of massive gravity describing a massive spin-2 field by requiring the absence of ghosts. The theory breaks the linearised diffeomorphism of GR resulting in the propagation of 5 degrees of freedom. Years later, in 1970, van Dam and Veltman [83] and independently Zakharov [84] showed that in the massless limit of the linear theory of massive gravity, GR is not recovered. The name given to this discrepancy is the famous *vDVZ* discontinuity. Vainshtein resolved the discontinuity two years later by realising that the inclusion of non-linear interactions, which promote the linear Fierz-Pauli theory to a non-linear theory, allows the recovery of GR in the massless limit. Written another way, the linear approximation of gravity outside of a source breaks down at distances larger than the gravitational radius, so the massless limit of FP massive gravity does not correspond to GR. In the same year however, Boulware and Deser showed that generic non-linear theories of massive gravity propagate an extra degree of freedom, which turned out to be a ghost and was dubbed the *Boulware-Deser* ghost [85]. The early 2000's saw developments in the effective field theory (EFT) description of a massive graviton [86]. It was found that massive gravity theories typically have a UV cut-off of $\Lambda_5 \sim (M_p m^4)^{\frac{1}{5}}$, and for a Hubble scale graviton mass $m \sim H_0$ yields $\Lambda_5^{-1} \sim 10^{11}$km, which is a very low cut-off. In 2010 there was a breakthrough, de-Rham, Gabadadze and Tolley constructed the unique, ghost free theory of massive gravity [87, 88] (dRGT massive gravity) with a higher UV cut-off of $\Lambda_3 \sim \left(M_p m^2\right)^{\frac{1}{3}}$, which assuming $m \sim H_0$ yields $\Lambda_3^{-1} \sim 10^3$km. Here Λ_3 is also referred to as the strong coupling scale of dRGT theory, which corresponds to the energy scale at which unitary is broken: so at higher energy scales than Λ_3 the theory loses predictability. Note here that to obtain massive gravity to be perturbative down to distances of $\mathcal{O}$(mm), i.e. laboratory scales, the graviton mass must be $m > \mathcal{O}(10^{-3})$eV which would render the theory incompatible with GR on large distances [89]. dRGT massive gravity will form

the framework model for which we will work in this thesis.

In this Section we first briefly review linearised GR and ouline the history of massive gravity from the first ideas by Fierz and Pauli to dRGT, mathematically highlighting the key developments and problems summarised in this Section. This Section is largely based on the review [90]. We then discuss the application of dRGT massive gravity to cosmology and study its viability.

2.1 Fierz-Pauli Massive Gravity

To study Fierz-Pauli massive gravity, we first have to discuss linearised GR. We consider purely the gravity sector with no cosmological constant for this discussion, and work with a spacetime which is close to flat described by

$$g_{\mu\nu} = \eta_{\mu\nu} + h_{\mu\nu}, \tag{2.3}$$

where $\eta_{\mu\nu}$ is the flat 4 dimensional Minkowski metric and $h_{\mu\nu}$ is the spin-2 metric perturbation. Upon substituting (2.3) into the action (1.1) and expanding to second order in $h_{\mu\nu}$ yields,

$$S^{(2)} = \frac{1}{8\pi G}\int d^4x\left(-\frac{1}{2}\partial_\lambda h_{\mu\nu}\partial^\lambda h^{\mu\nu} + \partial_\mu h_{\nu\lambda}\partial^\nu h^{\mu\lambda} - \partial_\mu h^{\mu\nu}\partial_\nu h + \frac{1}{2}\partial_\lambda h\partial^\lambda h\right), \tag{2.4}$$

where $h = \eta^{\mu\nu}h_{\mu\nu}$ is the trace of $h_{\mu\nu}$. The question we now ask is, what if the field $h_{\mu\nu}$ has a mass? At linear level (or quadratic at the level of the action), there are two possible terms that can be added when adding a mass term to (2.4),

$$L^{(2)} = m^2\left(ah^{\mu\nu}h_{\mu\nu} + bh^2\right), \tag{2.5}$$

where m is a parameter which controls the size of the graviton mass and a and b are constants. Requiring the absence of ghosts imposes constraints on the form of a and b. In order to show this, we expand (2.5) in terms of the metric perturbation components,

$$L^{(2)} = m^2\left((a+b)h_{00}^2 - 2ah_{0\mathrm{i}}^2 + ah_{\mathrm{ij}}^2 - 2bh_{00}h_{\mathrm{ii}} + bh_{\mathrm{ii}}^2\right). \tag{2.6}$$

In this work we are not concerned with the full Hamiltonian analysis and what follows is a rather heuristic way of counting the degrees of freedom (a more complete way would be performing a full Hamiltonian analysis, see [90]). With this in mind, we require that h_{00} appears linearly in the action to ensure there are no ghost degrees of freedom. In

order to achieve this, the only solution is $a = -b$, this is known as the *Fierz-Pauli tuning*. With this, we can can construct the action for Fierz-Pauli massive gravity [82],

(2.7)
$$S_{\rm FP} = \frac{1}{8\pi G}\int d^4x\left(-\frac{1}{2}\partial_\lambda h_{\mu\nu}\partial^\lambda h^{\mu\nu} + \partial_\mu h_{\nu\lambda}\partial^\nu h^{\mu\lambda} - \partial_\mu h^{\mu\nu}\partial_\nu h + \frac{1}{2}\partial_\lambda h\partial^\lambda h - \frac{m^2}{2}\left(h^{\mu\nu}h_{\mu\nu} - h^2\right)\right).$$

The Fierz-Pauli action is the unique action at the quadratic level that can describe the dynamics of a massive spin-2 field. Any deviation from the structure of (2.7) would result in extra degrees of freedom propagating, which would represent a ghost, or fewer than 5 degrees of freedom would propagate and the structure of the theory would be broken. To count the degrees of freedom, we calculate the equations of motion stemming from the action (2.7). Varying with respect to $h^{\mu\nu}$ yields,

$$\frac{\delta S_{\rm FP}}{\delta h^{\mu\nu}} = \Box h_{\mu\nu} - \partial_\lambda\partial_\mu h^\lambda_\nu - \partial_\lambda\partial_\nu h^\lambda_\mu + \eta_{\mu\nu}\partial_\lambda\partial_\gamma h^{\lambda\gamma} + \partial_\mu\partial_\nu h - \eta_{\mu\nu}\Box h - m^2\left(h_{\mu\nu} - \eta_{\mu\nu}h\right) = 0. \tag{2.8}$$

Taking the divergence of (2.8) yields the following constraint equation,

$$m^2\left(\partial^\mu h_{\mu\nu} - \eta_{\mu\nu}\partial^\mu h\right) = 0, \tag{2.9}$$

and assuming a non-zero m, we plug the solution of (2.9) into the equations of motion (2.8) to obtain,

$$\Box h_{\mu\nu} - \partial_\mu\partial_\nu h - m^2\left(h_{\mu\nu} - \eta_{\mu\nu}h\right) = 0. \tag{2.10}$$

Taking the trace of (2.10) yields $h = 0$, and using this in (2.9) results in $\partial^\mu h_{\mu\nu} = 0$. Therefore, we have the following 3 equations describing the dynamics of a linear theory of massive gravity in a flat spacetime,

$$\left(\Box - m^2\right)h_{\mu\nu} = 0,\ \partial^\mu h_{\mu\nu} = 0,\ h = 0. \tag{2.11}$$

The first of (2.11) is a wave equation describing the propagation of a massive spin-2 field. As $h_{\mu\nu}$ is symmetric, this equation implies 10 propagating degrees of freedom in 4 dimensions. The constraint $h = 0$ removes one degree of freedom, whilst the divergence of $h_{\mu\nu}$, given by the second equation, is in fact four equations which remove another 4 degrees of freedom. Therefore the total number of degrees of freedom is $10 - 1 - 4 = 5$, as expected from a theory of massive gravity. Now that we understand how the vacuum field equations behave, we investigate the behaviour of Fierz-Pauli massive gravity in response to an external matter source. Here we encounter the first setback in the history of massive gravity, the vDVZ discontinuity.

2.2 vDVZ discontinuity

To couple Fierz-Pauli massive gravity to matter, we consider an action of the form,

$$S = S_{FP} + \int d^4x h_{\mu\nu} T^{\mu\nu}. \tag{2.12}$$

Varying (2.12) results in the following equation of motion,

$$\Box h_{\mu\nu} - \partial_\lambda \partial_\mu h^\lambda_\nu - \partial_\lambda \partial_\nu h^\lambda_\mu + \eta_{\mu\nu}\partial_\lambda \partial_\gamma h^{\lambda\gamma} + \partial_\mu \partial_\nu h - \eta_{\mu\nu}\Box h - m^2\left(h_{\mu\nu} - \eta_{\mu\nu} h\right) = -8\pi G T_{\mu\nu}. \tag{2.13}$$

Again, applying the operator ∂^μ on (2.13) results in,

$$\partial^\mu h_{\mu\nu} - \partial_\nu h = \frac{8\pi G}{m^2}\partial^\mu T_{\mu\nu}, \tag{2.14}$$

where, due to a non-zero m, the conservation of energy momentum is no longer implied, $\partial^\mu T_{\mu\nu} \neq 0$. However, we assume a conserved source for this discussion, which is a valid assumption at the classical level [2]. Furthermore, if we do not consider a conserved source then in the limit $m \to 0$ then the right hand side of (2.14) diverges, indicating strong coupling. We will use this assumption later on in this chapter when identifying the origin of the vDVZ discontinuity (see footnote 3 in section 2.3). Substituting (2.14) into (2.13) and taking the trace yields,

$$h = -\frac{8\pi G}{3m^2} T. \tag{2.15}$$

Using the results of (2.15) and (2.14) in the equations of motion yields to the following 3 equations

$$\begin{aligned} (\Box - m^2) h_{\mu\nu} &= -8\pi G\left(T_{\mu\nu} - \frac{1}{3}\left(\eta_{\mu\nu} T - \frac{1}{m^2}\partial_\mu \partial_\nu T\right)\right), \\ \partial^\mu h_{\mu\nu} &= \frac{-8\pi G}{3m^2}\partial_\nu T, \\ h &= -\frac{8\pi G}{3m^2} T. \end{aligned} \tag{2.16}$$

Finding the solution of the first equation of (2.16) is sufficient since after some manipulations the other two equations are implied. Furthermore, we neglect the term proportional to $\partial_\mu \partial_\nu T$ as this term has no observable consequences on a test body under conservation of energy momentum [91]. Therefore, the equation for the massive spin-2 perturbation we wish to solve reduces to,

$$(\Box - m^2) h_{\mu\nu} = -8\pi G\left(T_{\mu\nu} - \frac{1}{3}\eta_{\mu\nu} T\right). \tag{2.17}$$

[2] For the type of sources we consider here, matter is conserved. The presence of the Fierz-Pauli term just means we cannot use the Bianchi identity to assume a conserved source.

Substituting the fields in terms of their Fourier transforms,

$$h_{\mu\nu}(x) = \int \frac{d^4p}{(2\pi)^4} e^{ip_\sigma x^\sigma} \tilde{h}_{\mu\nu}(p),$$
$$T_{\mu\nu}(x) = \int \frac{d^4p}{(2\pi)^4} e^{ip_\sigma x^\sigma} \tilde{T}_{\mu\nu}(p),$$
$$T(x) = \int \frac{d^4p}{(2\pi)^4} e^{ip_\sigma x^\sigma} \tilde{T}(p), \tag{2.18}$$

yields,

$$\tilde{h}_{\mu\nu}(p) = \frac{8\pi G}{p^\sigma p_\sigma + m^2}\left[\tilde{T}_{\mu\nu}(p) - \frac{1}{3}\eta_{\mu\nu}\tilde{T}(p)\right]. \tag{2.19}$$

Considering for the matter sector a point source located at the origin which is described by [90],

$$T_{\mu\nu}(x) = M\delta^0_\mu\delta^0_\nu\delta^3(\vec{x}), \tag{2.20}$$

and using the property of the Dirac delta in momentum space yields,

$$\tilde{T}_{\mu\nu}(p) = 2\pi M\delta^0_\mu\delta^0_\nu\delta(p_0), \quad \tilde{T}(p) = -2\pi M\delta(p_0). \tag{2.21}$$

Using (2.19) and (2.21) in (2.18) we obtain,

$$h_{\mu\nu}(x) = 8\pi GM\int \frac{d^4p}{(2\pi)^3}\frac{e^{ip_\sigma x^\sigma}}{p_\sigma p^\sigma + m^2}\left[\delta^0_\mu\delta^0_\nu + \frac{1}{3}\eta_{\mu\nu}\right]\delta(p_0). \tag{2.22}$$

We split the integral into the time and spatial components,

$$h_{\mu\nu}(x) = 8\pi GM\int dp_0\int \frac{d^3\vec{p}}{(2\pi)^3}\frac{e^{i(-p_0x_0+\vec{p}.\vec{x})}}{-p_0^2+p^2+m^2}\delta(p_0)\left(\delta^0_\mu\delta^0_\nu + \frac{1}{3}\eta_{\mu\nu}\right), \tag{2.23}$$

and integrate over p_0 to obtain,

$$h_{\mu\nu}(x) = 8\pi GM\int \frac{d^3\vec{p}}{(2\pi)^3}\frac{e^{i\vec{p}.\vec{x}}}{p^2+m^2}\left(\delta^0_\mu\delta^0_\nu + \frac{1}{3}\eta_{\mu\nu}\right). \tag{2.24}$$

Finally, we solve (2.24) using contour integration and express the result in component form,

$$h_{00}(x) = \frac{16\pi GM}{3}\int \frac{d^3\vec{p}}{(2\pi)^3}\frac{e^{i\vec{p}.\vec{x}}}{p^2+m^2} = \frac{4}{3}\frac{GM}{r}e^{-mr},$$
$$h_{0i}(x) = 0,$$
$$h_{ij}(x) = \frac{8\pi GM}{3}\delta_{ij}\int \frac{d^3\vec{p}}{(2\pi)^3}\frac{e^{i\vec{p}.\vec{x}}}{p^2+m^2} = \frac{2}{3}\frac{GM}{r}e^{-mr}\delta_{\rm ij}. \tag{2.25}$$

We now use the results in (2.25) to identify the two gravitational potentials using the following decomposition of $h_{\mu\nu}$ [16],

$$\begin{aligned} h_{00}(x) &= -\phi(r), \\ h_{ij}(x) &= -\psi(r), \end{aligned} \tag{2.26}$$

to yield,

$$\begin{aligned} \phi^{\mathrm{FP}}(r) &= -\frac{4}{3}\frac{GM}{r}e^{-mr}, \\ \psi^{\mathrm{FP}}(r) &= -\frac{2}{3}\frac{GM}{r}e^{-mr}. \end{aligned} \tag{2.27}$$

Whilst in the case of GR the result is the usual Newtonian gravitational potentials,

$$\begin{aligned} \phi^{\mathrm{GR}}(r) &= -\frac{GM}{r}, \\ \psi^{\mathrm{GR}}(r) &= -\frac{GM}{r}. \end{aligned} \tag{2.28}$$

We can also look at the bending angle of a light ray around a massive object with impact parameter given by b. As $\psi(r) = \gamma\phi(r)$, where γ is a constant referred to as the PPN parameter [92], and $\phi(r) = -k/r$ [90], where $k = GM$ is a constant, the deflection angle can be written as,

$$\delta\theta = \frac{2k}{b}(1+\gamma). \tag{2.29}$$

We now are in a position to exhibit the vDVZ discontinuity. Taking the solutions in Fierz-Pauli massive gravity (2.27) and applying the massless limit $m \to 0$ yields,

$$\begin{aligned} \phi^{\mathrm{FP}}(r) &= -\frac{4}{3}\frac{GM}{r}, \\ \psi^{\mathrm{FP}}(r) &= -\frac{2}{3}\frac{GM}{r}. \end{aligned} \tag{2.30}$$

We can immediately see here that the massless limit of Fierz-Pauli massive gravity does not recover the result of GR (2.28). However, the light bending angle is coherent with the result in GR.

$$\delta\theta^{\mathrm{FP}} = \delta\theta^{\mathrm{GR}} = \frac{4GM}{b}. \tag{2.31}$$

One should note here, however, that by rescaling $G \to 3/4G$ in (2.30) the same Newtonian potential can be recovered as in GR, but this modifies the light bending angle by 25

percent. This result is precisely the vDVZ discontinuity discovered by Van dam, Veltman and Zakharov [83, 84]. To see how well constrained the light bending angle is, we can re-write (2.31) as,

$$\delta\theta = \left(\frac{1+\gamma_{\rm PPN}}{2}\right)\frac{4GM}{b}, \tag{2.32}$$

where $\gamma_{\rm PPN}$ is known as the Eddington light bending parameter, which has been introduced to parameterise deviations away from GR and has been constrained to be $\gamma_{\rm PPN} < 10^{-5}$ by the Cassini probe. This implies that the maximum modification to the Newton constant can be at the 10^{-5} level, therefore completely ruling out $\mathcal{O}(1)$ modifications.

Due to the degeneracy from being able to rescale the gravitational constant to obtain the same Newtonian potential, another observation is required to falsify FP massive gravity. For example, one could calculate the prediction for the orbital period of the moon using Newton's third law,

$$T^2 \propto \frac{a^3}{GM}, \tag{2.33}$$

where T is the orbital period and a is the semi-major axis of the orbit. Rescaling G to obtain the same Newtonian potential will modify the light bending angle, whilst keeping the orbital period the same. However, not rescaling G will modify the lunar period. So, using a combination of these probes FP massive gravity can be ruled out.

Inspecting the form of the action (2.7) and taking $m = 0$ results in simply linearised GR and shows no inconsistency, so it is peculiar how at the level of the gravitational potentials we are witnessing $\mathcal{O}(1)$ departures from GR when taking the massless limit. The key to understanding this is to realise that the massless limit of Fierz-Pauli massive gravity is not GR. To see this, the action given by (2.7) propagates 5 degrees of freedom as expected from a healthy theory of a massive spin-2 field, and breaks the 4D diffeomorphism invariance of GR. Taking the massless limit means we are losing information about the extra degrees of freedom present in Fierz-Pauli massive gravity, and simply sending $m \to 0$ in (2.7) does not yield a smooth limit to GR.

2.3 Stückelberg Trick

In the previous Section, we found that the massless limit of Fierz-Pauli massive gravity does not produce GR due to the information lost from the extra degrees of freedom. To understand the origin of the vDVZ discontinuity, we introduce new fields to restore gauge

symmetry, but seek to maintain the physical predictions of the original theory. This the essence of the Stückelberg trick, introduced by Ernst Stückelberg in 1957 when studying the properties of massive photons [93].

To begin, we recall the Fierz-Pauli action with minimal coupling to an external matter source (2.12),

$$S = \int d^4x \left(\mathscr{L}_{\rm GR} - \frac{1}{2} m^2 \left(\hat{h}_{\mu\nu}\hat{h}^{\mu\nu} - \hat{h}^2 \right) + \frac{1}{M_p} \hat{h}_{\mu\nu} T^{\mu\nu} \right), \tag{2.34}$$

where $M_p^{-2} = 8\pi G$ and $\mathscr{L}_{\rm GR}$ is shorthand for the linearised Einstein Hilbert action. Here we have also canonically normalised the spin-2 perturbation $h_{\mu\nu}$ as $h_{\mu\nu} = \frac{\hat{h}_{\mu\nu}}{M_p}$, which ensures the coefficient of the kinetic term is normalised correctly. Redefining the canonically normalised spin-2 field $\hat{h}_{\mu\nu}$ as,

$$\hat{h}_{\mu\nu} \to \hat{h}_{\mu\nu} + \partial_\mu A_\nu + \partial_\nu A_\mu, \tag{2.35}$$

and substituting into the action (2.34) yields,

$$\begin{aligned} S = \int d^4x \Big(& \mathscr{L}_{\rm GR} - \frac{1}{2} m^2 \left(\hat{h}_{\mu\nu}\hat{h}^{\mu\nu} - \hat{h}^2 \right) - \frac{1}{2} m^2 F^{\mu\nu} F_{\mu\nu} - 2m^2 \left(\hat{h}_{\mu\nu}\partial^\mu A^\nu - \hat{h}\partial^\mu A_\mu \right) \\ & + \frac{1}{M_p} \hat{h}_{\mu\nu} T^{\mu\nu} - \frac{2}{M_p} A_\mu \partial_\nu T^{\mu\nu} \Big). \end{aligned} \tag{2.36}$$

As (2.35) looks like a gauge transformation, analogous to (1.90), and as $\mathscr{L}_{\rm GR}$ is gauge invariant, this piece remains unaltered by (2.35). Here, $F_{\mu\nu} = \partial_\mu A_\nu - \partial_\nu A_\mu$ is the Faraday field strength tensor and appears in (2.36) as the $U(1)$ gauge invariant quantity $F_{\mu\nu}F^{\mu\nu}$. Canonically normalising A_μ in (2.36) as $A_\mu \to \frac{1}{m} A_\mu$ we obtain,

$$\begin{aligned} S = \int d^4x \Big(& \mathscr{L}_{\rm GR} - \frac{1}{2} m^2 \left(\hat{h}_{\mu\nu}\hat{h}^{\mu\nu} - \hat{h}^2 \right) - \frac{1}{2} F^{\mu\nu} F_{\mu\nu} - 2m \left(\hat{h}_{\mu\nu}\partial^\mu A^\nu - \hat{h}\partial^\mu A_\mu \right) \\ & + \frac{1}{M_p} \hat{h}_{\mu\nu} T^{\mu\nu} - \frac{2}{mM_p} A_\mu \partial_\nu T^{\mu\nu} \Big). \end{aligned} \tag{2.37}$$

Now, we consider a conserved source[3] and take the massless limit. We obtain an action describing a massless spin-2 and massless spin-1 field, which propagate a total of 4 degrees of freedom,

$$S = \int d^4x \Big(\mathscr{L}_{\rm GR} - \frac{1}{2} F^{\mu\nu} F_{\mu\nu} + \frac{1}{M_p} \hat{h}_{\mu\nu} T^{\mu\nu} \Big). \tag{2.38}$$

[3] If we do not consider a conserved source, then in the massless limit the spin-1 field becomes strongly coupled to the source.

This is already an improvement on the original formulation of Fierz-Pauli: by introducing an extra field in the form of a field redefinition we have gained an extra two degrees of freedom in the massless limit. However, we are still 1 short of the 5 expected from a massive spin-2 field. Naturally, the next step is to utilise again the Stückelberg trick, this time with the addition of a spin-0 field. Taking the action (2.37) and performing the field redefinition,

$$A_\mu \to A_\mu + \frac{1}{m}\partial_\mu \phi, \tag{2.39}$$

results in,

$$\begin{aligned} S = \int d^4x \Big(\mathscr{L}_{\rm GR} &- \frac{1}{2}m^2\left(\hat{h}_{\mu\nu}\hat{h}^{\mu\nu} - \hat{h}^2\right) - \frac{1}{2}F^{\mu\nu}F_{\mu\nu} \\ &- 2m\left(\hat{h}_{\mu\nu}\partial^\mu A^\nu - \hat{h}\partial^\mu A_\mu\right) - 2\left(\hat{h}_{\mu\nu}\partial^\mu\partial^\nu\phi - \hat{h}\partial_\mu\partial^\mu\phi\right) \\ &- \frac{2}{mM_p}A_\mu\partial_\nu T^{\mu\nu} + \frac{2}{m^2M_p}\phi\partial_\mu\partial_\nu T^{\mu\nu} + \frac{1}{M_p}\hat{h}_{\mu\nu}T_{\mu\nu}. \end{aligned} \tag{2.40}$$

Like in the previous case, we take the massless limit of (2.40) assuming a conserved source to yield,

$$S = \int d^4x \left(\mathscr{L}_{\rm GR} - \frac{1}{2}F^{\mu\nu}F_{\mu\nu} - 2\left(\hat{h}_{\mu\nu}\partial^\mu\partial^\nu\phi - \hat{h}\partial_\mu\partial^\mu\phi\right) + \frac{1}{M_p}h_{\mu\nu}T^{\mu\nu} \right). \tag{2.41}$$

The action (2.41) describes a massless spin-2, massless spin-1 and massless spin-0 field, thus the theory represented propagates 5 degrees of freedom. The vector is completely decoupled from the tensor and scalar, whilst the latter two are mixed together. To disentangle the mixing between the scalar and tensor modes, we perform a conformal transformation at the expense of the non-minimal coupling to the energy-momentum tensor [90],

$$\hat{h}_{\mu\nu} = \bar{h}_{\mu\nu} + \pi\eta_{\mu\nu}. \tag{2.42}$$

The transformation to the gauge invariant GR piece is,

$$\mathscr{L}_{\rm GR}(h) = \mathscr{L}_{\rm GR}(\bar{h}) + 2\left(\partial_\lambda\bar{h}\partial^\lambda\pi - \partial^\mu\bar{h}_{\mu\nu}\partial^\nu\pi + \frac{3}{2}\partial_\lambda\pi\partial^\lambda\pi \right), \tag{2.43}$$

which inserted into (2.41) along with (2.42), setting $\pi = \phi$ and integrating by parts yields,

$$S = \int d^4x \left(\mathscr{L}_{\rm GR}(\bar{h}) - \frac{1}{2}F^{\mu\nu}F_{\mu\nu} - 3\partial_\lambda\phi\partial^\lambda\phi + \frac{1}{M_p}\bar{h}_{\mu\nu}T^{\mu\nu} + \frac{1}{M_p}\phi T \right). \tag{2.44}$$

Upon rescaling $A_\mu \to 1/\sqrt{2}A_\mu$ and $\phi \to 1/\sqrt{6}\phi$ to obtain the correct factors in front of the kinetic terms we finally obtain,

$$S = \int d^4x \left(\mathscr{L}_{\rm GR}(\bar{h}) - \frac{1}{4}F^{\mu\nu}F_{\mu\nu} - \frac{1}{2}\partial_\lambda\phi\partial^\lambda\phi + \frac{1}{M_p}\bar{h}_{\mu\nu}T^{\mu\nu} + \frac{1}{\sqrt{6}M_P}\phi T \right). \tag{2.45}$$

Here we have exposed the origin of the vDVZ discontinuity. In the massless limit of Fierz-Pauli massive gravity, the scalar ϕ remains coupled to energy momentum. The conclusion here is that the massless limit of Fierz-Pauli massive gravity does not correspond to GR, but a scalar tensor theory non-minimally coupled to energy momentum. From (2.45) it is also clear why for light bending the result is continuous in the massless limit, as the trace of energy momentum for a photon vanishes as $T = 0$ [4] but the metric potentials show an $\mathscr{O}(1)$ deviation from GR.

2.4 Non-linear massive gravity

We learned from the previous Section that in the massless limit of Fierz-Pauli massive gravity, solar system tests are violated and GR is not recovered. Arkady Vainshtein remedied this by realising that the vDVZ discontinuity was in fact an artefact of the linear theory [94], and by extending Fierz-Pauli to a non-linear theory, continuity with GR was obtained in the massless limit. The key concept here is identifying the scale at which the linear theory breaks down, which corresponds to a regime in which the theory becomes non-linear. The Vainshtein mechanism allows the smooth recovery of GR on solar system scales. Before we discuss the Vainshtein mechanism, we first address the concept of non-linearities in GR.

Being a non-linear theory, GR will also have a certain scale where the linear approximation is no longer applicable to describe gravitational interactions, and non-linear effects have to be included. To identify this scale in GR, we schematically expand the Einstein-Hilbert action to include non-linear terms with at most 2 derivatives,

$$S^{NL}_{EH} = \int d^4x \; \partial^2\hat{h}^2 + \frac{1}{M_p}\partial^2\hat{h}^3 + \frac{1}{M_P^2}\partial^2\hat{h}^4 + ... + \frac{1}{M_P^n}\partial^2\hat{h}^{n+2}, \tag{2.48}$$

[4] To see this, the stress tensor for a massless photon in a spacetime described by the metric $g_{\mu\nu}$ is

$$T^{\mu\nu} = F^{\mu\alpha}F^{\nu}_{\alpha} - \frac{1}{4}g^{\mu\nu}F_{\alpha\beta}F^{\alpha\beta}. \tag{2.46}$$

Tracing results in,

$$T = F^{\mu\alpha}F_{\mu\alpha} - \delta^\mu_\mu\frac{1}{4}F^{\alpha\beta}F_{\alpha\beta} = 0. \tag{2.47}$$

This can also be seen from the fact the equation of state of radiation is $w_R = 1/3$.

with $\hat{h}$ representing the canonically normalised field as in Section 2.3. Recalling the linear field profile for $\hat{h}$ around a massive body,

$$\hat{h} \sim \frac{M}{M_p r}, \tag{2.49}$$

and from (2.48) we have that the non-linear terms are suppressed with respect to the linear terms by the factor,

$$\frac{\frac{1}{M_p}\partial^2 \hat{h}^3}{\partial^2 \hat{h}^2} \sim \frac{\hat{h}}{M_p}. \tag{2.50}$$

Using (2.49) and the result above, we obtain that the distance with which the non-linear terms begin to dominate is $r_{NL} \sim M/M_p^2$ which roughly corresponds to the Schwarzschild radius r_s of a massive body, which is given by $r_s = 2GM$ [95, 96]. Working this out for the sun we obtain $r_s \sim 3$km. This means that we can trust the linear approximation of GR at distances $r > 3$km away from solar mass objects, and only at distances $r \sim 3$km we need to consider the non-linear effects. We can still do computations and make predictions below the Schwarzschild radius, we just need to consider non-linear effects. It is only when we hit the cutoff scale that we can no longer trust the results of GR. To find the cut-off scale, consider a $2 \to 2$ scattering of two gravitons [90] at energy scale E, the amplitude $\mathscr{A}$ for the scattering is $\mathscr{A} \propto \left(\frac{E}{M_p}\right)^2$. At energy scales $E \sim M_p$, unitarity is broken and we lose all predictability of the system. Therefore, from this we conclude that GR has a cutoff of M_p.

Now, we want to find the radius at which non-linear terms in massive gravity start to dominate. To do this, we follow the procedure of Vainshtein [90, 94] and consider a minimal non-linear model of massive gravity where we have full non-linear Einstein gravity but keep the linear Fierz-Pauli mass term.

$$S = \frac{M_p^2}{2}\int d^4x \left[\left(\sqrt{-g}R\right) - \sqrt{-g^{(0)}}\frac{m^2}{4} g^{(0)\,\mu\alpha} g^{(0)\,\nu\beta}\left(h_{\mu\nu}h_{\alpha\beta} - h_{\mu\alpha}h_{\nu\beta}\right)\right], \tag{2.51}$$

where $g_{\mu\nu} = g^{(0)}_{\mu\nu} + h_{\mu\nu}$ is the full metric and $g^{(0)}_{\mu\nu}$ is a background fiducial metric. Here, $g^{(0)}_{\mu\nu}$ is required to create non-trivial interactions as constructing scalar quantites out of 1 metric simply yields a cosmological constant $g_{\mu\nu}g^{\mu\nu} = $ c. To derive the radius at which non-linearities begin to dominate, we work at the level of the equations of motion. Varying (2.51) with respect to $g^{\mu\nu}$ yields,

$$\sqrt{-g}G_{\mu\nu} + \sqrt{-g^{(0)}}\frac{m^2}{2}\left(g^{(0)}_{\mu\alpha}g^{(0}_{\nu\beta}h^{\alpha\beta} - g^{(0)}_{\alpha\beta}h^{\alpha\beta}g^{(0)}_{\mu\nu}\right) = 0. \tag{2.52}$$

We assume a static spherically symmetric source and a spherically symmetric ansatz for g,

$$g_{\mu\nu}dx^\mu dx^\nu = -B(r)dt^2 + C(r)dr^2 + A(r)r^2 d\Omega^2, \tag{2.53}$$

where $d\Omega^2$ is the metric on a 2-sphere. Furthermore, we consider a flat fiducial metric,

$$g^{(0)}_{\mu\nu}dx^\mu dx^\nu = -dt^2 + dr^2 + r^2 d\Omega^2. \tag{2.54}$$

Substituting the above ansatz into the equations of motion (2.52), and solving the equations recursively by expanding the functions in (2.53) as $A \to 1 + \epsilon A_1 + \epsilon^2 A_2 + ...$ we obtain,

$$\begin{aligned} A(r) - 1 &= \frac{4}{3}\frac{GM}{4\pi m^2 r^3}\left(1 - 4\frac{GM}{m^4 r^5} + ...\right) \\ B(r) - 1 &= -\frac{8}{3}\frac{GM}{r}\left(1 - \frac{1}{6}\frac{GM}{m^4 r^5} + ...\right) \\ C(r) - 1 &= -\frac{8}{3}\frac{GM}{m^2 r^3}\left(1 - 14\frac{GM}{m^4 r^5} + ...\right). \end{aligned} \tag{2.55}$$

The solutions in (2.55) are an expansion in the following quantity

$$\sim \left(\frac{R_V}{r}\right)^5 \tag{2.56}$$

where we define the *Vainshtein radius* as

$$R_V = \left(\frac{GM}{m^4}\right)^{\frac{1}{5}}. \tag{2.57}$$

The Vainshtein radius is the radius at which the linear theory becomes no longer applicable, and higher order interactions must be considered. As we send $m \to 0$, R_V grows and the regime in which we can trust the solution is reduced to zero. Vainshtein therefore concluded that the linear theory cannot make predictions below R_V as the perturbative expansion breaks down, and that the solutions to the full non-linear equations may show a smooth limit to GR [94, 97, 98]. Analogous to the case of GR, we can estimate the radius at which linear perturbation theory breaks down for a solar mass object. We have to specify the parameter m, and for cosmological purposes it is natural to assume $m \sim H_0$. Plugging into (2.57) we obtain that $R_V \sim 10^{18}$km, which is approximately the size of the Milky Way galaxy. Therefore we cannot use linear Fierz-Pauli massive gravity to describe light bending or other solar system tests, we have to use the full non-linear theory. For the moment, we do not comment on the cutoff of non-linear massive gravity, this will become apparent in the next Section.

2.5 Higher order interactions

As we found for the linear case, adding a Lorentz-invariant non-derivative term to the Einstein-Hilbert action required the addition of a non-dynamical reference metric. In this section, we briefly summarise the development of the unique, non-linear theory of massive gravity starting from a general potential. A candidate non-linear theory of massive gravity takes the form,

$$S = \frac{M_p^2}{2}\int d^4x\left[\sqrt{-g}R - \sqrt{-g}\frac{1}{4}m^2U(g^{(0)},h)\right], \tag{2.58}$$

where $g_{\mu\nu} = g^{(0)}_{\mu\nu} + h_{\mu\nu}$ and $U(g^{(0)},h) = U_2(g^{(0)},h) + U_3(g^{(0)},h) + U_4(g^{(0)},h) + ... +$ where the individual terms are given by,

$$\begin{aligned}
U_2(g^{(0)},h) &= [h^2] - [h]^2 \\
U_3(g^{(0)},h) &= c_1[h^3] + c_2[h^2][h] + c_3[h]^3 \\
U_4(g^{(0)},h) &= d_1[h^4] + d_2[h^3][h] + d_3[h^2][h]^2 + d_4[h^2]^2 + d_5[h]^4 \\
&\quad + \sum_{n=5}^{\infty} U_n(g^{(0)},h).
\end{aligned} \tag{2.59}$$

In (2.59) the square brackets denote trace operation with respect to the background metric, i.e.

$$[h] = g^{(0)\mu\nu}h_{\mu\nu},\ [h^2] = g^{(0)\mu\alpha}h_{\alpha\beta}g^{(0)\beta\nu}h_{\mu\nu} \tag{2.60}$$

etc.. and the minus sign in U_2 has been chosen to match Fierz-Pauli [82] at the linear level, so at least at the linear level there are no ghost degrees of freedom.

As we have seen, utilising the Stückelberg trick allows us to restore diffeomorphism invariance at the expense of introducing new degrees of freedom. We choose to let the full metric $g_{\mu\nu}$ transform covariantly, and introduce the Stückelberg fields via the fiducial metric as in [86, 90],

$$H_{\mu\nu}(x) = g_{\mu\nu}(x) - g^{(0)}_{AB}(\phi(x))\partial_\mu\phi^A\partial_\nu\phi^B, \tag{2.61}$$

where ϕ^A are the 4 Stückelberg fields. Substituting (2.61) into the action (2.58) and setting $\phi^A = x^A$, where x^A represent the spacetime coordinates, we obtain the original Fierz-Pauli action at the linear level. This choice is known as the *unitary gauge*.

As before, we are interested in separating out the different helicities present in the theory, so we write $\phi^\alpha = x^\alpha - \pi^\alpha$. We also change the field space index to a greek index as

π^μ will eventually transform as a Lorentz 4-vector [99, 100]. We therefore expand (2.61) as

$$H_{\mu\nu} = h_{\mu\nu} + g^{(0)}_{\mu\beta}\partial_\nu\pi^\beta + g^{(0)}_{\alpha\nu}\partial_\mu\pi^\alpha - g^{(0)}_{\alpha\beta}\partial_\mu\pi^\alpha\partial_\nu\pi^\beta + \mathcal{G}(\partial g^{(0)}), \tag{2.62}$$

where $h_{\mu\nu} = g_{\mu\nu} - g^{(0)}_{\mu\nu}$ and $\mathcal{G}(\partial g^{(0)})$ is schematic for derivatives of the fiducial metric. Specialising to the case of a flat fiducial metric, and further expanding the 4-vector π^α as $\pi^\alpha \to \pi^\alpha + \partial^\alpha\phi$ to extract the longitudinal mode yields,

$$H_{\mu\nu} = h_{\mu\nu} + \partial_\mu\pi_\nu + \partial_\nu\pi_\mu + 2\partial_\mu\partial_\nu\phi - \partial_\mu\pi^\alpha\partial_\nu\pi_\alpha - \partial_\mu\pi^\alpha\partial_\nu\partial_\alpha\phi - \partial_\mu\partial^\alpha\phi\partial_\nu\pi_\alpha - \partial_\mu\partial^\alpha\phi\partial_\nu\partial_\alpha\phi. \tag{2.63}$$

After substituting (2.63) into the action (2.58) as in [90, 91, 100] and canonically normalising the fields as,

$$\hat{h}_{\mu\nu} = \frac{1}{2}M_p h_{\mu\nu}, \quad \hat{\pi}^\mu = \frac{1}{2}mM_p\pi^\mu, \quad \hat{\phi} = \frac{1}{2}m^2M_p\phi, \tag{2.64}$$

we obtain a plethora of interaction terms between the different helicity modes. A generic interaction term takes the form [90, 100, 101],

$$m^2M_p^2\sqrt{-g}U \supset m^2M_p^2 h^{n_h}(\partial\pi)^{n_\pi}\left(\partial^2\phi\right)^{n_\phi} \sim \Lambda_\lambda^{4-n_h-2n_\pi-3n_\phi}\hat{h}^{n_h}(\partial\hat{\pi})^{n_\pi}\left(\partial^2\hat{\phi}\right)^{n_\phi}, \tag{2.65}$$

where

$$\Lambda_\lambda = \left(M_p m^{\lambda-1}\right)^{\frac{1}{\lambda}}, \quad \lambda = \frac{3n_\phi + 2n_\pi + n_h - 4}{n_\phi + n_\pi + n_h - 2}. \tag{2.66}$$

In (2.65) $\hat{h}$ always appears with no derivatives, π with 1 derivative and ϕ with 2 derivatives. Here Λ_λ is the energy scale corresponding to the outlined interaction. As $m \ll M_P$, the smaller the λ the higher the energy scale the interaction appears at. Furthermore, $n_h + n_\pi + n_\phi \geq 3$. The term suppressed by the smallest scale will be the most important at low energies. For the system (2.65), the term suppressed by the lowest scale is that of the cubic scalar which contributes as,

$$\sim (\partial^2\hat{\phi})^3, \tag{2.67}$$

where $n_h = 0$, $n_\pi = 0$, $n_\phi = 3$. Therefore, the corresponding energy scale associated with this interaction is,

$$\Lambda_5 = \left(M_p m^4\right)^{\frac{1}{5}}, \tag{2.68}$$

which is the strong coupling scale of the theory, or in other words, the scale at which the theory becomes non-predictive. In this non-linear theory, as with the Vainshtein radius,

we can estimate the energy scale Λ_5 for a solar mass object and a Hubble scale graviton mass. We find that $\Lambda_5 \sim 10^{-11}\text{km}^{-1}$. This is an unnacceptably low scale, and renders this theory uninteresting for cosmological purposes. To make matters worse, as was found by Boulware and Deser [85], the theory described by the action (2.58) with generic coefficients propagates an extra scalar mode which was dubbed the Boulware-Deser (BD) ghost. However, efforts to raise the strong coupling scale and exorcise the BD ghost were made at the start of this century and the next section describes these developments.

2.6 dRGT massive gravity

As we saw in the last section, generic non-linear theories of massive gravity have a very low cutoff and propagate a 6th degree of freedom which corresponds to the BD ghost. We recall the generic non-linear potential $U(g,h) = U_2(g,h) + U_3(g,h) + U_4(g,h) + U_5(g,h) +$ ....+, where the individual terms are given by,

$$\begin{aligned}
U_2(g,h) &= [h^2] - [h]^2 \\
U_3(g,h) &= c_1[h^3] + c_2[h^2][h] + c_3[h]^3 \\
U_4(g,h) &= d_1[h^4] + d_2[h^3][h] + d_3[h^2][h]^2 + d_4[h^2]^2 + d_5[h]^4 \\
U_5(g,h) &= f_1[h^5] + f_2[h^4][h] + f_3[h^3][h]^2 + f_4[h^3][h^2] + f_5[h^2]^2[h] + f_6[h]^2[h]^3 + f_7[h]^5 \\
&+ \sum_{n=6}^{\infty} U_n(g,h),
\end{aligned} \tag{2.69}$$

where we included the explicit 5th order term for illustrative purposes. This time we choose to write the interaction potential as a function of the full metric $g_{\mu\nu}$ and $h_{\mu\nu}$. This means indices are raised with respect to the full metric and the equivalence between the two ways of writing the potential can be seen by expanding the inverse metric as,

$$g^{\mu\nu} = g^{(0)\mu\nu} - h^{\mu\nu} + h^{\mu\lambda}h^{\nu}_{\lambda} + \mathcal{O}(h^3), \tag{2.70}$$

and the matrix determinant as,

$$\sqrt{-g} = \sqrt{-g^{(0)}}\left[1 + \frac{1}{2}[h] - \frac{1}{4}\left([h^2] - \frac{1}{2}[h]^2\right) + \mathcal{O}(h^3)\right]. \tag{2.71}$$

Next we recall the culprit interaction for the lowest energy scale Λ_5, which was the cubic scalar self interaction

$$\frac{1}{\Lambda_5^5}\left(\partial^2\hat{\phi}\right)^3, \tag{2.72}$$

and we identify the next lowest scale $\Lambda_4 = \left(M_p m^3\right)^{\frac{1}{4}}$, which appears in the interactions,

$$\frac{1}{\Lambda_4^8}(\partial^2\hat{\phi})^4, \quad \frac{1}{\Lambda_4^4}(\partial\hat{\pi})^2\left(\partial^2\hat{\phi}\right)^2. \tag{2.73}$$

The next scale is $\Lambda_3 = (M_p m^3)^{\frac{1}{3}}$ and is only carried by the interactions,

$$\frac{1}{\Lambda_3^{3(n-1)}}\hat{h}\left(\partial^2\hat{\phi}\right)^n, \quad \frac{1}{\Lambda_3^{3n}}(\partial\hat{\pi})^2\left(\partial^2\hat{\phi}\right)^n. \tag{2.74}$$

It was shown in [86, 102] that arranging the scalar self interactions into total derivatives, the cutoff scale could be raised to Λ_3. However in [103] it was argued that any massive gravity theory with cutoff of Λ_3 would propagate a ghost, but a sign error in [103] proved this to be a wrong conclusion.

To raise the cutoff scale, it is sufficient to consider only scalar interactions, so (2.63) becomes simply,

$$H_{\mu\nu} = 2\partial_\mu\partial_\nu\phi - \partial_\mu\partial^\alpha\phi\partial_\nu\partial_\alpha\phi, \tag{2.75}$$

and by defining $\Pi_{\mu\nu} = \partial_\mu\partial_\nu\phi$ (2.75) it becomes,

$$H_{\mu\nu} = 2\Pi_{\mu\nu} - \Pi^\alpha_\mu\Pi_{\nu\alpha}. \tag{2.76}$$

We can construct total derivative combinations of the matrix Π up to quartic order [87, 101, 104]

$$\begin{aligned}
\mathscr{L}_0^{\rm der} &= 1 \\
\mathscr{L}_1^{\rm der} &= [\Pi] \\
\mathscr{L}_2^{\rm der} &= [\Pi]^2 - [\Pi^2] \\
\mathscr{L}_3^{\rm der} &= [\Pi]^3 - 3[\Pi][\Pi^2] + 2[\Pi^3] \\
\mathscr{L}_4^{\rm der} &= [\Pi]^4 - 6[\Pi^2][\Pi]^2 + 8[\Pi^3][\Pi] + 3[\Pi^2]^2 - 6[\Pi^4].
\end{aligned} \tag{2.77}$$

In fact, the total derivative combinations vanish for $\mathscr{L}^{\rm der}_{n>4}$. Defining a generic 4×4 matrix S, the determinant expansion of $\det(I_4 + S) = \sum_{n=0}^4 \mathscr{U}_n(S)$ can be written in terms of the

elementary symmetric polynomials $\mathscr{U}_n(S)$,

$$\begin{aligned}
\mathscr{U}(S) &= 1 \\
\mathscr{U}_1(S) &= [S] \\
\mathscr{U}_2(S) &= \frac{1}{2!}\left([S]^2 - [S^2]\right) \\
\mathscr{U}_3(S) &= \frac{1}{3!}\left([S]^3 - 2[S][S]^2 + 2[S^3]\right) \\
\mathscr{U}_4(S) &= \frac{1}{4!}\left([S]^4 - 6[S^2][S]^2 + 8[S^3][S] - 6[S]^4\right) \\
\mathscr{U}_{n>4}(S) &= 0.
\end{aligned} \tag{2.78}$$

By using the result in (2.78), we deduce that $\mathscr{U}_n(S) = n!\mathscr{L}_n^{\rm der}(S)$.

By tuning the coefficients in (2.69) ensuring that the dangerous interactions suppressed by the scales Λ_5 and Λ_4 arrange into the total derivative combinations (2.77), the lowest scale at which interactions arise can be promoted to Λ_3. The authors in [87, 104] performed this analysis in the decoupling limit[5], order by order, and removed the dangerous interactions characterised by $\left(\partial^2\hat{\phi}\right)^n$.

Finally, the last step in the construction of dRGT massive gravity came when the infinite set of interactions in (2.69) were re-summed into an action with a finite number of terms [88]. First we define a new tensor $\mathscr{K}$ as,

$$\mathscr{K}^\mu_\nu = \delta^\mu_\nu - \sqrt{\delta^\mu_\nu - H^\mu_\nu} = \sum_{n=1}^{\infty} d_n \left(H^n\right)^\mu_\nu, \tag{2.79}$$

where $H^\mu_\nu = g^{\mu\alpha}H_{\alpha\nu}$, $(H^n)^\mu_\nu = H^\mu_{\lambda_1}H^{\lambda_1}_{\lambda_2}..H^{\lambda_{n-1}}_\nu$ and

$$d_n = -\frac{(2n)!}{(1-2n)(n!)^2 4^n}. \tag{2.80}$$

It was shown that in the decoupling limit, this time keeping the scale Λ_3 fixed, the $\mathscr{K}$ tensor reduces to

$$\mathscr{K}^{DL}_{\mu\nu}\big|_{h_{\mu\nu}=0} = \partial_\mu\partial_\nu\phi. \tag{2.81}$$

To see this, we write the relation (2.79) as,

$$\begin{aligned}
\mathscr{K}^{DL}_{\mu\nu}\big|_{h_{\mu\nu}=0} &= g_{\mu\nu} - \sqrt{\eta_{\alpha\beta}\partial_\mu\pi^\alpha\partial_\nu\pi^\beta} \\
&\implies g_{\mu\nu} - \sqrt{\eta_{\mu\nu} - 2\Pi_{\mu\nu} + \Pi_{\mu\beta}\Pi^\beta_\nu},
\end{aligned} \tag{2.82}$$

[5]The decoupling limit is used to isolate the leading order interactions in the theory. For this purpose, it is described by $M_p \to \infty$, $m \to 0$, $\hat{h}, \hat{\phi}$ and the scale Λ_5 fixed.

which after expanding the square root for small Π yields precisely to (2.81)[6]. By replacing the tensor $\mathscr{K}^{DL}$ into (2.69), the graviton potential can be written as,

$$W(g,\mathscr{K}) = [\mathscr{K}^2] - [\mathscr{K}]^2 + \tilde{c}_1[\mathscr{K}^3] + \tilde{c}_2[\mathscr{K}^2][\mathscr{K}] + ...+, \tag{2.83}$$

and from the structure of (2.81) it is clear that the structure is that of in (2.77), so $W(g,\Pi) = W(g,\mathscr{K})$. The key point here is that in 4 dimensions, the potential can be written as,

$$W(g,\mathscr{K}) = \sum_{n=0}^{4} \frac{\alpha_n}{n!} \mathscr{L}_n^{\text{der}}(\mathscr{K}), \tag{2.84}$$

where the sum truncates at $n = 4$ as the total derivative combinations vanish for $n > D$, as in (2.78). Here α_n are generic coefficients which can be related to the original coefficients in (2.69). Since we want to describe the full non-linear theory, including all interactions including the vector, we move away from the decoupling limit and write down the full non-linear action for massive gravity [87, 88, 101],

$$S = \frac{M_p^2}{2} \int d^4x\sqrt{-g}\left(R + 2m^2 \sum_{n=0}^{4} \alpha_n \mathscr{U}_n(\mathscr{K})\right), \tag{2.85}$$

where $\mathscr{U}_n$ are the dRGT potential terms constructed in such a way as to not excite the BD ghost and to be total derivatives in the decoupling limit.

We can rewrite $\mathscr{K}$ by remembering that $H_{\mu\nu}$ is defined, in the case of a flat field space metric as,

$$H_{\mu\nu} = g_{\mu\nu} - \eta_{\alpha\beta}\partial_\mu\phi^\alpha\partial_\nu\phi^\beta. \tag{2.86}$$

Acting on (2.86) with the inverse metric $g^{\mu\nu}$ yields,

$$H^\mu_\nu = \delta^\mu_\nu - g^{\gamma\mu}\eta_{\alpha\beta}\partial_\gamma\phi^\alpha\partial_\nu\phi^\beta \equiv \delta^\mu_\nu - g^{\gamma\mu}f_{\gamma\nu}, \tag{2.87}$$

which implies,

$$\delta^\mu_\nu - H^\mu_\nu = g^{\gamma\mu}f_{\gamma\nu}, \tag{2.88}$$

where $f_{\mu\nu}$ is defined as

$$f_{\mu\nu} = \eta_{ab}\partial_\mu\phi^a\partial_\nu\phi^b. \tag{2.89}$$

[6]Note that this holds only around Minkowski backgrounds.

Using this result, we can express the square root in (2.79) as the matrix product of the full metric g and the background fiducial metric f,

$$\mathcal{K}^{\mu}_{\nu} = \delta^{\mu}_{\nu} - \left(\sqrt{g^{-1}f}\right)^{\mu}_{\nu}. \tag{2.90}$$

There is also an equivalent formulation of the dRGT theory in terms of β_n parameters [105],

$$S = \frac{M_p^2}{2}\int d^4x\sqrt{-g}\left(R - 2m^2\sum_{n=0}^{3}\frac{\beta_n}{n!}\mathcal{U}_n(g^{-1}f)\right), \tag{2.91}$$

in which the β parameters are related to the α parameters via [101, 106],

$$\beta_n = (-1)^{n+1}\sum_{k=0}^{4}\frac{n!}{(n-k)!}\alpha_n. \tag{2.92}$$

We finish this Section by commenting on the structure of the action given by (2.85). The term proportional to $\alpha_0\mathcal{U}_0$ is simply a cosmological constant and $\alpha_1\mathcal{U}_1$ corresponds to a linear term whose existence does not allow Minkowksi space as a solution. The higher order interactions $\mathcal{U}_{3,4}$ are allowed if and only if $\mathcal{U}_2$ is present, and any deviation from the structure of dRGT would be pathological.

dRGT massive gravity is a ghost free theory of massive gravity [107–111] with a UV cutoff scale of Λ_3 and a Vainshtein screening mechanism to allow the recovery of GR on local scales, see [112] for full details on the Vainshtein mechanism in the decoupling limit of dRGT. The Vainshtein radius around a point mass M in the Λ_3 decoupling limit is given by,

$$R_V^3 = \left(\frac{M}{\Lambda_3^3 M_p}\right), \tag{2.93}$$

which for a Hubble scale graviton mass and solar mass object is roughly $R_V \sim \mathcal{O}(\text{pc})$. An example of how the Vainshtein mechanism works in the cubic galileon theory, which arises in the decoupling limit of dRGT massive gravity, is outlined in Appendix A. Furthermore, illustrated in Fig.2.1 is a schematic picture of the different length scales in dRGT away from a body of mass M, which is inspired off a diagram in [90].

Now, we turn our attention towards the cosmological implications of dRGT massive gravity, and investigate the viability and phenomenology of cosmologies in the dRGT framework.

2.7 Cosmology of dRGT

Shortly after the construction of the ghost free theory of massive gravity, it was shown that the gravitational mass term can invoke an energy density which exerts a negative pressure and drives the accelerated expansion of the universe via the helicity-0 mode of the graviton [113]. In this Section, we briefly review the attempts to find a stable cosmology in massive gravity. To begin the study of dRGT cosmology, we work with the action given by (2.85) and show the presence of open FLRW solutions at the background level [114, 115]. It was shown in [116] that cosmologies with a flat FLRW solution are not allowed due to the time evolution of the scale factor being forbidden. Furthermore, since Minkowski space cannot be put into a closed FLRW chart, no closed FLRW solutions exist either. Therefore, we seek the form of the open FLRW solution which was shown to be in agreement with ΛCDM [117]. In order to achieve an isotropic and homogeneous universe for both the physical and fiducial metric, we need $f_{\mu\nu}$ to have the same FLRW symmetries as $g_{\mu\nu}$ in the same coordinate system, since they are coupled via $g^{-1}f$. Note that we are considering homogeneous and isotropic solutions as the cosmological perturbations for a non FLRW case are very complicated [114, 116] and requires a full re-addressing of how to perform perturbative analysis. For a Minkowski field space metric the background fiducial metric is,

$$f_{\mu\nu} = \eta_{ab}\partial_\mu\phi^a\partial_\nu\phi^b, \tag{2.94}$$

and the unique field configuration compatible with these symmetries is

$$\begin{aligned}
\phi^0 &= f(t)\sqrt{1+\kappa(x^2+y^2+z^2)}\,,\\
\phi^1 &= f(t)\sqrt{\kappa}\,x\,,\\
\phi^2 &= f(t)\sqrt{\kappa}\,y\,,\\
\phi^3 &= f(t)\sqrt{\kappa}\,z\,.
\end{aligned} \tag{2.95}$$

where $\kappa = |K| = -K$ is the absolute value of the negative constant curvature of the spatial slice. With this definition, the fiducial metric has the same form as an open FLRW solution [114]

$$f_{\mu\nu}dx^\mu dx^\nu = -\dot{f}(t)^2dt^2 + \kappa f(t)^2\Omega_{ij}dx^i dx^j\,, \tag{2.96}$$

where an overdot denotes time derivative and Ω_{ij} is the metric of the constant time hypersurfaces with constant negative curvature

$$\Omega_{ij}dx^i dx^j = dx^2 + dy^2 + dz^2 - \frac{\kappa(xdx+ydy+zdz)^2}{1+\kappa(x^2+y^2+z^2)}\,. \tag{2.97}$$

Our metric ansatz is then an open FLRW

$$g_{\mu\nu}dx^\mu dx^\nu = -N^2dt^2 + a(t)^2\Omega_{ij}dx^i dx^j\,. \tag{2.98}$$

We substitute the metric ansatz into the dRGT action, with $\alpha_0 = \alpha_1 = 0$ for now, and setting $\alpha_2 = 1$ yields to the background action,

$$S = \frac{M_p^2 V}{2}\int N\,dt\,a^3\left[-\frac{6\kappa}{a^2} - \frac{6\dot{a}^2}{a^2N^2} + 2m^2(U_2 + \alpha_3 U_3 + \alpha_4 U_4)\right], \tag{2.99}$$

where

$$\begin{aligned} U_2 &= 3\left(1-\frac{\sqrt{\kappa}f}{a}\right)\left(2-\frac{\sqrt{\kappa}f}{a}-\frac{\dot{f}}{N}\right),\\ U_3 &= \left(1-\frac{\sqrt{\kappa}f}{a}\right)^2\left(4-\frac{\sqrt{\kappa}f}{a}-\frac{3\dot{f}}{N}\right),\\ U_4 &= \left(1-\frac{\sqrt{\kappa}f}{a}\right)^3\left(1-\frac{\dot{f}}{N}\right). \end{aligned} \tag{2.100}$$

Varying (2.99) with respect to f we obtain the Stückelberg equation of motion which encodes all the information about the dynamics of the 4 Stückelberg fields,

$$\left(H-\frac{\sqrt{\kappa}}{a}\right)\left[(\xi-2)+(\xi-1)(\xi-4)\alpha_3+(\xi-1)^2\alpha_4\right] = 0, \tag{2.101}$$

where $\xi = \frac{f\sqrt{\kappa}}{a}$ is the ratio of the scale factors of the background and dynamical metrics respectively. The equation (2.101) has 2 branches of solutions. The first branch with solution,

$$H = \frac{\sqrt{\kappa}}{a}, \tag{2.102}$$

corresponds to an empty universe, or in other words the open chart of Minkowski space-time which is the same as the f-metric. It is uninteresting for cosmology as expansion is prohibited. The other branch arises from solving the following algebraic equation for ξ,

$$(\xi-2)+(\xi-1)(\xi-4)\alpha_3+(\xi-1)^2\alpha_4 = 0, \tag{2.103}$$

where with respect to (2.101) we have removed the trivial solution. The other two solutions are,

$$\xi^\pm = \frac{1+2\alpha_3+\alpha_4 \pm \sqrt{1+\alpha_3+\alpha_3^2-\alpha_4}}{\alpha_3+\alpha_4}. \tag{2.104}$$

In this branch, ξ is constant and exhibits self acceleration as the contribution from the graviton mass term to the Friedmann equation acts like a cosmological constant [114]. Note here that the above solutions do not exist in the limit $\kappa \to 0$, which is consistent with the result of no stable closed or flat FLRW solutions [114, 116]. It was shown that the solutions on the self-accelerating branch suffer from a non-linear instability [115, 118] as the kinetic terms vanish for the scalar and vector sectors at the level of the quadratic action for cosmological perturbations. The upshot of this is that the modes are infinitely strongly coupled and standard perturbative analysis cannot be performed.

The open FLRW can be generalised to include any choice for the field space metric which can be written in FLRW form in some coordinate system as in [119] via,

$$f_{\mu\nu} = -n^2(\varphi^0)\partial_\mu\varphi^0\partial_\nu\varphi^0 + \alpha^2(\varphi^0)\Omega_{ij}(\varphi^k)\partial_\mu\varphi^i\partial_\nu\varphi^j, \tag{2.105}$$

where φ^i represent Stückelberg fields which have undergone a change of variables with respect to the original ones. It was shown in [120] that this generalisation does not revive the BD ghost. Deriving the Stückelberg equation, 3 solutions are again found [115, 119]. The first can be written as,

$$aH = \alpha H_f, \tag{2.106}$$

where $H = \frac{\dot{a}}{aN}$ and $H_f = \frac{\dot{\alpha}}{\alpha n}$ are the Hubble rates for the physical and fiducial metric respectively. By choosing a maximally symmetric spacetime [120], the normal branch outlined in (2.106) can support a cosmological solution. However, in the case of a de-Sitter reference metric [121] the Higuchi ghost[7] is also present [122] and is unstable under linear perturbations [105, 123]. Choosing the form of the metric to be anti de-Sitter, the cosmology cannot sustain acceleration [125]. The other branch of solution has exactly the same structure as in (2.104) and can accommodate self-acceleration. However, this branch of solution suffers from the same non-linear instability [115, 119] as before so the solutions are unstable. With this result, we understand that all homogeneous and isotropic solutions in dRGT massive gravity are unstable and breaking some underlying assumptions about the theory are required to seek stable cosmologies.

Giving up isotropy and homogeneity, a stable ghost free anisotropic universe can be achieved with the presence of a late time attractor solution [126]. Furthermore, in the Stückelberg field space an inhomogeneous fiducial metric can be allowed [127–130].

[7]The Higuchi ghost is present when the Higuchi bound is violated. The Higuchi bound ensures the positivity of the kinetic term of the helicity-0 mode of the graviton. It was first studied by Higuchi considering de-Sitter backgrounds [122] but was generalised in [123, 124] to arbitrary flat FLRW spacetimes.

With this choice the Stückelberg fields are,

$$\phi^0 = f(t,r), \quad \phi^i = g(t,r)\frac{x^i}{r}, \tag{2.107}$$

which again results in an effective cosmological constant appearing in the Friedmann equation which then exhibits self-acceleration. However, it was shown that these solutions are also unstable [131] due to a ghost instability arising from an unbounded hamiltonian. The lack of stable cosmologies in massive gravity led some authors to consider extensions to dRGT and we briefly comment on some of them in the next Section.

2.8 Extensions to dRGT

The first extension to consider is mass-varying massive gravity (MVMG) [132, 133], where the free α parameters and the graviton mass parameter in the dRGT action are promoted to functions of a scalar field $\alpha \to \alpha(\psi)$ where ψ is a scalar field which appears with its own kinetic term. The action is modified in the following way,

$$S = \frac{M_p^2}{2}\int d^4x\sqrt{-g}\left[R + 2V(\psi)\sum_n \alpha_n(\psi)\mathcal{U}_n - \frac{1}{2}\left(\partial\psi\right)^2 - \tilde{V}(\psi)\right]. \tag{2.108}$$

In this model the graviton mass becomes a function of the background scalar field. The mass varying theory was shown to be stable under linear perturbations [133], but propagates 6 degrees of freedom. This model can approximate self-acceleration, but to get a cosmological constant requires the extra scalar to be slowly varying which almost approximates constant mass dRGT.

Another extension is the quasidilaton massive gravity [134], which introduces another scalar field but not in a way which promotes free parameters to functions. The scalar field σ, or the quasidilaton, is coupled to the fiducial metric via a conformal transformation. The quasidilaton can source the late time acceleration of the universe. The scalar field and Stückelberg fields satisfy the following transformation properties,

$$\sigma \to \sigma + \sigma_0, \quad \phi^a \to e^{-\sigma_0/M_p}\phi^a, \tag{2.109}$$

and with these definitions the building block tensor is modified to be,

$$\mathcal{K}^\mu_\nu = \delta^\mu_\nu - e^{-\sigma/M_p}\left(\sqrt{g^{-1}f}\right)^\mu_\nu. \tag{2.110}$$

Whilst there are flat self-accelerating solutions, it was shown that a ghost instability is always present in the theory [133, 135, 136]. The quasidilaton can be extended by adding derivative operators [137] and it was hoped a stable cosmology could be achieved with self-acceleration [138–141]; however it was shown that even in the extended theory there is an instability [142, 143].

So far we have only mentioned Lorentz invariant theories, but by breaking Lorentz invariance one can construct the minimal theory of massive gravity [144] which is a massive gravity theory that propagates 2 degrees of freedom. It was shown that this theory is pathology free [145] and can lead to self acceleration without the need of a cosmological constant or other dark energy fluid. There is also the minimal quasidilaton [146] with a Horndeski extension [147] and the resulting phenomenology has been studied in [148, 149]. The main result of these extensions is that they are stable with respect to the Lorentz invariant ones, at the price of abandoning Lorentz invariance. The minimal theory also has interesting implications for the early universe, as blue tilted primordial gravitational waves can be generated [150] which could potentially be detected by interferometers [151–154]. Other versions of Lorentz breaking massive gravity are detailed in [155–158] and references therein.

2.9 Quantum corrections and mass bounds

We end this chapter by mentioning quantum corrections and the observational bounds on the graviton mass. Quantum corrections to the graviton mass scale as $m^2 \to m^2 + \mathcal{O}(1)m^2$ [55, 159]. Therefore a small mass is technically natural as the corrections are proportional to the mass itself, unlike the cosmological constant. So if the graviton mass is small, it remains small.

A plethora of observations which operate at different scales which constrain the mass of different helicities of the graviton are outlined in [160]. The most stringent bound on the scalar mass is from Lunar laser ranging [161], which interestingly places an upper bound one order of magnitude higher than the dark energy scale,

$$M_S < 10^{-32}\text{eV}. \tag{2.111}$$

This result is obtained from analysing the decoupling limit of dRGT, which describes a linearised massive spin-2 mode and a quartic galileon field theory. The vector is also present in the decoupling limit but does not couple directly to matter [159], so does not influence the result. This result is the same order of magnitude as obtained from the

decoupling limit of DGP, which is a linearised spin-2 mode plus a cubic galileon scalar interaction.

The bound from gravitational waves on the spin-2 mass, which arises from the dispersion relation, places an upper bound of

$$M_T < 10^{-22}\text{eV}. \tag{2.112}$$

This result is obtained from the time delay difference between the light signal from the gamma ray burst and the arrival of the gravitational wave. The observation of more gravitational wave events with optical counterpart could tighten the bound on the mass of the tensor modes, although at the moment they remain weaker than the bounds on the scalar graviton mass.

2.10 Conclusions

The conclusion to this chapter is that there are many extensions to dRGT (for more see [101, 162] and references therein), but finding a pathology free, Lorentz invariant massive gravity theory, which can describe the late time acceleration of the universe has been a challenge. Early on in this chapter we outlined the construction of dRGT massive gravity, starting from the linear theory first studied by Fierz and Pauli. The next chapter describes the cosmology of bigravity, which is an extension to dRGT which promotes the background fiducial metric to be a dynamical variable. Extending the theory in this way was hoped to alleviate some of the issues which has plagued cosmologies in dRGT.

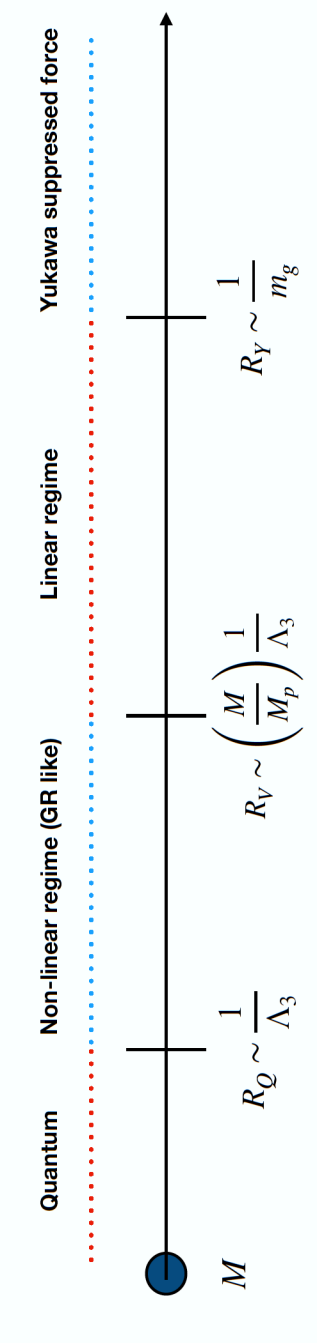

Figure 2.1: Schematic representation of the different length scales in dRGT away from a body of mass M. R_Q is the cutoff of the theory, in which quantum corrections become important. This scale in dRGT is given by $\Lambda_3 \sim \left(M_p m^2\right)^{\frac{1}{3}}$. Then there is the intermediate regime in which non-linear interactions are important and GR is recovered. The next regime is the linear regime where there is a fifth force active, and finally a large scale regime where the force of gravity is exponentially suppressed due to the mass of the graviton, which roughly corresponds to its Compton wavelength.

CHAPTER 3

COSMOLOGY OF BIGRAVITY

Introduction

In this chapter we introduce the theory of bigravity. We then study the background cosmology and discuss the branches of background solutions which exist in the bigravity framework, assuming homogeneity and isotropy. We then discuss the theoretical inconsistencies with one of these branches and move on to describe the cosmology of the *low energy model* of bigravity and investigate the cosmological viability of it. To achieve this, we study the background evolution and linear perturbations by deriving the Poisson's equation. Next, we describe the derivation of the non-linear equations of motion which allows us to identify the Vainshtein radius. We conclude this chapter with a discussion of the viability of bigravity theories for dark energy. This chapter is based on published results in [163].

3.1 Bigravity Theory

Bigravity is an extension to dRGT massive gravity where the background fiducial metric is promoted to a dynamical variable. The ghost free bigravity theory, which was constructed by Hassan and Rosen [54], modifies the dRGT action by imposing that the bigravity theory propagates 7 degrees of freedom. In this way, the form of the kinetic term for the f-metric is fixed to be that of the Einstein-Hilbert. Therefore the action for

bigravity is,

(3.1)
$$S = \frac{M_g^2}{2}\int d^4x\sqrt{-g}R[g] + \frac{M_f^2}{2}\int d^4x\sqrt{-f}R[f] + m^2M_g^2\int d^4x\sqrt{-g}\sum_{n=0}^{4}\alpha_n\mathcal{U}_n + \int d^4x\sqrt{-g}\mathcal{L}_m,$$

where matter is coupled only to the g-metric and $\mathcal{U}_n$ are the dRGT interaction terms (2.85).

The question of which metric to couple matter to is an interesting one, as there are two metrics to choose from. In GR the weak equivalence principle is satisfied, that is to say all matter couples to gravity in the same way, typically through a term like $\sqrt{-g}\mathcal{L}_m(g,\psi^i)$, but the presence of a second dynamical metric adds a sense of ambiguity. If all matter couples universally in a two-metric theory then the weak equivalence principle can be satisfied. The first and most simple form of matter coupling is to couple matter to only one tensor, through $\sqrt{-g}\mathcal{L}_m(g,\psi^i)$; this was considered in the original formulation of Hassan and Rosen bigravity and is inherently ghost free [54]. The advantage of the single coupling scenario is that the metric tensor, which describes the dynamics of spacetime, is clearly the metric which matter couples to. It is this type of matter coupling we will work with in this thesis. The logical next step is to consider a doubly coupled scenario and here there are two possibilities. The first is to couple g and f to the same matter field via,

(3.2)
$$S_m = \int d^4x\sqrt{-g}\mathcal{L}_m(g,\psi^i) + \int d^4x\sqrt{-f}\mathcal{L}_m(f,\psi^i).$$

This form of coupling creates a conceptual problem about which of g or f is the metric tensor, however one can find a combination of the two which acts as the metric. In this coupling scenario it was shown that a ghost is present [164], however there is a special form of effective metric built out of both g and f which is ghost free in the decoupling limit [164] and at the level of the background action. The structure of such a matter action takes the form,

(3.3)
$$S_m = \int d^4x\sqrt{-g^{\text{eff}}}\mathcal{L}_m(g^{\text{eff}},\psi^i),$$

where

(3.4)
$$g^{\text{eff}} = \alpha^2 g_{\mu\nu} + 2\alpha\beta g_{\mu\alpha}\left(\sqrt{g^{-1}f}\right)^{\alpha}_{\nu} + \beta^2 f_{\mu\nu},$$

and (α, β) are constants. Another form of coupling we discuss here is where different matter fields can couple to each metric via,

$$S_m = \int d^4x\sqrt{-g}\,\mathscr{L}_m^g(g,\psi^i) + \int d^4x\sqrt{-f}\,\mathscr{L}_m^f(f,\phi^i). \tag{3.5}$$

This model was studied in [165], where it was found that the doubly coupled scenario could explain the origin of dark matter. There are also other dark matter candidates in the literature which arise out of the bigravity theory [166–168].

We turn our attention to the single coupling scenario and to the application of bigravity theory as a solution to the dark energy problem. To obtain the Einstein equations, we vary the action (3.1) with respect to g and f, and as both metrics are dynamical they satisfy their own Einstein equations. For a derivation of the variation of the mass term see Appendix B. The equations of motion are,

$$\begin{aligned} \mathscr{E}^{(g)}_{\mu\nu} &\equiv G_{\mu\nu} - \frac{1}{M_g^2}T_{\mu\nu} - m^2\sum_{n=0}^{4}\alpha_n\left(g_{\mu\nu}\mathscr{L}_n - 2\frac{\delta\mathscr{U}_n}{\delta g^{\mu\nu}}\right) = 0\,, \\ \mathscr{E}^{(f)}_{\mu\nu} &\equiv \mathscr{G}_{\mu\nu} + \frac{2m^2\sqrt{-g}M_g^2}{\sqrt{-f}M_f^2}\sum_{n=0}^{4}\alpha_n\frac{\delta\mathscr{U}_n}{\delta f^{\mu\nu}} = 0\,, \end{aligned} \tag{3.6}$$

where $G_{\mu\nu}$ and $\mathscr{G}_{\mu\nu}$ are the Einstein tensors built out of the g and f metrics respectively, and

$$T_{\mu\nu} \equiv -\frac{2}{\sqrt{-g}}\frac{\delta}{\delta g^{\mu\nu}}(\sqrt{-g}\mathscr{L}_m), \tag{3.7}$$

is the energy-momentum tensor for the matter sector. Taking the divergence of (3.6) and assuming matter conservation yields,

$$\sum_{n=0}^{4}\alpha_n\nabla_g^\mu\left(g_{\mu\nu}\mathscr{L}_n - 2\frac{\delta\mathscr{U}_n}{\delta g^{\mu\nu}}\right) = \sum_{n=0}^{4}\alpha_n\nabla_f^\mu\frac{\delta\mathscr{U}_n}{\delta f^{\mu\nu}} = 0. \tag{3.8}$$

The previous equation is analogous to the energy-momentum conservation equation for the matter fluid in (1.12), as the two-metric interaction produces an effective energy-momentum tensor. Note here, that ∇_g and ∇_f are covariant derivatives compatible with the g and f metrics respectively.

3.2 Background Cosmology

In this section we study the background cosmology of the bigravity theory under the ansatz that both metrics take flat Friedmann Lemaître Robertson Walker (FLRW) form

in the same coordinate system:

$$
\begin{aligned}
ds_g^2 &= -N(t)^2 + a(t)^2 \delta_{ij} dx^i dx^j \\
ds_f^2 &= -n(t)^2 + \alpha(t)^2 \delta_{ij} dx^i dx^j ,
\end{aligned} \tag{3.9}
$$

where $N(t), n(t)$ denote the lapse functions, while $a(t)$, $\alpha(t)$ represent the scale factors for the g and f metrics respectively. For the matter content we consider a perfect fluid described by the energy-momentum tensor:

$$
T_{\mu\nu} = \rho u_\mu u_\nu + P(g_{\mu\nu} + u_\mu u_\nu), \tag{3.10}
$$

where u_μ is the 4-velocity of the fluid and satisfies the condition $u_\mu u^\mu = -1$, P the pressure and ρ the energy density. In accordance with the homogeneous and isotropic metric ansatze, the background values for the pressure and energy density are functions of time only, while $u_\mu = -\delta^0_\mu N$. In what follows, we will restrict our discussion to a matter sector consisting only of a pressureless non-relativistic fluid, $P = 0$.

For the background metrics (3.9) and a perfect fluid (3.10), the equations of motion (3.6) reduce to four independent equations and the matter equation of motion [169]

$$
3H^2 = m^2 \rho_{m,g} + \frac{\rho}{M_g^2} , \tag{3.11}
$$

$$
3H_f^2 = \frac{m^2}{\tilde{\kappa}} \rho_{m,f} , \tag{3.12}
$$

$$
\frac{2\dot{H}}{N} = m^2 \xi \, J(\tilde{c} - 1) - \frac{\rho}{M_g^2} , \tag{3.13}
$$

$$
\frac{2\dot{H}_f}{n} = -\frac{m^2}{\tilde{\kappa} \xi^3 \tilde{c}} J(\tilde{c} - 1), \tag{3.14}
$$

$$
\frac{\dot{\rho}}{N} + 3H\rho = 0, \tag{3.15}
$$

where a dot represents a time derivative and we define the following functions in accordance with the notation of Ref.[169]:

$$
\begin{aligned}
\rho_{m,g}(\xi) &\equiv U(\xi) - \frac{\xi}{4} \partial_\xi U(\xi), \\
\rho_{m,f}(\xi) &\equiv \frac{1}{4\xi^3} \partial_\xi U(\xi), \\
J(\xi) &\equiv \frac{1}{3} \partial_\xi \left(U(\xi) - \frac{\xi}{4} \partial_\xi U(\xi) \right),
\end{aligned} \tag{3.16}
$$

with $U(\xi) \equiv -\alpha_0 + 4\alpha_1(\xi - 1) - 6(\xi - 1)^2 + 4\alpha_3(\xi - 1)^3 - \alpha_4(\xi - 1)^4$ and

$$
\xi \equiv \frac{\alpha}{a}, \qquad \tilde{c} \equiv \frac{n\,a}{N\,\alpha}, \qquad \tilde{\kappa} \equiv M_f^2 / M_g^2 . \tag{3.17}
$$

The conservation of the energy-momentum tensor arising from the two-metric interaction (3.8) yields,

$$J(H - \xi H_f) = 0\,. \tag{3.18}$$

One final point we should make here is that the constraint equation derived from the derivative of (3.18) is

$$\frac{d(H - \xi H_f)}{dt} = 0. \tag{3.19}$$

Using the background equations (3.11,3.18) we obtain,

$$2(\tilde{c} - 1)W = \frac{\rho}{M_g^2}, \tag{3.20}$$

where W is defined to be,

$$W \equiv \frac{m^2 J(1 + \tilde{\kappa}\xi^2)}{2\tilde{\kappa}\xi} - H^2. \tag{3.21}$$

The quantity W plays a role in the perturbative stability conditions [163, 169], and $W > 0$ is the bigravity generalisation of the Higuchi bound.

3.3 Bigravity Cosmologies

The constraint equation (3.18) branches out into two solutions, the self-accelerating branch $J = 0$ and the normal branch of solution $H = \xi H_f$. The self-accelerating branch clearly has $\xi = \text{const}$ which forces $\rho_{m,g}$ and $\rho_{m,f}$ to be constant. This branch of solution is problematic, and is analogous to the self-accelerating branch in massive gravity. There are only 4 degrees of freedom propagating which correspond to two tensor modes and the kinetic terms for the vectors and scalars vanish [170, 171].

Focusing on the normal branch, there are a couple of different options to take to obtain a cosmological solution. We briefly summarise the results here, but refer the reader to the reviews [162, 172, 173] for more details.

The normal branch is given by the solution $H = \xi H_f$ which links the evolution of the f metric to the evolution of the g metric. The consistency of the two Friedmann equations results in,

$$\left(3H^2 - m^2\rho_{m,g} - \frac{\rho}{M_g^2}\right) - \xi^2\left(3H_f^2 - \frac{m^2}{\tilde{\kappa}}\rho_{m,f}\right) = 0, \tag{3.22}$$

which gives an algebraic relation between ξ and the matter density ρ

$$\hat{\rho}_m(\xi) = -\frac{\rho}{m^2 M_g^2}\,, \tag{3.23}$$

where

$$\hat{\rho}_m(\xi) \equiv \rho_{m,g} - \frac{\xi^2}{\tilde{\kappa}}\rho_{m,f}\,. \tag{3.24}$$

This equation determines ξ as a function of ρ and in general it is a quartic equation for ξ. For late time cosmology, we desire a quasi de-Sitter phase and when the equation for ξ (3.23) is in the late universe regime, the right hand side tends to zero as the density redshifts away. From the Friedmann equation, for late time acceleration we require that $m \sim H_0$, which appears to be a natural choice to match observations without any fine tuning of the model parameters. Furthermore, $m \sim H_0$ corresponds to a value of m which is roughly the dark energy scale, so in this sense this is a natural value for m. For the early universe the behaviour of the equation for ξ is different. The right hand side of (3.23) gets very large at early times, therefore ξ can either be very large or very small to satisfy this condition. Here we discuss both options. Note that the following discussion is valid in the high energy regime, i.e. the early universe.

3.3.1 Branch 1: Infinite branch

Taking the first option, a large ξ means we can approximate (3.23) as,

$$(\alpha_3 + \alpha_4)\,\xi^3 \sim -\frac{\rho}{m^2 M_g^2}. \tag{3.25}$$

This branch is known as the *infinite* branch of solution [173–175] and requires $\alpha_3 + \alpha_4 < 0$ as ξ is strictly positive. This branch of solution was shown to be unstable at early times [176], but here we comment briefly on it. We can derive a relation for the time derivative of ξ,

$$\dot{\xi} = \frac{\dot{\alpha}}{a} - \frac{\alpha}{a^2}\dot{a}. \tag{3.26}$$

Using the background equation $H = \xi H_f$ and the definition of $\tilde{c}$ (3.17) we can re-write (3.26) as,

$$\dot{\xi} = NH(\tilde{c} - 1)\xi, \tag{3.27}$$

on which using (3.20) becomes,

$$\dot{\xi} = \frac{NH\xi}{2M_g^2} \times \frac{\rho}{W}. \tag{3.28}$$

As ξ is a decreasing function in time, this implies that either $W < 0$ which violates the Higuchi bound [122], or the matter sector has negative energy density. Both of these are unphysical so we can conclude that this branch is unstable [177, 178]. Furthermore, perturbations around this branch have been studied around FLRW backgrounds and in general, even though for a specific set of parameters the branch is free from instabilities [179], this branch contains ghost instabilities [180–182] and does not pass theoretical consistency tests.

3.3.2 Branch 2: Finite branch

Taking the other extreme, $\xi \ll 1$ which is known as the *finite* branch, the equation for ξ becomes.

$$\frac{\alpha_1 + 3 + 3\alpha_3 + \alpha_4}{\xi\tilde{\kappa}} = \frac{\rho}{m^2 M_g^2}. \tag{3.29}$$

In this branch, ξ increases in time until the energy density dilutes away and ξ tends to a constant value as the universe enters a late time de-Sitter phase [176]. At the background level this branch appears to be stable. Moving on to the perturbations, it was shown that while tensor and vector modes are well behaved, a gradient instability is generated in the scalar sector at early times. [170, 171, 179, 182, 183]. A couple of resolutions to this problem have been proposed. The first one is to work in the GR limit of the theory, which is equivalent to taking $\tilde{\kappa} \to 0$ [184]. This effectively freezes the dynamics of the second metric and decouples the massive graviton from the matter sector. It was shown that in this limit the time the gradient instability appears can be pushed to arbitrarily early times beyond the limit of the effective field theory. In this branch, the cosmology becomes GR-like which has the advantage of being stable, however the theory becomes indistinguishable from GR and therefore finding observational signatures are difficult, however multiple works are still investigating the phenomenology and effects on large scale structure of this model [185–188]. Another option is that a Vainshtein-like mechanism could be present [189, 190] which screens the effect of the instability at early times recovering GR.

3.3.3 Branch 3: Exotic branch

There is also another branch of solution in the literature which is known as the exotic branch. It arises from explicitly solving the quartic equation (3.23) for ξ. These branches of solution do not assume a monotonous evolution for the density ρ, and avoid the early

time instability via a bounce or describe a static cosmology. However, all these solutions were shown to be unstable [181].

To conclude this discussion, the only viable bigravity models which could be interesting for dark energy lie on the finite branch of solution. Imposing a hierarchy between the Planck scales of the two metrics, one can recover GR at early times and push the gradient instability out of reach of the effective field theory. Another way to resolve the problem is the invoking of a Vainshtein-like mechanism to screen the effect of the instability and allow GR to be recovered at early times.

However, abandoning the assumption that $m \sim H_0$ it was shown to lead to another solution, which could potentially avoid the instability at the expense of fine tuning of model parameters. In the rest of the chapter we focus on the cosmological viability of this model, which was first introduced in [191].

3.4 Low Energy Limit

We now study the phenomenology of the *low energy* model of bigravity. This was proposed in [191], and a healthy background cosmology was found. Implications on this model from primordial gravitational waves and early universe physics were studied in [192], where mild bounds on the parameter space of the model are found. The low energy limit is defined by,

$$\rho \ll m^2 M_g^2 . \tag{3.30}$$

This regime allows us to avoid the early time gradient instability in the normal branch of solution [171] by pushing the instability beyond the reach of the effective field theory [169, 191]. This model also has interesting implications for gravitational waves: Ref. [191] studied the gravitational wave signal generated by this model and found an inverse chirp signal could be detected by future gravitational wave experiments. For the physical sector, gravitational waves propagate at the speed of light so are not constrained by the binary neutron star merger, and for the second metric propagate at speed $c_f = 1 + \mathcal{O}\left(H^2/m^2\right)$ [191]. An interesting feature of this bigravity theory is that due to the two-metric coupling, the gravitational waves oscillate from the hidden sector to the physical sector and it can produce a detectable signal.

Our goal for this chapter is to analyse the cosmological viability of the low energy limit of the bigravity theory. Studying the equation for (3.23) we notice that in the far future, the density ρ redshifts as a^{-3}, and the solution for ξ converges to a constant value

ξ_c defined by

$$\hat{\rho}_m(\xi_c) = 0\,. \tag{3.31}$$

To describe the evolution close to this late time attractor, we linearise Eq.(3.23) around $\xi = \xi_c$ to relate the departure from this point to the matter density:

$$m^2\left[\frac{3(1+\tilde{\kappa}\xi_c^2)J_c}{\tilde{\kappa}\xi_c^2} - \frac{2\Lambda}{m^2\xi_c}\right](\xi-\xi_c) \sim \frac{\rho}{M_g^2}\,, \tag{3.32}$$

where $\Lambda \equiv m^2\rho_{m,g}(\xi_c)$ and the subscript c corresponds to the values of functions evaluated at the de-Sitter attractor. Following Ref.[169], we now assume $|\Lambda/(m^2 J_c)| \ll 1$. Using these results, we find that the Friedmann equation (3.11) can be approximated as

$$3H^2 \simeq \frac{\rho}{\tilde{M}_g^2} + \Lambda\,, \tag{3.33}$$

where the effective Planck scale is $\tilde{M}_g^2 \equiv (1+\tilde{\kappa}\xi_c^2)M_g^2$, and we now identify Λ as the effective cosmological constant [1].

3.5 Cosmological perturbations

In this section we consider perturbations around the low energy background model and determine the effect of the two-metric interaction on the linear growth of structure. We outline the method adopted to study the perturbations, the process to isolate the scalar mode in the Poisson's equation and the extension to non-linear order. In this work, we only consider scalar perturbations as they are the only relevant ones for the large scale structure.

3.5.1 Linear perturbations

To start the study of cosmological perturbations, we perturb both metrics around the backgrounds (3.9) in the Newtonian gauge for the g metric

$$\begin{aligned} ds_g^2 &= -(1+2\phi)dt^2 + a^2\left(\delta_{ij} + 2\delta_{ij}\psi\right)dx^i dx^j\,,\\ ds_f^2 &= -n^2(1+2\phi_f)dt^2 + 2n\,a\,\partial_i b\,dt\,dx^i + \alpha^2\left[\delta_{ij} + 2\delta_{ij}\psi_f + \left(\partial_i\partial_j - \frac{\delta_{ij}}{3}\nabla^2\right)S\right]dx^i dx^j\,, \end{aligned} \tag{3.34}$$

[1] Notice that Λ has a contribution from α_0, which is simply a bare cosmological constant. In Sec.3.6, we will set $\alpha_0 = 0$ such that the accelerated expansion is solely due to the two-metric coupling.

where $(\phi, \psi, b, S, \phi_f, \psi_f)$ are the perturbation variables and we fixed the time coordinate such that $N = 1$. The perturbations in the matter sector are introduced via $\rho = \rho(t) + \delta\rho$ and $u^\mu = (1-\phi, \partial^i v)$ which leads to the following form for $T_{\mu\nu}$,

$$\begin{aligned} T_{00} &= \rho\left(1 + 2\phi + \frac{\delta\rho}{\rho}\right), \\ T_{0i} &= -a^2\,\rho\,\partial_i v\,, \\ T_{ij} &= 0\,. \end{aligned} \tag{3.35}$$

With these decompositions and using the quasi-static approximation [193] we can derive an analogue of Poisson's equation for the potential ϕ [169]. Here we briefly summarise the derivation.

To begin with, we substitute the perturbed metrics into the equations of motion, whilst in the process setting all time derivatives of the fields to zero in accordance with the quasi-static approximation and evaluating everything at the late time attractor. Due to the complex nature of the dRGT potential term, the calculation of the square-root tensor is complicated for non-diagonal metrics. An algorithm used for this procedure is presented in Appendix C. The equations take the following form, up to non-zero factors

$$\begin{aligned} \mathcal{E}^{(g)}_{00} &= \frac{\delta\rho}{M_g^2} - \frac{2k^2\psi}{a^2} - 3J_c m^2 \xi_c(\psi - \psi_f), \\ \mathcal{E}^{(g)}_{tr} &= \left(-3J_c m^2\xi_c - 2(k^2/a^2)\right)\phi + 3J_c m^2\xi_c\phi_f - 6J_c m^2\xi_c\psi - 2(k^2/a^2)\psi + 6J_c m^2\xi_c\psi_f\,, \\ \mathcal{E}^{(g)}_{\rm tl} &= J_c m^2\xi_c a^2 S + 2(\phi + \psi), \\ \mathcal{E}^{(f)}_{00} &= -k^2\tilde{\kappa}\xi_c(k^2 S + 6\psi_f) + a^2(9J_c m^2\psi - 9J_c m^2\psi_f), \\ \mathcal{E}^{(f)}_{tr} &= -3a^2(3J_c m^2\phi - 3J_c m^2\phi_f + 6J_c m^2\psi - 6J_c m^2\psi_f) + k^2\tilde{\kappa}\xi_c(k^2 S + 6(\phi_f + \psi_f)), \\ \mathcal{E}^{(f)}_{\rm tl} &= -3J_c m^2 a^2 S + \tilde{\kappa}\xi_c(k^2 S + 6(\phi_f + \psi_f)). \end{aligned} \tag{3.36}$$

where a subscript 00 represents the time-time component, tr is the trace of the spatial components and tl is the traceless combination. We then solve the equations

$\left(\mathscr{E}^{(g)}_{\rm tl},\mathscr{E}^{(f)}_{00},\mathscr{E}^{(f)}_{tr},\mathscr{E}^{(f)}_{\rm tl}\right)$ for the variables (S,ϕ_f,ψ_f,ψ). The explicit solutions are as follows;

$$\psi = \frac{1}{2}\left(-J_c m^2 \xi_c a^2 S - 2\phi\right), \tag{3.37}$$

$$\psi_f = -\frac{\xi_c S\left(9J_c^2 m^4 a^4 + 2\tilde{\kappa}k^4\right) + 18 J_c m^2 a^2 \phi}{6\left(3J_c m^2 a^2 + 2\tilde{\kappa}k^2\xi_c\right)}, \tag{3.38}$$

$$\phi_f = \frac{J_c m^2 a^2\left[\left(3J_c m^2 a^2(1+\tilde{\kappa}\xi_c^2) + \tilde{\kappa}\xi_c k^2\right)S + 6\tilde{\kappa}\xi_c\phi\right]}{2\tilde{\kappa}\xi_c\left(3J_c m^2 a^2 + 2\tilde{\kappa}k^2\xi_c\right)}, \tag{3.39}$$

$$S = -\frac{4\tilde{\kappa}^2 k^2 \xi_c^2 \phi}{J_c m^2 a^2\left(3J_c m^2 a^2\left(\tilde{\kappa}\xi_c^2+1\right) + \tilde{\kappa}k^2\xi_c\left(4\tilde{\kappa}\xi_c^2+3\right)\right)}. \tag{3.40}$$

Substituting solutions (3.37-3.40) into $\mathscr{E}^{(g)}_{00}$ and performing the re-definitions

$$M_g = \frac{\tilde{M}_g}{\sqrt{1+\tilde{\kappa}\xi_c^2}}, \quad J_c = \frac{2\tilde{\kappa}\xi_c W}{m^2(1+\tilde{\kappa}\xi_c^2)}, \tag{3.41}$$

yields equation (3.42). Note that the trace part of the g-metric equations $\mathscr{E}^{(g)}_{tr}$ is automatically satisfied.

$$\phi = -\frac{\delta\rho}{2\tilde{M}_g(k^2/a^2)}\left[\frac{6W + (3+4\tilde{\kappa}\xi_c^2)(k^2/a^2)}{6W + 3(k^2/a^2)}\right], \tag{3.42}$$

where k is the momentum of the mode in the plane-wave expansion and W is defined in (3.20).

Inspecting the form of the Poisson's equation, we find it is similar to the one in the presence of a scalar field source. The traceless part of the g equations of motion is given by $\mathscr{E}^{(g)}_{\rm tl}$,

$$J_c m^2 \xi_c a^2 S + 2(\phi+\psi) = 0, \tag{3.43}$$

and reveals that the perturbation S acts as a source for anisotropic stress.

3.5.2 Vainshtein radius

We now move on to the study of second order perturbations and to identify the scale at which the perturbative expansion breaks down. This will allow us to determine the Vainshtein radius where the scalar graviton decouples from the matter sector and the evolution closely follows GR. The workings of the Vainshtein mechanism are that derivative self interactions of the scalar are enhanced around a matter source such as a star, so that the effect of the fifth force is screened below the Vainshtein radius.

In order to do this, a few approximations are in order. In addition to restricting the study to the de Sitter attractor, we consider scales where the expansion can be neglected. We also focus on small scales and assume $\nabla^2 \gg m^2$. Keeping the metric perturbations up to second order in the equations of motion, we find that unlike the g-metric equations, the non-linear f-metric equations do not exhibit the enhancement ∇^2/m^2 with respect to the linear part. This allows us to solve the linear f-metric equations and substitute the solutions for (ψ_f, ϕ_f, ϕ) into the non-linear components of the g-metric equations. The solutions are:

$$\begin{aligned} \phi_f &= \frac{J_c m^2 S}{4\tilde{\kappa}\xi_c}\,, \\ \psi_f &= \frac{1}{6}\nabla^2 S + \frac{J_c m^2 S}{4\tilde{\kappa}\xi_c}\,, \\ \phi &= \frac{3 J_c m^2 S}{4\tilde{\kappa}\xi_c} - 2\psi\,, \end{aligned} \tag{3.44}$$

Upon substitution of equations (3.44) into the g-metric equations we obtain

$$\mathscr{E}^{(g)}_{00} = \frac{m^2\xi_c^3}{16(\xi_c-1)}\left[(\nabla^2 S)^2 - \left(\partial_i\partial_j S\partial^i\partial^j S\right)\right] + \frac{1}{2}J_c m^2\xi_c\nabla^2 S + 2\nabla^2\psi + \frac{\delta\rho(t)}{M_g^2}\,, \tag{3.45}$$

$$\mathscr{E}^{(g)}_{tr} = \frac{m^2\xi_c^3}{16(\xi_c-1)}\left[(\nabla^2 S)^2 - \left(\partial_i\partial_j S\partial^i\partial^j S\right)\right] + \frac{3+2\tilde{\kappa}\xi_c^2}{2\tilde{\kappa}}J_c m^2\nabla^2 S - 2\nabla^2\psi\,, \tag{3.46}$$

where we kept only the second order terms that are enhanced in the limit $\nabla^2/J_c m^2 \gg 1$. Using Eq. (3.46) to replace $\nabla^2\psi$ and the definition of $\tilde{M}_g$, Eq. (3.45) reduces to

$$\frac{m^2}{8\xi_c}\left\{\frac{\xi_c^4}{(\xi_c-1)(1+\tilde{\kappa}\xi_c^2)}\left[(\nabla^2 S)^2 - \left(\partial_i\partial_j S\right)^2\right]\right\} + \frac{m^2}{8\xi_c}\left(\frac{12J_c}{\tilde{\kappa}}\nabla^2 S\right) + \frac{\delta\rho}{\tilde{M}_g^2} = 0\,, \tag{3.47}$$

where the non-linear term has the expected galileon-like structure. The scale at which the non-linear terms become important depends on the normalisation of the field. We define

$$\tilde{S} = -\frac{m^2 J_c\xi_c}{2}S\,, \tag{3.48}$$

such that the linear traceless equation of motion (3.43) reduces to $\tilde{S} = \psi + \phi$. With this normalisation, the non-linear equation (3.47) becomes

$$\nabla^2\tilde{S} - \frac{C}{6}\left[(\nabla^2\tilde{S})^2 - \left(\partial_i\partial_j\tilde{S}\right)^2\right] = \frac{\tilde{\kappa}\,\xi_c^2\delta\rho}{3\tilde{M}_g^2}\,, \tag{3.49}$$

where

$$C \equiv \frac{\tilde{\kappa}\xi_c^3}{J_c^2 m^2(\xi_c-1)(1+\tilde{\kappa}\xi_c^2)}\,. \tag{3.50}$$

Thus the non-linear term dominates for $C\nabla^2\tilde{S} \sim \mathcal{O}(1)$, revealing the order of the Vainshtein radius as

$$R_V \sim (C\, r_g)^{\frac{1}{3}}, \tag{3.51}$$

where r_g corresponds to the Schwarzschild radius of a spherical body. This result is similar to the one obtained in section 2 in (2.93). This result is consistent with a similar calculation performed in Ref.[191].

3.6 Fixing Model Parameters

We are now ready to fix the model parameters without introducing the bare cosmological constant term, which is equivalent to setting $\alpha_0 = 0$. On the other hand, we keep α_1 non-zero. This means that the theory does not admit the Minkowski solution, which is not a problem as we are interested in cosmological solutions.

We start by trading α_3 for ξ_c using the definition of the de-Sitter fixed point (3.31) and obtain $\alpha_3 = \alpha_3(\xi_c, \alpha_1, \alpha_4, \tilde{\kappa})$ as

$$\alpha_3 = \frac{3(\xi_c - 1)\left(\xi_c - 2 - \frac{1}{\tilde{\kappa}\xi_c}\right) + \left(4 + \frac{1}{\tilde{\kappa}\xi_c} - 3\xi_c\right)\alpha_1 - (\xi_c - 1)^3\left(\frac{1}{\tilde{\kappa}\xi_c} + 1\right)\alpha_4}{(\xi_c - 1)^2\left[\xi_c - 4 - \frac{3}{\xi_c\tilde{\kappa}}\right]} \tag{3.52}$$

We then fix α_4 matching the effective cosmological constant Λ in the approximate Friedmann equation (3.33) to the observed value, which is equivalent to solving,

$$\rho_{m,g} = \left(\frac{H_0}{m}\right)^2. \tag{3.53}$$

The solution for $\alpha_4 = \alpha_4(\xi_c, \alpha_1, \tilde{\kappa})$ is,

$$\alpha_4 = \frac{6}{(\xi_c - 1)^2} - \frac{8\alpha_1}{(\xi_c - 1)^3} + \left(\frac{H_0}{m}\right)^2 \frac{3 - \tilde{\kappa}\xi_c(\xi_c - 4)}{(\xi_c - 1)^4}. \tag{3.54}$$

Finally, the last parameter is fixed by requiring a sensible Vainshtein radius which ensures that the effects of modified gravity are hidden below a certain distance scale to recover GR on solar system and galactic scales. The relation we will consider is,

$$R_V^3 = r_c^2 r_g\,. \tag{3.55}$$

We introduce the parametrisation

$$r_c = b\, H_0^{-1}, \tag{3.56}$$

where $b \sim \mathcal{O}(0.1-1)$ [194, 195] and allows us to tune the size of the Vainshtein radius. b can be seen as the effective coupling to matter as in [195], where the authors considered a cubic galileon model with an $\mathcal{O}(1)$ coupling, and tested the theory using supermassive black holes via the strong equivalence principle. Black holes are a good test of galileon like theories as they have no hair, i.e. the coupling to matter induced by the presence of an extra scalar mode should vanish. Therefore, black holes can provide strong constraints on galileon theories. It was shown that $\mathcal{O}(1)$ couplings are disfavoured, so we consider an $\mathcal{O}(1)$ coupling as the maximum. The equation which relates the model parameters to the Vainshtein radius is (3.51)

$$C = \frac{b^2}{H_0^2}. \tag{3.57}$$

From this relation we then fix α_1,

$$\alpha_1 = \frac{\xi_c - 1}{2} \pm \frac{\sqrt{\tilde{\kappa}\xi_c(\xi_c-1)}}{2b\sqrt{1+\tilde{\kappa}\xi_c^2}}\frac{H_0}{m} + \mathcal{O}\left(\frac{H_0}{m}\right)^2, \tag{3.58}$$

where we made use of the fact that $H_0 \ll m$. Noting that the solution with the + sign leads to a negative W (defined in Eq.(3.21)), we will choose the − sign solution in the following. Moreover, the solution only exists for $\xi_c > 1$.

After this procedure, we have reduced the number of free parameters down to two: ξ_c and $\tilde{\kappa}$. We now check whether there are any inconsistencies in the background equations of motion. Expanding the left hand side of Eq.(3.23) around the attractor, we have

$$\left.\frac{d\hat{\rho}_m}{d\xi}\right|_{\xi=\xi_c}(\xi-\xi_c) + \left.\frac{d^2\hat{\rho}_m}{d\xi^2}\right|_{\xi=\xi_c}(\xi-\xi_c)^2 + \mathcal{O}(\xi-\xi_c)^3 = -\frac{\rho}{m^2 M_g^2}. \tag{3.59}$$

In the limit $H_0 \ll m$, the coefficients of the linear and quadratic terms are,

$$\begin{aligned}\left.\frac{d\hat{\rho}_m}{d\xi}\right|_{\xi=\xi_c} &= \frac{3\sqrt{1+\tilde{\kappa}\xi_c^2}}{b\sqrt{\tilde{\kappa}\xi_c(\xi_c-1)}}\frac{H_0}{m} + \mathcal{O}\left(\frac{H_0}{m}\right)^2, \\ \left.\frac{d^2\hat{\rho}_m}{d\xi^2}\right|_{\xi=\xi_c} &= \frac{3(1+\tilde{\kappa}\xi_c^2)}{\tilde{\kappa}\xi_c(\xi_c-1)} + \mathcal{O}\left(\frac{H_0}{m}\right).\end{aligned} \tag{3.60}$$

In Section 3.2, we used the linear term to obtain the approximate Friedmann equation (3.33). However, we see that the first derivative is suppressed by H_0/m, while the second derivative term is manifestly positive. As a result, when the quadratic term dominates, there is no real solution to this equation. This observation allows us to determine the parameter range which grants a physical evolution. The linear term is dominant if

$$|\xi - \xi_c| \lesssim \frac{1}{b}\frac{H_0}{m}, \tag{3.61}$$

in which case, the solution to (3.59) behaves as

$$|\xi - \xi_c| \sim b \left(\frac{H_0}{m}\right)^{-1} \frac{\rho}{m^2 M_g^2}. \tag{3.62}$$

Using the condition (3.61), the above relation yields an upper bound on b;

$$b < \frac{H_0 M_g}{\sqrt{\rho}}. \tag{3.63}$$

Since the matter density today is of order of $H_0^2 M_g^2$, we use $\rho \sim H_0^2 M_g^2 / a^3$, giving

$$b < a^{3/2}. \tag{3.64}$$

Therefore, the solution exists for

$$a > a_{in} = b^{3/2}. \tag{3.65}$$

Turning this relation around, given a parameter b, the cosmological description can go as far back as a_{in}, before which no physical evolution exists. Although we set $\alpha_0 = 0$ in order not to introduce a bare cosmological constant, we can check that this conclusion holds even if $\alpha_0 \neq 0$.

As an example, we impose that we wish to describe the evolution of the scale factor up from the last scattering surface onward. Therefore, we set $a_{in} = a_{CMB} = 10^{-3}$. In order to have the low energy limit (3.30) be valid at the time of CMB, the minimum mass parameter allowed is $m = H_{CMB}$, where H_{CMB} is the Hubble parameter at the last scattering surface. From Eq. (3.65), this initial value of the scale factor corresponds to a value of $b = 10^{-9/2}$. In order to check this estimate, we compared the exact numerical solution of Eq.(3.23) to the linear approximation. The comparison is summarised in figure 3.1. The exact solution only appears around $a \sim 10^{-3}$, after which the value of ξ becomes closer to the de Sitter attractor value ξ_c.

We close this Section with a discussion of the effect on the large scale structure. From Eq. (3.42) we can determine the consequences of the several tunings: in order to have an observable effect, the quantity W has to be comparable to the k^2 contribution. The function W can be interpreted as the effective mass of the gravity perturbations, and behaves as $W \sim m^2 J$. It encodes the information about the scale at which the modifications to gravity appear. Using the approximate expression,

$$W \sim m^2 \left[\left(\frac{1}{b} \frac{H_0}{m} \right) + \mathcal{O}\left(\frac{H_0}{m}\right)^2 \right], \tag{3.66}$$

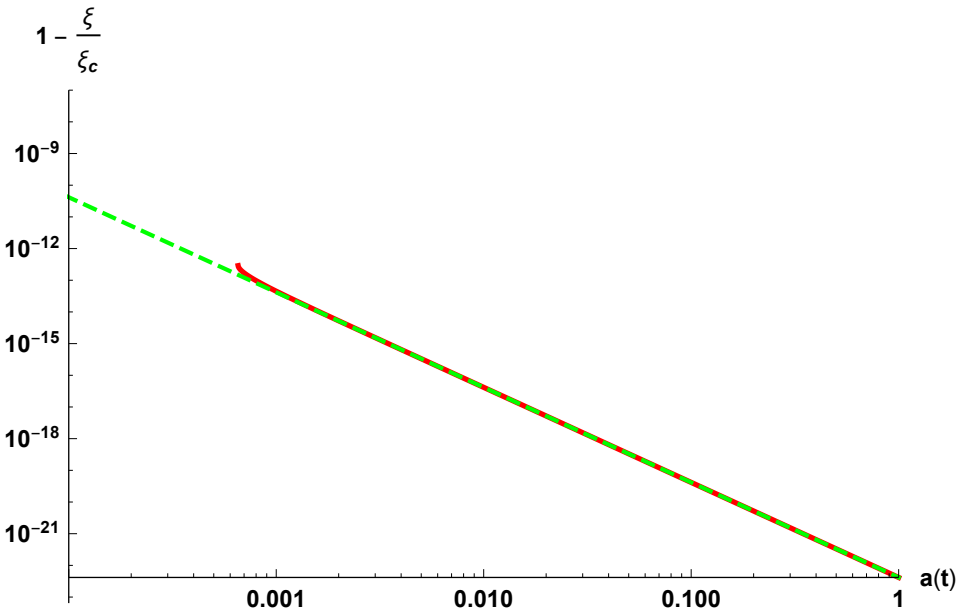

Figure 3.1: The evolution of $1-\xi/\xi_c$ with the scale factor. The dashed green line shows the linear approximation (3.32) while the solid red line corresponds to the numerical solution obtained by solving the exact equation (3.23). The Vainshtein radius tuning parameter, defined in Eq.(3.56), is $b = 10^{-9/2}$, while the other parameters are set to $\tilde{\kappa} = 1$, $\xi_c = 8$.

we can estimate its value, using $m \sim H_{CMB} \sim 10^{9/2} H_0$,

$$W \sim \frac{1}{\left(10^{3/2}\text{Mpc}\right)} \left(\frac{10^3 \text{Mpc}}{H_0^{-1}}\right)^2 , \tag{3.67}$$

which implies that the effect of the two-metric interaction appears only at scales smaller than ~ 0.1Mpc where linear perturbation theory is no longer applicable.

3.7 Conclusions

In this chapter we have presented an analysis of the linear and non-linear perturbations in bigravity, where non-derivative two-metric coupling is introduced as in [54] so as not to generate the Boulware-Deser ghost. We considered a perfect fluid with equation of state $P = 0$ coupled to the g-metric and studied metric perturbations around FLRW, whilst adopting the healthy branch of solution with $H = \xi H_f$. We then adopted the low energy limit of the theory as it was thought this model could support a healthy cosmology. Poisson's equation was derived at the linear level in perturbations and we identified the modification to the Poisson's equation due to the extra degrees of freedom present from

the massive graviton. Furthermore, we studied perturbations going beyond linear order and identified the Vainshtein radius, below which the derivative self-interactions of the scalar screen the effect of the fifth force and conspire to reproduce GR on local scales.

We then looked at the effect of fixing three of the model parameters on the background cosmology of the theory. We use the following requirements: ensuring the existence of the late-time de-Sitter attractor, matching the effective cosmological constant in the Friedmann equation to the value we observe and proposing we have a Vainshtein radius. Bigravity in the low energy limit can admit a sensible cosmological solution, but this comes with a cost of lowering the Vainsthein radius. With a value of $b = 10^{-9/2}$, for which the Vainshtein radius is given by $R_V^3 = 10^{-9} H_0^{-2} r_g$, we are able to describe the evolution of the scale factor up until the last scattering surface at $a_{in} = 10^{-3}$. However, to satisfy the observational constraints, we need to impose $b = \mathcal{O}(0.1 - 1)$, which results in a very short window of the viable cosmological evolution.

The main conclusion of this chapter is that the stable bigravity model that is distinguishable from GR does not provide a reasonable description for the late time acceleration of the universe. With this result, we have established that none of the exact cosmological solutions to dRGT massive gravity/bigravity theory, where matter couples to a single metric, admit a viable and testable dark energy model. However, there are two possible ways out from this no-go result for bigravity: (i) impose a hierarchy between the two Planck scales, effectively decoupling the massive graviton from the matter sector, thus making the model indistinguishable from GR [184], or (ii) invoke a Vainshtein-like mechanism [189, 190] to screen the effect of the instability at early times.

CHAPTER 4

STABILITY OF GENERALISED MASSIVE GRAVITY

Introduction

As seen in the previous chapter, finding a stable cosmology in the framework of massive gravity continues to be a challenge. In the case of bigravity, most models are pathological or show no deviation away from GR so are not testable. There are, however, other extensions to dRGT which do not add extra gravitational degrees of freedom which have so far not been studied in detail. The *Generalised Massive Gravity* (GMG) remains one of these theories. First introduced in [106], the authors showed the stability of GMG in a decoupling limit with all 5 graviton modes propagating, but the stability of the full theory was yet to be studied. In addition, it was shown the theory admits self-accelerating and exact FLRW solutions as well as an active Vainshtein mechanism. Whilst our results in this chapter qualitatively match [106], how to perform a formal quantitative comparison is unclear, but we stress that in this chapter we make no assumptions so our results hold in generality.

GMG modifies dRGT massive gravity without introducing any new gravitational degrees of freedom, which is an advantage with respect to many other extensions of dRGT. This is achieved by breaking the translation invariance in the field space by promoting the mass parameters to functions of $\eta_{ab}\phi^a\phi^b$, while preserving Lorentz invariance. One might argue that by promoting constants to functions decreases the attractiveness of the theory in terms of an Occam's razor perspective, but we shall see that by minimally modifying the original dRGT theory can lead to interesting phenemenology.

This construction preserves the dRGT tuning that removes the Boulware-Deser mode [196]. In this chapter, we perform a full stability analysis with a k-essence fluid acting as the matter field. We choose a k-essence field as it represents a simple choice for analysing matter at the level of the action, but we stress that the results in this chapter hold independently of the matter field considered. We derive the quadratic action for the tensor, vector and scalar modes and derive stability conditions by requiring the absence of ghosts and gradient instabilities. As gaining an analytic understanding of extended theories of gravity can be challenging, we introduce the *minimal* theory of generalised massive gravity. In the framework of this model, where we allow only one of the mass functions to vary, we investigate the stability for a self-accelerating cosmological background. We conclude this chapter by identifying a parameter space in which the theory is pathology-free and in which the effective energy density arising from the mass term approximates a cosmological constant. The work in this chapter is based on the publication [197].

4.1 The Set-Up

In this section we outline the GMG theory and discuss the field configuration for cosmological solutions.

The gravitational action consists of the Einstein-Hilbert term and the generalised mass terms

$$S = \frac{M_p^2}{2}\int d^4x\sqrt{-g}\left[R + 2m^2\sum_{n=0}^{4}\alpha_n(\phi^a\phi_a)\,\mathcal{U}_n[\mathcal{K}]\right] + S_{matter}\,. \tag{4.1}$$

In the case of GMG, $f_{\mu\nu}$ is non-dynamical and is written in terms of the four Stückelberg scalar fields,

$$f_{\mu\nu} \equiv \eta_{ab}\partial_\mu\phi^a\partial_\nu\phi^b\,, \tag{4.2}$$

with $(a,b = 0,1,2,3)$. In standard dRGT massive gravity ϕ^a are the Stückelberg fields, arising from the reintroduction of diffeomorphism invariance. However, if the translation invariance in the field space is broken, the four fields can also appear in the Lorentz invariant combination $\eta_{ab}\phi^a\phi^b$; in GMG theory, the mass parameters α_n are promoted to functions of this combination [106].

For the matter sector we consider a k-essence field with action

$$S_{matter} = \int d^4x\sqrt{-g}\,P(X), \tag{4.3}$$

with

$$X \equiv -g^{\mu\nu}\partial_\mu\varphi\partial_\nu\varphi\,. \tag{4.4}$$

In order to achieve an isotropic and homogeneous universe for both the physical and fiducial metric, we need $f_{\mu\nu}$ to have the same FLRW symmetries as $g_{\mu\nu}$ in the same coordinate system, since they are coupled via $g^{-1}f$. Moreover, we also need to ensure that $\phi^a\phi_a$ stays uniform. For a Minkowski field space metric the unique field configuration that is compatible with these symmetries is

$$\begin{aligned}
\phi^0 &= f(t)\sqrt{1+\kappa(x^2+y^2+z^2)}\,,\\
\phi^1 &= f(t)\sqrt{\kappa}x\,,\\
\phi^2 &= f(t)\sqrt{\kappa}y\,,\\
\phi^3 &= f(t)\sqrt{\kappa}z\,.
\end{aligned} \tag{4.5}$$

where $\kappa = |K| = -K$ is the absolute value of the negative constant curvature of the spatial slice. With this definition, the fiducial metric has the same form as an open FLRW solution [114]

$$f_{\mu\nu}dx^\mu dx^\nu = -\dot{f}(t)^2dt^2 + \kappa f(t)^2\Omega_{ij}dx^i dx^j\,, \tag{4.6}$$

where an overdot denotes time derivative and Ω_{ij} is the metric of the constant time hypersurfaces with constant negative curvature

$$\Omega_{ij}dx^i dx^j = dx^2+dy^2+dz^2 - \frac{\kappa(xdx+ydy+zdz)^2}{1+\kappa(x^2+y^2+z^2)}\,. \tag{4.7}$$

Our metric ansatz is then an open FLRW

$$g_{\mu\nu}dx^\mu dx^\nu = -dt^2 + a(t)^2\Omega_{ij}dx^i dx^j\,. \tag{4.8}$$

The background field value is chosen to be uniform, i.e. $\varphi = \varphi(t)$. In this case, the k-essence can be interpreted as an irrotational fluid with pressure $P(\dot\varphi^2)$, while the energy density ρ and sound speed c_s of the analogue fluid is given by

$$\rho = 2P'(\dot\varphi^2)\dot\varphi^2 - P(\dot\varphi^2), \qquad c_s^2 = \frac{P'(\dot\varphi^2)}{2P''(\dot\varphi^2)\dot\varphi^2 + P'(\dot\varphi^2)} \tag{4.9}$$

where a prime denotes differentiation with respect to the argument.

4.2 Background Dynamics

We now can use the field configurations outlined in the previous section to determine the background dynamics of cosmology. We take the approach of calculating the background action to obtain the background equations of motion. The total action in the mini-superspace approximation is

(4.10)
$$S = \frac{M_p^2 V}{2}\int N\,dt\,a^3\left[-\frac{6\kappa}{a^2}-\frac{6\dot{a}^2}{a^2N^2}+2m^2(\alpha_0U_0+\alpha_1U_1+\alpha_2U_2+\alpha_3U_3+\alpha_4U_4)+\frac{2a^3}{M_p^2}P(\dot{\varphi}^2)\right],$$

where $\alpha_n = \alpha_n[-f(t)^2]$ and

$$\begin{aligned}
U_0 &= 1\,,\\
U_1 &= 4-\frac{3\sqrt{\kappa}f}{a}-\frac{\dot{f}}{N}\,,\\
U_2 &= 3\left(1-\frac{\sqrt{\kappa}f}{a}\right)\left(2-\frac{\sqrt{\kappa}f}{a}-\frac{\dot{f}}{N}\right),\\
U_3 &= \left(1-\frac{\sqrt{\kappa}f}{a}\right)^2\left(4-\frac{\sqrt{\kappa}f}{a}-\frac{3\dot{f}}{N}\right),\\
U_4 &= \left(1-\frac{\sqrt{\kappa}f}{a}\right)^3\left(1-\frac{\dot{f}}{N}\right).
\end{aligned} \tag{4.11}$$

Varying the action (4.10) with respect to N, a and φ, then fixing the cosmological time $N=1$, we get the following equations of motion [106]

$$\begin{aligned}
3\left(H^2-\frac{\kappa}{a^2}\right) &= m^2L+\frac{\rho}{M_p^2}\,,\\
2\left(\dot{H}+\frac{\kappa}{a^2}\right) &= m^2J(r-1)\xi-\frac{\rho+P}{M_p^2}\,,\\
\dot{\rho} &= -3H(\rho+P)\,,
\end{aligned} \tag{4.12}$$

where for convenience, we defined[1]

$$H\equiv\frac{\dot{a}}{a}\,,\qquad \xi\equiv\frac{\sqrt{\kappa}f}{a}\,,\qquad r\equiv\frac{a\dot{f}}{\sqrt{\kappa}f}\,. \tag{4.13}$$

We also defined two combinations of the mass parameters

$$\begin{aligned}
L &\equiv -\alpha_0+(3\xi-4)\alpha_1-3(\xi-1)(\xi-2)\alpha_2+(\xi-1)^2(\xi-4)\alpha_3+(\xi-1)^3\alpha_4\,,\\
J &\equiv \alpha_1+(3-2\xi)\alpha_2+(\xi-1)(\xi-3)\alpha_3+(\xi-1)^2\alpha_4\,,
\end{aligned} \tag{4.14}$$

[1] Note that r defined here is the equivalent of $\tilde{c}$ in the previous chapter.

where from the background equations, we infer that $m^2M_p^2L^2$ is the effective energy density coming from the mass term while $m^2M_p^2J(1-r)\xi$ corresponds to the sum of the effective density and pressure. In standard dRGT, the quantity J is forced to vanish, yielding a constant ξ solution. As a result, the contribution to the Friedmann equation m^2L becomes an effective cosmological constant. In contrast, in the GMG theory, this is no longer the case. By varying the action (4.10) with respect to f, or equivalently using the contracted Bianchi identities, we obtain the Stückelberg constraint equation

$$3HJ(r-1)\xi - \dot{L} = 0\,. \tag{4.15}$$

Using the definition of L from Eq. (4.14), we can also rewrite this equation in the following form

$$3\left(H - \frac{\sqrt{\kappa}}{a}\right)J = -\frac{2a\xi}{\sqrt{\kappa}}\left[-\alpha_0' + (3\xi-4)\alpha_1' - 3(\xi-1)(\xi-2)\alpha_2' + (\xi-1)^2(\xi-4)\alpha_3' + (\xi-1)^3\alpha_4'\right]. \tag{4.16}$$

In this form, the dRGT limit can be trivially taken by $\alpha_n' \equiv \partial\alpha_n/\partial(-f^2) \to 0$. In this constant mass limit, there are two branches: the normal branch with $H = \sqrt{\kappa}a$ which prevents expansion, while $J = 0$ branch gives rise to a self-acceleration. The generalised mass term thus prevents the branching by breaking the factorised form of the constraint equation. Although this means that generically the mass term is no longer an effective cosmological constant, this also solves the problem of infinite strong coupling of scalar perturbations, whose kinetic terms are proportional to J in standard dRGT [119].

4.3 Cosmological Perturbations

In this section we derive the stability conditions by calculating the quadratic action for the tensors, vectors and scalars. To calculate the quadratic action we need to first introduce perturbations to the physical metric, whilst working in the unitary gauge for the f-metric which leaves it un-perturbed,

$$g_{\mu\nu}dx^\mu dx^\nu = -(1+2\phi)dt^2 + (\partial_i B + B_i)\,dt\,dx^i + h_{ij}, \tag{4.17}$$

with h_{ij} decomposed as

$$h_{ij} = 2\psi\Omega_{ij} + \left(D_iD_j - \frac{1}{3}\Omega_{ij}D_lD^l\right)E + \frac{1}{2}\left(D_iE_j + D_jE_i\right) + \gamma_{ij}\,, \tag{4.18}$$

[2]Note here that L is the equivalent of $\rho_{m,g}$ in chapter 3.

D_i is the covariant derivative associated with the 3-metric Ω_{ij} and the spatial indicies are raised by the inverse metric Ω^{ij}. The vectors in the above decomposition are divergence-free $D^i E_i = D^i B_i = 0$, while the tensor is divergence and trace-free $D^i \gamma_{ij} = \Omega^{ij}\gamma_{ij} = 0$. We also introduce matter perturbations through

$$\varphi = \varphi_0 + \delta\varphi\,, \tag{4.19}$$

with quantities in the fluid analogue P, ρ and c_s all defined with respect to the background field. For the four scalar fields ϕ^a we exploit the diffeomorphism invariance to fix their perturbations to zero, depleting all the gauge freedom in the system.

In this decomposition, the scalars (ϕ, B, ψ, E, $\delta\varphi$), vectors (E_i, B_i) and tensor (γ_{ij}) perturbations decouple at quadratic order in the action. We will therefore study them separately in the following.

4.3.1 Tensors

Starting with the tensor sector, we expand (4.1) to second order in tensor perturbations, we find

$$S_T^{(2)} = \frac{M_p^2}{8}\int d^4x\,\sqrt{\Omega}\,a^3\left[\dot\gamma_{ij}\dot\gamma^{ij} + \frac{1}{a^2}\gamma_{ij}D_lD^l\gamma^{ij} + \left(\frac{2\kappa}{a^2} - m^2\,\Gamma\right)\gamma_{ij}\gamma^{ij}\right]. \tag{4.20}$$

We expand γ_{ij} in terms of tensor harmonics (see e.g. [74])

$$\gamma_{ij} = \int d^3k\,\gamma_{|\vec k|}Y_{ij}(\vec k,\vec x), \tag{4.21}$$

with $D_lD^lY_{ij} = -k^2Y_{ij}$ and $D^iY_{ij} = \Omega^{ij}Y_{ij} = 0$. Using the orthornormality condition,

$$\int d^3x\sqrt{\Omega}Y_{ij}(\vec k,\vec x)Y^{ij}(\vec k',\vec x) = \delta^{(3)}(\vec k - \vec k'), \tag{4.22}$$

the action can be written as,

$$S_T^{(2)} = \frac{M_p^2}{8}\int dtd^3k\int d^3k'\left[\dot\gamma_{|\vec k|}\dot\gamma_{|\vec k'|} - \frac{k^2}{a^2}\gamma_{|\vec k|}\gamma_{|\vec k'|} + \left(\frac{2\kappa}{a^2} - m^2\Gamma\right)\gamma_{|\vec k|}\gamma_{|\vec k'|}\right]\delta^{(3)}(\vec k - \vec k'). \tag{4.23}$$

Integrating over $\vec k'$ allows us to reduce the above action to

$$S_T^{(2)} = \frac{M_p^2}{8}\int dtd^3k\,a^3\left[|\dot\gamma|^2 - \omega_T^2|\gamma|^2\right], \tag{4.24}$$

where the tensor dispersion relation is

$$\omega_T^2 = \left(\frac{k^2}{a^2} - \frac{2\kappa}{a^2} + m^2\,\Gamma\right). \tag{4.25}$$

The mass of the tensor mode $m\sqrt{\Gamma}$ is given in terms of the mass functions as

(4.26)
$$\Gamma \equiv \xi\left[\alpha_1+(3-2\xi)\alpha_2+(\xi-1)(\xi-3)\alpha_3+(\xi-1)^2\alpha_4\right]+(r-1)\xi^2\left[-\alpha_2+(\xi-2)\alpha_3+(\xi-1)\alpha_4\right].$$

This expression agrees with the standard dRGT tensor mass with constant α_n [119].

From (4.24) it is clear the tensors show no ghost or gradient instabilities since their kinetic term directly follows from a standard Einstein-Hilbert action. However one can place restrictions on Γ requiring that $\Gamma > 0$ to avoid a tachyonic instability. On the other hand, for $|m^2\Gamma| \sim \mathcal{O}(H_0^2)$, the instability generically takes the age of the universe to develop, thus an imaginary mass is not necessarily a cause for concern.

4.3.2 Vectors

We next calculate the action (4.1) at quadratic order in vector modes. The shift vector B_i is non-dynamical so it can be integrated out by solving its algebraic equation of motion

$$B_V = \frac{a(1+r)(k^2+2\kappa)}{2\left[(k^2+2\kappa)(r+1)+2m^2a^2J\xi\right]}\dot{E}_V\,, \tag{4.27}$$

where we expanded the perturbations in terms of vector harmonics

$$Q_i = \int d^3k Q_{V,|\vec{k}|}Y_i(\vec{k},\vec{x}), \tag{4.28}$$

with $D_iD^iY_j = -k^2Y_j$ and $D^iY_i = 0$. Upon substituting (4.27) into the action, only one propagating vector remains,

$$S_V^{(2)} = \frac{M_p^2}{8}\int d^3k\,dt\,a^3\left[\mathcal{T}|\dot{E}_V|^2 - \frac{k^2+2\kappa}{2}m^2\,\Gamma\,|E_V|^2\right], \tag{4.29}$$

where the kinetic term is

$$\mathcal{T} = \left(\frac{2}{k^2+2\kappa}+\frac{1+r}{m^2a^2J\xi}\right)^{-1}. \tag{4.30}$$

For avoiding ghost instability, the following condition must hold at sub-horizon scales

$$\mathcal{T}\Big|_{k\gg aH} = \frac{m^2a^2J\xi}{1+r} > 0\,. \tag{4.31}$$

The sound speed for the vector modes can be calculated by taking the ratio of the two terms in Eq.(4.29) in the sub-horizon limit

$$c_V^2 = \frac{m^2a^2\Gamma}{2\mathcal{T}}\Big|_{k\gg aH} = \frac{(1+r)\Gamma}{2JX}. \tag{4.32}$$

The squared-sound speeds should be positive to avoid gradient instability $c_V^2 \geq 0$.

4.3.3 Scalars

We now expand the action (4.1) up to quadratic order in scalar perturbations. Unfortunately, the full calculation involves expressions not suitable for presentation as they are very lengthy and non-intuitive. However, we describe the procedure here and show some intermediate results.

At this stage we have an action with five degrees of freedom, $(\phi,\psi,B,E,\delta\varphi)$. However, the lapse and shift perturbations appear in the action without any time derivatives and can be integrated out. By first expanding all perturbations in terms of scalar harmonics

$$Q = \int d^3k Q_{S,|\vec{k}|} Y(\vec{k},\vec{x}), \tag{4.33}$$

with $D_i D^i Y = -k^2 Y$, we solve the equation of motion for the shift B,

$$B = \frac{a(1+r)\left[3\delta\varphi(\rho+P)+M_p^2\dot{\varphi}\left[(k^2+3\kappa)\dot{E}+6(\dot{\psi}-H\phi)\right]\right]}{3M_p^2\left[2(r+1)\kappa+m^2a^2J\xi\right]\dot{\varphi}}. \tag{4.34}$$

where we omitted the subscript $S,|\vec{k}|$ and we will do so for all other perturbations in the following. Upon substituting the solution for B back in the action, we then solve for the lapse perturbation ϕ, which is,

$$\begin{aligned}\phi =& \frac{M_p^2c_s^2\left[2\kappa(r+1)+m^2a^2J\xi\right]}{2M_p^2c_s^2H^2\left[2(k^2+3\kappa)(r+1)+3m^2a^2J\xi\right]-\left[2\kappa(r+1)+m^2a^2J\xi\right](\rho+P)}\\ &\times\left\{\frac{2k^2H(1+r)}{3\left[2\kappa(1+r)+m^2a^2J\xi\right]}\left[\frac{3(\rho+P)}{M_p^2\dot{\varphi}}\delta\varphi+(k^2+3\kappa)\dot{E}+\frac{3}{k^2}\left(2(k^2+3\kappa)+\frac{3m^2a^2J\xi}{1+r}\right)\dot{\psi}\right]\right.\\ &\left.+\frac{k^2(k^2+3\kappa)}{3a^2}E+\frac{2(k^2+3\kappa)+3m^2a^2J\xi}{a^2}\psi-\frac{(\rho+P)}{M_p^2c_s^2\dot{\varphi}}\delta\dot{\varphi}\right\}.\end{aligned} \tag{4.35}$$

With the solution (4.35) we reduce the quadratic action to a system with 3 degrees of freedom $(\psi,E,\delta\varphi)$. Formally, the action is the following;

$$S_S^{(2)} = \frac{M_p^2}{2}\int d^3k\,dt\,a^3\left(\dot{\tilde{\Psi}}^\dagger\tilde{\mathcal{K}}\dot{\tilde{\Psi}}+\frac{1}{2}\dot{\tilde{\Psi}}^\dagger\tilde{\mathcal{G}}\tilde{\Psi}+\frac{1}{2}\tilde{\Psi}^\dagger\tilde{\mathcal{G}}^T\dot{\tilde{\Psi}}-\tilde{\Psi}^\dagger\tilde{\mathcal{M}}\tilde{\Psi}\right), \tag{4.36}$$

where $\tilde{\Psi}\equiv(\psi,E,\delta\varphi)$ is the field array and where $\tilde{\mathcal{K}}$, $\tilde{\mathcal{G}}$ and $\tilde{\mathcal{M}}$ are the real 3×3 kinetic, mixing and mass matrices respectively. The absence of the Boulware-Deser ghost requires that we can integrate out one more non-dynamical degree of freedom. Indeed, at this stage $\det\tilde{\mathcal{K}}=0$, indicating that at least one combination of the fields has a vanishing kinetic term. To explicitly see this we define the quantity Q

$$Q\equiv\psi+\frac{k^2(r+1)(k^2+3\kappa)}{9m^2a^2J\xi+6(r+1)(k^2+3\kappa)}E-\left(\frac{H}{\dot{\varphi}}\right)\delta\varphi. \tag{4.37}$$

When we remove $\delta\varphi$ in favour of Q, the kinetic part of the action becomes diagonal and the non-dynamical nature of ψ becomes manifest. We identify ψ in this basis as the would-be Boulware-Deser mode and integrate it out. Unfortunately, the solution is not suitable to be presented here, but upon substitution into the action we obtain a system with two dynamical fields in a basis $\Psi = (Q, E)$, with the action formally

$$S_S^{(2)} = \frac{M_p^2}{2}\int d^3k\, dt\left(\dot{\Psi}^\dagger \mathscr{K}\,\dot{\Psi} + \frac{1}{2}\dot{\Psi}^\dagger \mathscr{G}\,\Psi + \frac{1}{2}\Psi^\dagger \mathscr{G}^T\dot{\Psi} - \Psi^\dagger \mathscr{M}\,\Psi\right), \tag{4.38}$$

where $\mathscr{K}$, $\mathscr{G}$ and $\mathscr{M}$ are now the 2×2 kinetic, mixing and mass matrices respectively in the new basis, with $\mathscr{K} = \mathscr{K}^T$, $\mathscr{M} = \mathscr{M}^T$.

4.3.3.1 No-ghost Conditions

The conditions for the absence of ghosts can be obtained by studying the positivity of the eigenvalues of the kinetic matrix $\mathscr{K}$ in the sub-horizon limit, which corresponds to taking $k \to \infty$. The two eigenvalues are determined as

$$e_1 = \mathscr{K}_{11}, \qquad e_2 = \frac{\det \mathscr{K}}{\mathscr{K}_{11}}. \tag{4.39}$$

The exact expressions are,

$$\begin{aligned}
e_1 &= \left[\frac{M_p^4 c_s^2 H^2}{2(\rho+P)} - \left(\frac{4\left[2(k^2+3\kappa)(r+1)+3m^2a^2J\xi\right]}{M_p^2\left[2\kappa(r+1)+m^2a^2J\xi\right]} + \mathscr{B}_1\right)^{-1}\right]^{-1},\\
e_2 &= \left\{\frac{3M_p^2}{k^2(k^2+3\kappa)} + \frac{2M_p^2(r+1)}{k^2m^2a^2J\xi}\right.\\
&\quad \left. + \frac{4M_p^2 r^2}{3m^2a^2}\left[J\xi\left[-2\sqrt{\kappa}\,a\left(H-\frac{\sqrt{\kappa}}{a}\right)r + a^2\left(-4H^2 + r\left(\frac{\rho+P}{M_p^2}+m^2J\xi\right)\right)\right] + 2a^2H(2H\Gamma - \dot{J}\xi)\right]^{-1}\right\}^{-1}
\end{aligned} \tag{4.40}$$

where

$$\begin{aligned}
\mathscr{B}_1 \equiv{}& \frac{4m^2J^2r^2(r+1)\xi^2\left[6\kappa+2(k^2+3\kappa)r+3m^2a^2J\xi^2\right]^2}{M_p^2\left[2\kappa(r+1)+m^2a^2J\xi\right]}\\
&\times\left\{m^2J^2r\xi^2\left[-2k^2r^3-6\kappa(r-1)(1+r)^2-3m^2a^2J(r^2-1)\xi\right]\right.\\
&\left.+H\xi\left[2\kappa(r+1)+m^2a^2J\xi\right]\left[\mathscr{B}_2 J - 6(r+1)\left(-\frac{2H\Gamma}{X}+\dot{J}\right)\right]\right\}^{-1},\\
\mathscr{B}_2 \equiv{}& -\frac{3r(r+1)}{H^2}\left[\frac{2\sqrt{\kappa}H}{a}+\frac{4H^2}{r}-\frac{2\left[3\kappa+(k^2+3\kappa)r\right]}{3a^2(1+r)}-\frac{\rho+P}{M_p^2}\right].
\end{aligned} \tag{4.41}$$

In the dRGT limit $J, \dot{J} \to 0$, the second eigenvalue vanishes, in agreement with [119]. However, with the varying mass functions, the strong coupling problem is resolved.

We now expand the eigenvalues in the sub-horizon limit, obtaining

$$e_1 = \frac{2(\rho+P)}{M_p^2 c_s^2 H^2} + \mathcal{O}\left(k^{-2}\right),$$

(4.42)

$$e_2 = \frac{3m^2a^4H}{2M_p^2r^2}\left[\frac{rJ\xi}{2H}\left(\frac{2\kappa}{a^2} - \frac{2\sqrt{\kappa}H}{a} - \frac{4H^2}{r} + m^2J\xi + \frac{\rho+P}{M_p^2}\right) + 2H\Gamma - \dot{J}X\right] + \mathcal{O}\left(k^{-2}\right).$$

To avoid ghost instabilities, we need $e_1 > 0$ and $e_2 > 0$. The first no-ghost condition is simply the null-energy condition, so we identify the first eigenmode as the matter sector. The second one is therefore the scalar graviton mode. However, from the subhorizon expression for e_2 we see that it no longer vanishes in the dRGT limit $J, \dot{J} \to 0$. The reason for this apparent discrepancy is that the sub-horizon limit does not commute with the dRGT limit.

This peculiar behaviour can be understood by inspecting the terms in e_2. In the second of Eq.(4.40), there are some terms that vanish in any order of the limits. Neglecting these, we are left with two terms that dominate according to which limit is applied first

$$e_2 \simeq \frac{1}{M_p^2}\left(\frac{2(r+1)}{k^2m^2a^2J\xi} + \frac{r^2}{3m^2a^4H^2\Gamma}\right)^{-1}. \tag{4.43}$$

In the above, the first term dominates in the dRGT limit while the second term dominates in the large momentum limit. In order to control which limit is stronger, we define the quantity

$$\mathscr{E} \equiv \frac{k^2J}{a^2H^2}. \tag{4.44}$$

The case $\mathscr{E} \ll 1$ then corresponds applying the dRGT limit first, while $\mathscr{E} \gg 1$ corresponds to applying the sub-horizon limit first. To make this argument clearer, we rewrite this new parameter in terms of the relevant length scales in the problem

$$\mathscr{E} = \frac{l_H\, l_{GMG}}{\lambda^2}, \tag{4.45}$$

where $\lambda = a/k$ is the physical wavelength, the horizon length is $l_H \equiv 1/H$, while we define the length scale associated with varying mass parameters as $l_{GMG} \equiv J/H$. We summarise the possible values of the wavelength with respect to these scales in Figure 4.1. For a small departure from constant mass dRGT, the two characteristic lengths obey $l_H > l_{GMG}$.

For modes with wavelengths $\lambda \ll l_{GMG}$, the variation of the mass parameters is non-negligible, thus this case corresponds to the $\mathscr{E} \gg 1$ limit. For $l_{GMG} \ll \lambda \ll l_H$, the modes are sub-horizon, but the departure from standard dRGT is negligible, corresponding to $\mathscr{E} \ll 1$. One can see that $\mathscr{E}$ must always be less than one in this case as if $\mathscr{E} > 1$ then

$$l_H l_{GMG} > \lambda^2 \implies \lambda < \sqrt{J}/H, \tag{4.46}$$

which is not allowed as in the dRGT limit $J \to 0$.

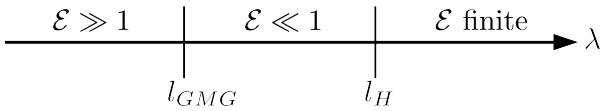

Figure 4.1: Schematic representation of different length scales. In this diagram, we assumed that $l_{GMG} < l_H$, which corresponds to small departures from standard dRGT.

4.3.3.2 Sound Speeds

Instead of obtaining the full dispersion relations of eigenmodes, we will make use of the fact that the frequency is dominated by the gradient term at high momenta. We first vary the action (4.38) with respect to the fields $\Psi^\dagger$, what results is the following equation of motion

$$\mathscr{K}\ddot{\Psi} + \left(\frac{\mathscr{G} - \mathscr{G}^T}{2} + 3H\mathscr{K} + \dot{\mathscr{K}}\right)\dot{\Psi} + \left(\frac{\dot{\mathscr{G}}}{2} + \frac{3H\mathscr{G}}{2} + \mathscr{M}\right)\Psi = 0. \tag{4.47}$$

For a monochromatic wave of the form $\Psi \propto e^{-i\int \omega dt}$, and in the sub-horizon limit we have $|\dot{\omega}| \ll \omega^2$, so equation (4.47) can be converted into an eigenvalue equation to solve ω

$$\det\left[-\omega^2\mathscr{K} - i\omega\left(\frac{\mathscr{G} - \mathscr{G}^T}{2} + 3H\mathscr{K} + \dot{\mathscr{K}}\right) + \left(\frac{\dot{\mathscr{G}}}{2} + \frac{3H\mathscr{G}}{2} + \mathscr{M}\right)\right] = 0\,. \tag{4.48}$$

Since deep in the horizon, frequency is $\omega = C_S(k/a)$, we solve the above equation for the squared sound speed C_S^2. The equation is quadratic in C_S^2. The first solution coincides with the sound speed of the k-essence field

$$C_{S,1}^2 = c_s^2. \tag{4.49}$$

The second one provides the sound speed of the scalar graviton $C^2_{S,2}$,

$$
\begin{aligned}
C_S^2 = &\Big(18M_p^2H^3\dot{L}\big[6M_p^2H(r-1)^2\kappa\dot{L}+a^2(36M_p^2H^4(r-1)^2\Gamma-18M_p^2H^3(r-1)\dot{L}\,,\\
&+3H(r-1)^2(\rho_X+P_X)\dot{L}+m^2M_p^2(2r-1)\dot{L}^2+6M_p^2H^2(\dot{L}\dot{r}-(r-1)\ddot{L})\big]\Big)^{-1}\times\\
&\Big\{-36M_p^4H^2(r-1)^2\kappa^2\dot{L}^2-6M_p^2a^2H\kappa\dot{L}\big[36M_p^2H^4(r-1)^2(r(r-3)-2)\Gamma)+18M_p^2H^3(r^2+r-2)\dot{L}\\
&-6H(r-1)^2(\rho_X+P_X)\dot{L}+m^2M_p^2(r-1)(3r-2)\dot{L}^2+6M_p^2H^2((r-3)\dot{L}\dot{r}+2(r-1)\ddot{L})\big]+a^4\Big(\\
&1296M_p^4H^8(r-1)^3(r+1)\Gamma^2-216M_p^4H^7(r-1)^2(6+r)\Gamma\dot{L}+3m^2M_p^2H(r-1)(3r-2)(\rho_X+P_X)\dot{L}^3\\
&+m^4M_p^4(r(3-2r)-1)\dot{L}^4108M_p^4H^6(r-1)\big[(3-2r)\dot{L}^2+2\dot{L}((3+r)\Gamma\dot{r}+r(r-1)\dot{\Gamma})-4(r^2-1)\Gamma\ddot{L}\big]\\
&-M_p^2H^3\dot{L}\big[m^2M_p^2(r(5+2r)-6)\dot{L}^2-3(r-3)(\rho_X+P_X)\dot{L}\dot{r}-6(r-1)(\rho_X+P_X)\ddot{L}\big]+36M_p^2H^5\dot{L}\big[\\
&-3P_X(r-1)^2(2+3r)\Gamma-3(r-1)^2(2+3r)\Gamma\rho_X+M_p^2((5r-9)\dot{L}\dot{r}-2(r-3)(r-1)\ddot{L})\big]-3H^2\dot{L}^2\big[\\
&3P_X^2(r-1)^2+6P_X(r-1)^2\rho_X+3(r-1)^2\rho_X^2+2m^2M_p^4\big((r-3)\dot{L}\dot{r}-(r-2)(r-1)\ddot{L}\big)\big]\\
&+18M_p^2H^4\Big[P_X(r-1)(6+(4c_s^2+3)r)\dot{L}^2+2m^2M_p^2(r-1)(r(5r-1)-2)\Gamma\dot{L}^2-6\rho_X\dot{L}^2+2r\rho_X\dot{L}^2\\
&-3c_s^2r\rho_X\dot{L}^2+4r^2\rho_X\dot{L}^2+3c_s^2r^2\rho_X\dot{L}^2-4M_p^2\dot{L}^2\dot{r}^2-6M_p^2\dot{L}\dot{r}\ddot{L}+M_p^2r\dot{L}\dot{r}\ddot{L}-2M_p^2\ddot{L}^2+2M_p^2r^2\ddot{L}^2\\
&+2M_p^2r\dot{L}^2\ddot{r}-2M_p^2(r-1)r\dot{L}L^{(3)}\Big]\Big).\Big\}
\end{aligned}
\tag{4.50}
$$

Both of the squared-sound speeds should be positive to avoid gradient instability. In order to see how the stability conditions in this section can be satisfied, in the next section we consider a minimal model of GMG, which allows us to gain an analytic understanding of the system.

Before discussing the minimal model, we briefly discuss the advantages of GMG with respect to pure dRGT massive gravity. Inspecting the form of the vector kinetic term 4.31 and the scalar kinetic term 4.40, and taking the dRGT limit $J \to 0$, we see that the kinetic terms vanish. This is the problem with cosmologies in dRGT massive gravity. However, clearly from the form of the Stuckelberg constraint equation in GMG, the same problem is not manifested and the kinetic terms remain finite.

4.4 Minimal Generalised Massive Gravity

In this section we consider small departures of constant mass parameters by allowing only one of the α_n parameters to vary. This allows us to solve the Stückelberg constraint

(4.15) and evaluate the stability conditions in a concrete framework. In this minimal setup, the free $\alpha_n(\phi^a\phi_a)$ functions in the action (4.1) are

$$\begin{aligned}
\alpha_0(\phi^a\phi_a) &= \alpha_1(\phi^a\phi_a) = 0\,,\\
\alpha_2(\phi^a\phi_a) &= 1 + m^2\alpha_2'\phi_a\phi^a\,,\\
\alpha_3(\phi^a\phi_a) &= \alpha_3\,,\\
\alpha_4(\phi^a\phi_a) &= \alpha_4\,.
\end{aligned} \tag{4.51}$$

For the background configuration (4.5), we have $(\phi^a\phi_a) = -f(t)^2$. The above choice is basically the constant mass dRGT theory, with the only difference that we allowed α_2 to vary with the Stückelberg fields. The variation is assumed to be small $\alpha_2' \ll 1$, so we expect the solutions to be close to dRGT. In this case, the contribution from mass term to the Friedmann equation m^2L should be approximately constant, and if it is responsible for late time acceleration, positive. The conditions we impose are the positivity of the effective cosmological constant, the squared-tensor mass, vector and scalar gradient and kinetic terms.

We expand all background quantities for small α_2',

$$\begin{aligned}
\xi &= \xi_0 + \alpha_2'\xi_1 + \mathcal{O}\left(\alpha_2'\right)^2\,,\\
J &= J_0 + \alpha_2' J_1 + \mathcal{O}\left(\alpha_2'\right)^2\,.\\
&\vdots
\end{aligned} \tag{4.52}$$

At leading order, i.e. $\mathcal{O}(\alpha_2')^0$, all background quantities reduce to standard (constant mass) dRGT expressions. The Stückelberg equation (4.15) at this order is simply $J_0 = 0$, solved by [119]

$$\xi_{0\pm} = \frac{1 + 2\,\alpha_3 + \alpha_4 \pm \sqrt{1 + \alpha_3 + \alpha_3^2 - \alpha_4}}{\alpha_3 + \alpha_4}\,. \tag{4.53}$$

Moreover, since $\dot{\xi} = (-H + \sqrt{\kappa}\,r/a)\xi$, we can use that $\dot{\xi}_0 = 0$ to determine

$$r_0 = \frac{a_0 H_0}{\sqrt{\kappa}}\,. \tag{4.54}$$

To determine which solution of ξ_0 we need to use, we can use the squared tensor mass in dRGT [119],

$$\Gamma_0 = \pm\left(\frac{a_0 H_0}{\sqrt{\kappa}} - 1\right)\xi_{0\pm}^2\sqrt{1 + \alpha_3 + \alpha_3^2 - \alpha_4}\,. \tag{4.55}$$

Provided that curvature never dominates the expansion, the tensor mass is real only for the solution ξ_{0+}, which in turn leads to a positive vector gradient term (4.32). We therefore consider this solution in the remainder of this section.

We now discuss the parameter region where we have a real solution that leads to a positive cosmological constant. By definition, ξ_0 is a positive quantity, so the parameter region where the solution ξ_{0+} in (4.53) is positive corresponds to

$$\Big(\alpha_3 < -1 \wedge \alpha_4 < -3(1+\alpha_3)\Big) \vee \Big(\alpha_3 > -1 \wedge \alpha_4 > -\alpha_3\Big). \tag{4.56}$$

On the other hand the contribution to the Friedmann equation from the mass term is then an effective cosmological constant

$$\begin{aligned} L_0 &= (\xi_0 - 1)\left[6 + 4\alpha_3 + \alpha_4 - (3 + 5\alpha_3 + 2\alpha_4)\xi_0 + (\alpha_3 + \alpha_4)\xi_0^2\right], \\ &= -\frac{1}{(\alpha_3+\alpha_4)^2}\left[(1+\alpha_3)(2+\alpha_3+2\alpha_3^2-3\alpha_4) + 2(1+\alpha_3+\alpha_3^2-\alpha_4)^{3/2}\right]. \end{aligned} \tag{4.57}$$

In order to have a real and positive cosmological constant, we need to satisfy these conditions:

$$\alpha_3 > -1 \wedge \frac{3 + 2\alpha_3 + 3\alpha_3^2}{4} < \alpha_4 < 1 + \alpha_3 + \alpha_3^2. \tag{4.58}$$

The $\mathcal{O}(\alpha_2')$ terms are relevant only in the stability conditions, and they are exclusively introduced by the function J, whose $\mathcal{O}(\alpha_2')^0$ contribution vanishes. We can solve background equations (4.12),(4.15) for J_1 to obtain

$$\begin{aligned} J_1 = \frac{m^2 a_0^2}{(\alpha_3+\alpha_4)^3\left(\sqrt{\kappa}\, a_0 H_0 - \kappa\right)}\Big[&2(1+\alpha_3)\left(3\alpha_3^2 + \alpha_3(5-2\alpha_4) - (\alpha_4-1)(\alpha_4+4)\right) \\ &+ 2\sqrt{1+\alpha_3+\alpha_3^2-\alpha_4}\left(4 + \alpha_3(7+3\alpha_3) - \alpha_4 - 2\alpha_3\alpha_4 - \alpha_4^2\right)\Big]. \end{aligned} \tag{4.59}$$

This is the main quantity needed when calculating the kinetic terms of perturbations. For the region (4.58), where cosmological constant and tensor mass is positive, the positivity of J requires

$$\alpha_2'(\alpha_3 - \alpha_4 + 1) > 0\,. \tag{4.60}$$

We now discuss the conditions for avoiding ghost and gradient instability in the vector and scalar perturbations.

Schematically the action for the vector modes takes the form,

$$S_V^{(2)} = \int d^3k\, dt\, a^3\, \mathcal{T}_V \left(|\dot{V}|^2 - \frac{c_V^2 k^2}{a^2}|V|^2 + \ldots\right), \tag{4.61}$$

where ellipsis denotes other terms in the action, e.g. mass. For the vector modes, both limits of the parameter $\mathscr{E}$ give the same result for the sub-horizon expressions, with

$$\mathscr{T}_V \to \frac{m^2 a_0^2 J_1 \xi_0 \alpha_2'}{1+r_0}, \qquad c_V^2 \to \frac{(1+r_0)\Gamma_0}{2 J_1 \xi_0 \alpha_2'}. \tag{4.62}$$

Since r_0 given by (4.54) is positive, and we chose the branch where $\Gamma_0 > 0$, avoiding both ghost and gradient instability requires

$$J_1 \alpha_2' > 0, \tag{4.63}$$

which, in the regime where we have positive cosmological constant, corresponds to the range (4.60).

For the scalar mode that corresponds to the matter field, there is no ambiguity; as long as the equivalent fluid obeys the null energy condition, and has a real propagation speed, it is stable. For the scalar graviton, the action is formally

$$S_S^{(2)} = \int d^3k dt a^3 \mathscr{T}_S \left(|\dot{S}|^2 - \frac{c_S^2 k^2}{a^2} |S|^2 + \dots \right). \tag{4.64}$$

As discussed in the previous section, the sub-horizon limit for $\mathscr{T}_S$ depends also on the limit for the parameter $\mathscr{E}$. We find

$$\mathscr{T}_S \to \begin{cases} \dfrac{3 m^2 a_0^4 H_0^2 \Gamma_0}{M_p^2 r_0^2} & , \ \mathscr{E} \gg 1 \\ \\ \dfrac{m^2 a_0^2 k^2 \xi_0 J_1 \alpha_2'}{2 M_p^2 (r_0+1)} & , \ \mathscr{E} \ll 1 \end{cases}. \tag{4.65}$$

On the other hand, the sound speed for the scalar graviton has the same value when $\mathscr{E}$ is send to the either of the two extremes,

$$c_S^2 \to \frac{2(1+r_0)\Gamma_0}{3 J_1 \xi_0 \alpha_2'} = \frac{4}{3} c_V^2 \tag{4.66}$$

Regardless of the $\mathscr{E}$ limit, scalar kinetic term and squared-sound speed are positive in the region where cosmological constant is positive, tensor mass is real ($\Gamma_0 > 0$) and the vector mode stability condition (4.63) is satisfied.

In Fig.4.2, we summarise all the conditions obtained in this section for the minimal model. We show the region of the parameter space that has positive cosmological constant and stable perturbations in Fig.4.2. Depending on the sign of α_2' parameter, the allowed region is either constrained in a finite area ($\alpha_2' > 0$) or is open ($\alpha_2' < 0$).

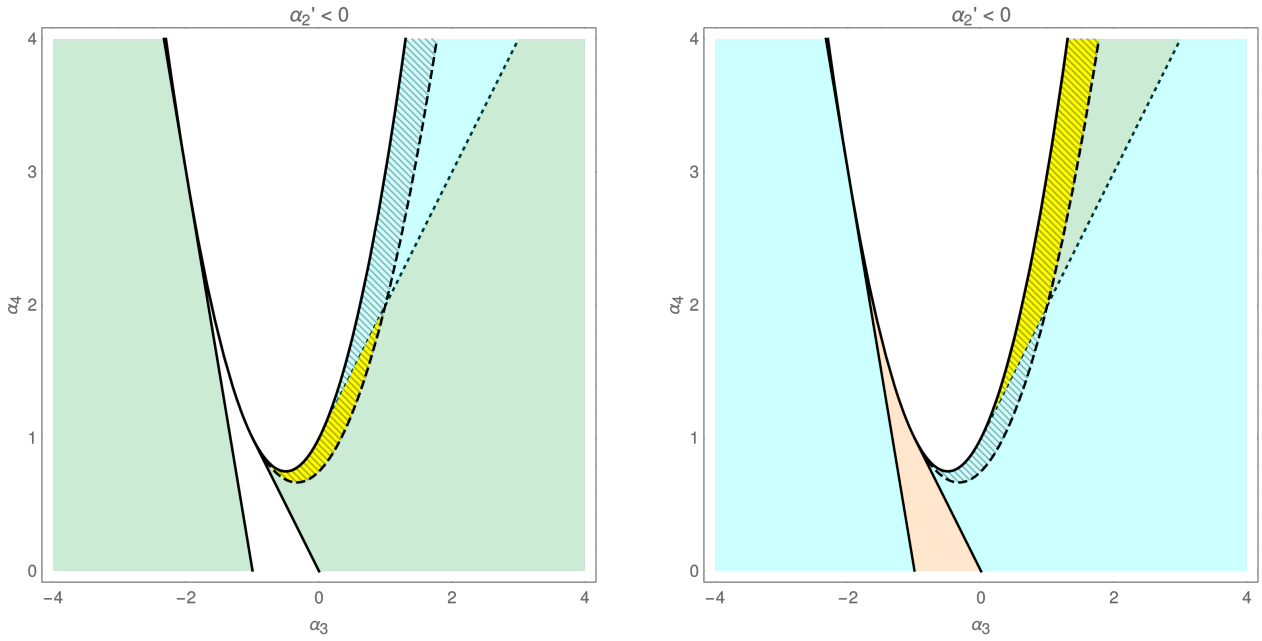

Figure 4.2: Allowed regions for $\alpha_2' > 0$ (left panel) and $\alpha_2' < 0$ (right panel). The blue region is $\xi_0 > 0$ (bounded by the solid lines), orange region is $\alpha_2' J_1 > 0$ (bounded with the solid and the dotted lines), the green region is where both conditions are satisfied. We also mark the positive cosmological constant as the shaded area (region between the solid and dashed lines). The region where all conditions are satisfied is highlighted in yellow.

4.5 Conclusions

In this chapter we have studied the cosmological perturbations of Generalised Massive Gravity with a k-essence fluid as the matter sector. We calculated the quadratic action for the tensor, vector and scalar sectors and identified the stability conditions. We found that, unlike in constant mass dRGT massive gravity, the kinetic terms for the vector and scalar gravitons are non-vanishing, and the background can be free from pathologies. As an example, we introduced a minimal version of the theory where only one mass function is allowed to vary slowly, which can be considered as a small variation from standard dRGT. In this model, the contribution to the Friedmann equation from the mass term is approximately a constant, which can be positive. In other words, the cosmology approximates GR with a cosmological constant. On the other hand, the effective cosmological constant continues to vary, and this variation allows the background to be perturbatively stable in a region of the parameter space, unlike constant mass dRGT theory. The tensor graviton has a time dependent mass and propagates at the speed

of light, while vector and scalar perturbations generically propagate at superluminal speeds. Superluminality is not generically a problem. However if the scalar graviton was sub-luminal, there would be a decay channel from photons to scalar gravitons [198] which has been heavily constrained by observations.

Our results in this chapter qualitatively match the results in [106], however quantatively the comparison is unclear when taking the dRGT limit. For instance, taking the dRGT limit on the vector action (4.29) results in a vanishing kinetic term, signalling the infinite strong coupling problem in dRGT cosmologies. However, taking the dRGT limit on the vector action in [106], the kinetic terms are non-vanishing. One possibility is that the apparent discrepancy is due to their choice of Fermi normal coordinates and the decoupling limit potentially probing a different background than the one considered here.

The cosmology of Generalised Massive Gravity has advantages over similar extensions outlined at the end of chapter 2. In addition to being an extension that has the same number of degrees of freedom as standard dRGT, the strong coupling problem can be tamed, unlike some other extensions. For instance, the problem of vanishing kinetic terms have been addressed in a similar manner in the mass-varying massive gravity [132], where the mass parameters are promoted to functions of a new dynamical field. On the other hand, in order to achieve self-acceleration the mass functions need to vary slowly, making the scalar and vector modes strongly coupled. In contrast, in this chapter, we showed that the scalar perturbations in the GMG theory effectively end up with finite kinetic terms provided that one considers modes that are sub-horizon and below the characteristic GMG length scale. This is an indication that the strong coupling problem of the dRGT theory becomes milder even with a slight variation of the model parameters.

As we have established a simple model of a stable cosmology with (approximate) self-acceleration, the next chapter presents a comprehensive study of the background cosmology and linear perturbations. To date, this is the only current Lorentz invariant model of massive gravity with 5 degrees of freedom that admits a stable cosmology.

CHAPTER 5

PHENOMENOLOGY OF GENERALISED MASSIVE GRAVITY

Introduction

In this section we study in detail the background cosmology and linear perturbations of the GMG theory. As was shown in the previous chapter, we found that a stable cosmology can be accommodated in the GMG framework. In this chapter, we build upon the analysis in chapter 4 and study the full background evolution, identifying the equation of state of dark energy and comparing the expansion history to that of ΛCDM. We then study linear perturbations at the level of the equations of motion, and derive the modified Poisson's equation sourced by the extra scalar mode. Due to the modified Poisson's equation, the effective Newton's constant is altered which results in a modification to the growth rate of structure, so we compare the growth rate in GMG to ΛCDM. Finally, we derive the equation of motion for the tensor modes and discuss their evolution. This chapter is based on published results in [199].

5.1 Background Set Up

We begin the study of the background by considering the background in chapter 4, except this time using the simplest matter source, a pressureless perfect fluid described by the

energy momentum tensor,

$$T_{\mu\nu} = \rho\, u_\mu u_\nu. \tag{5.1}$$

As mentioned in chapter 4, the results are independent of the matter field, and a pressureless perfect is the simplest choice for working at the level of the equations of motion. The background equations of motion take the same form as in (4.12). We then adopt the minimal model as studied in Chapter 4, which is outlined in (4.51) and derive the background Friedmann and Stückelberg equations, which take the following form:

$$3\left(H^2-\frac{\kappa}{a^2}\right)-m^2\left[-3(\xi-2)(\xi-1)(1-m^2f^2\alpha_2')+\alpha_3(\xi-1)^2(\xi-4)+\alpha_4(\xi-1)^3\right]=\frac{\rho}{M_p^2},$$

$$3\left(H-\frac{\sqrt{\kappa}}{a}\right)\left[(3-2\xi)(1-m^2f^2\alpha_2')+\alpha_3(\xi-3)(\xi-1)+\alpha_4(\xi-1)^2\right]=6m^2f(\xi-2)(\xi-1)\alpha_2'. \tag{5.2}$$

In order to investigate the mass term's effective equation of state and the Hubble rate, we first introduce dimensionless variables and re-write every dimensionful quantity in units of H_0 and M_p

$$\begin{aligned} m &\to H_0\mu, \\ H &\to H_0 h, \\ \kappa &\to a_0^2H_0^2\Omega_{\kappa 0}, \\ \alpha_2' &\to \frac{q}{\mu^2}, \\ \rho &\to \frac{3a_0^3H_0^2M_p^2\Omega_{m0}}{a^3}. \end{aligned} \tag{5.3}$$

With this choice the parameter q now controls how far away from dRGT we are, where $q\to 0$ is the dRGT limit. We also use Eq.(4.13) to replace $f(t)$ with $f(t)\to\frac{a\xi}{\sqrt{\kappa}}$. With these replacements, (5.2) becomes:

$$3\left(h^2-\frac{a_0^2\Omega_{\kappa 0}}{a^2}\right)-\mu^2\left[\frac{3(\xi-2)(\xi-1)(qa^2\xi^2-a_0^2\Omega_{\kappa 0})}{a_0^2\Omega_{\kappa 0}}+\alpha_3(\xi-1)^2(\xi-4)+\alpha_4(\xi-1)^3\right]=\frac{3a_0^3\Omega_{m0}}{a^3}, \tag{5.4}$$

$$3\left(h-\frac{\sqrt{\Omega_{\kappa 0}}a_0}{a}\right)\left[(3-2\xi)\left(1-\frac{qa^2\xi^2}{a_0^2\Omega_{\kappa 0}}\right)+\alpha_3(\xi-3)(\xi-1)+\alpha_4(\xi-1)^2\right]=\frac{6qa(\xi-2)(\xi-1)\xi}{a_0\sqrt{\Omega_{\kappa 0}}}. \tag{5.5}$$

The full evolution for h and ξ in terms of a can be determined by solving the above equations.

For numerical solutions, we will fix the following parameters [1]:

$$\Omega_{\kappa 0} = 3 \times 10^{-3}, \qquad \Omega_{m0} = 0.3, \qquad \alpha_3 = 0, \qquad \alpha_4 = 0.8\,, \tag{5.6}$$

where the specific choice of α_n parameters correspond to a simple choice within the allowed parameter space for stable cosmologies, depicted in Fig.4.2, as outlined in chapter 4. We stress that in this chapter we are not exploring all of the parameter space outlined in Fig.4.2. Our goal is to investigate the phenomenology and viability of the theory for a choice of parameters which give stability, at least at the level of the quadratic action for cosmological perturbations.

5.1.1 Varying q

In this section we study the background cosmology of GMG, whilst varying the parameter q which controls the deviation away from dRGT.

From here on we rescale q in the following way

$$Q \equiv 10^4 q\,, \tag{5.7}$$

as this is a typical value of q which will appear in later solutions and for the purpose of clarity later in the plots.

First, we outline the method taken to isolate the physical solution for $\xi(a)$ and $h(a)$. Initially, we keep μ arbitrary since it is sensitive to the value of Q and will later be fixed by requiring that the effective energy density from the mass term is consistent with the choice of cosmological parameters. We first solve the Stückelberg equation (5.5) for $h(\xi, a, Q, \mu)$. We then replace this solution in the Friedmann equation (5.4), which results in a 10th order polynomial equation for $\xi(a, Q, \mu)$. To choose the physical solution with positive real values, we compare the values of the roots of this equation to the value of ξ_{dRGT} at early times, where the contribution from α_2', or Q, is negligible. We do this because constant mass dRGT yields a cosmological constant with equation of state $w = -1$, which therefore means at early times we match ΛCDM. Whereas at late times, if we have departures from dRGT we can have departures also from ΛCDM. We set aside the roots that are closest. The solution for ξ in dRGT is [114],

$$\xi^{\pm}_{dRGT} = \frac{1 + 2\alpha_3 \pm \sqrt{1 + \alpha_3 + \alpha_3^2 - \alpha_4}\,\,+ \alpha_4}{\alpha_3 + \alpha_4}, \tag{5.8}$$

[1] Note we will allow $\Omega_{\kappa 0}$ to vary later in this section.

which arises from solving $J(\xi) = 0$, i.e. the quadratic equation (4.16) when the right hand side is zero. As shown in chapter 4, only the + root allows for a real tensor mass so we work with this solution. Using the parameter values (5.6), the solution is $\xi^{+}_{dRGT} = 2.80902$. We can then compare the solutions for ξ_{GMG} to this value. Fig. 5.1 shows the solution for ξ_{GMG} in comparison to ξ^{+}_{dRGT}: 8 of the other solutions do not converge to ξ^{+}_{dRGT} at early

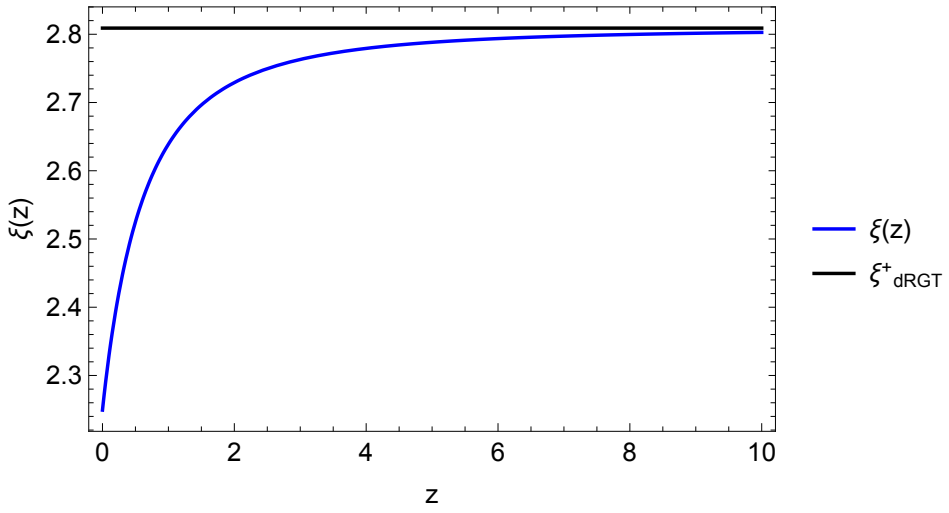

Figure 5.1: The black solid line shows the solution for ξ_{dRGT}. The blue curve shows the only physical solution for ξ_{GMG} which asymptotes to the solution for ξ_{dRGT} at early times. Parameter values taken are $Q = 1$ and those outlined in (5.6).

times, whilst the other ξ solution which tends to ξ^{+}_{dRGT} at early times does not satisfy both (5.4) and (5.5), leaving us with one physical solution.

We have reduced the system to one $\xi(a, Q, \mu)$ solution and its corresponding $h(a, Q, \mu)$ solution. We start by first determining the value of μ that would be compatible with the cosmological parameters today. We rewrite the Friedmann equation Eq.(5.4) as,

$$h^2 - \frac{a_0^2 \Omega_{\kappa 0}}{a^2} = \Omega_{DE} + \frac{a_0^3 \Omega_{m0}}{a^3}, \tag{5.9}$$

where we defined the density function for the effective dark energy as

$$\Omega_{DE} \equiv \frac{\rho_{DE}}{3H_0^2 M_p^2} = \frac{\mu^2 L}{3} = \frac{\mu^2}{30}(\xi - 1)\left[8(\xi - 1)^2 + (\xi - 2)\left(\frac{Q\,\xi^2 a^2}{a_0^2} - 30\right)\right]. \tag{5.10}$$

For a given value of Q, we evaluate this equation today $a = a_0$ using the root $\xi(a_0, Q, \mu)$. Since today we have $\Omega_{\kappa 0} + \Omega_{m0} + \Omega_{DE0} = 1$, we fix the value of μ using this relation.

We now investigate the effect of varying the parameter Q on the expansion rate and the equation of state of the effective fluid for the mass term. The effective equation of

state can be obtained by identifying the contribution $(P^{DE}+\rho^{DE})$ from the acceleration equation, i.e. the second line of Eq. (4.12)

$$P^{DE}+\rho^{DE}=-M_p^2 m^2 J(r-1)\xi\,, \tag{5.11}$$

then using the effective density defined in Eq.(5.10). As a result, we find

$$w_{DE}=\frac{P_{DE}}{\rho_{DE}}=-1-\frac{\mu^2 J(r-1)\xi}{3\Omega_{DE}}=-1-\frac{J(r-1)\xi}{L}\,. \tag{5.12}$$

The functions J and L, defined in (4.14), are functions of ξ and a only, so using the solution $\xi(a)$, we can determine their evolution with a. For the quantity r, we use Eq.(4.13) to write

$$r=\frac{a}{\sqrt{\kappa}}\left(H+\frac{\dot{\xi}}{\xi}\right), \tag{5.13}$$

which can be calculated by using the solutions h, ξ and its derivative.

We can now discuss the effect of Q on the evolution. In Fig.5.2 we show the effect of varying Q on the Hubble rate and the equation of state. Smaller values of Q lead to smaller deviations of the Hubble rate from the ΛCDM value, which are typically at 1% level. This is due to Q controlling how close we are to the dRGT background where the effective density from the mass term is constant. We note that the normalisation of μ parameter ensures that the value of H recovers the ΛCDM value today. The evolution of the equation of state parameter shows a late time departure from a cosmological constant, with maximum deviation at a 20% level with $w_{DE}<-1$, followed by a bounce back towards $w_{DE}=-1$. Notably, the value of Q does not affect the size of this departure but only the time it occurs. This behaviour can be understood as follows. The departure from dRGT is introduced in α_2 via Eq.(4.51)

$$\alpha_2=1-\frac{Q}{10^4}f^2, \tag{5.14}$$

Since f is an increasing function of time, with $f^2\propto(1+z)^{-2}$ a smaller value of Q will simply decrease the redshift where the deviation from dRGT starts and delays the bounce in w_{DE} to later times. Conversely, a large value of Q will cause the bounce at an earlier time, thus allowing w_{DE} to increase back up and cross $w_{DE}=-1$. From (5.12), this crossing occurs when either $J\sim 0$ or $r\sim 1$. When J crosses zero, the solutions collapse to the self-accelerating solutions of dRGT, and scalar and vector modes becomes infinitely strongly coupled [119]. On the other hand, there is no a priori reason that prevents

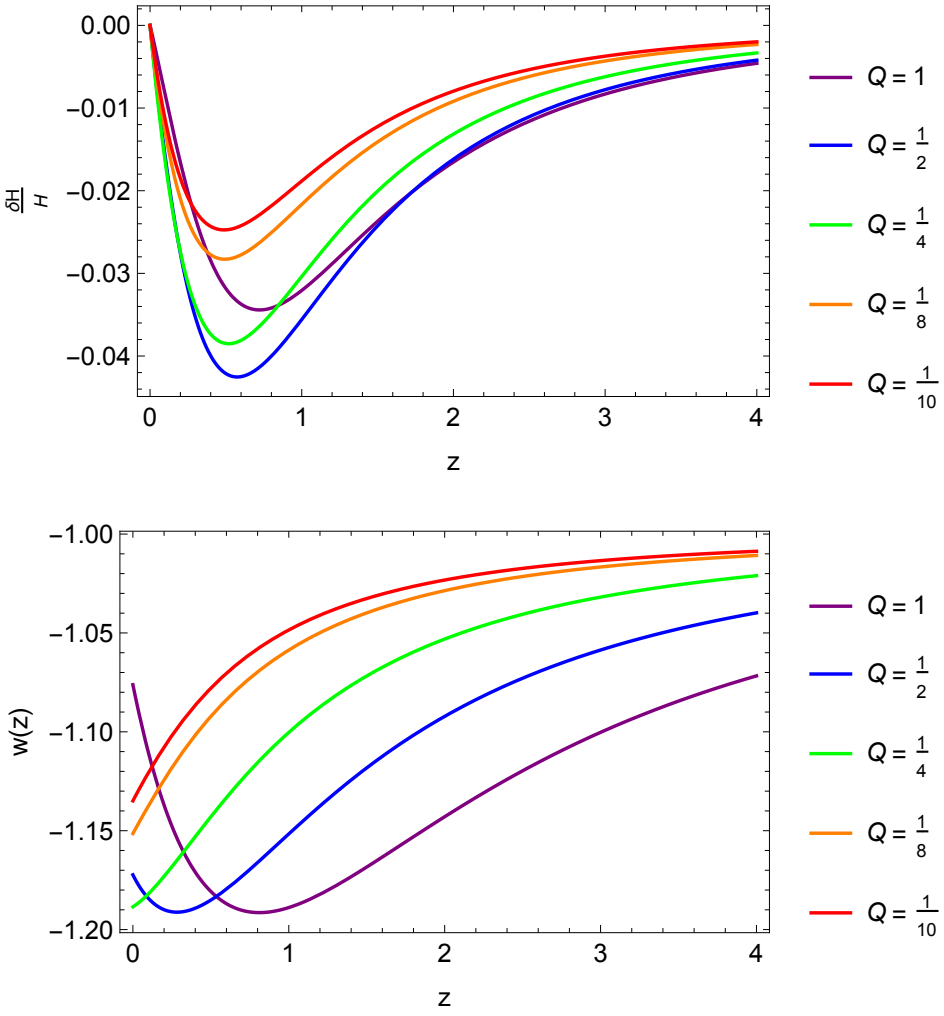

Figure 5.2: Left panel shows fractional deviation in the Hubble rate in GMG compared to ΛCDM with varying values of Q, where $\frac{\delta h}{h} = \frac{h - h_{\Lambda\text{CDM}}}{h_{\Lambda\text{CDM}}}$. The right panel shows the equation of state $w(z)$.

r from crossing 1. In the next section, we will determine the conditions for which the background solution exists and how, if at all, it breaks down.

To study the regime of applicability of the solution, we will impose the perturbative stability conditions derived in Chapter 4. We then evolve the background equations until one of the above conditions are broken, which then results in the theory no longer being applicable as a dark energy model.

5.1.2 Case Study: $Q = 1$

In this section we give a concrete example of the cosmological evolution for a value of $Q = 1$ with $\Omega_{\kappa 0} = 3 \times 10^{-3}$. We classify the evolution into several points.

1. The evolution starts at $z = 10$, at early times the solution tracks the dRGT evolution.

2. The equation of state undergoes a decrease away from $w = -1$ reaching a minimum value of $w \sim -1.19$ at $z \sim 0.8$, and there is a small deviation away from the ΛCDM value shown in the Hubble rate at about 2% level.

3. w then starts to bounce back to $w = -1$ and the difference in the Hubble rate decreases as it evolves towards $z = 0$ and into the future, past $z = 0$.

4. The critical point in the evolution now occurs. At $z_c \sim -0.178$, w crosses -1 which is caused by $r = 1$. At this point Γ also crosses 0 which generates a tachyonic instability in the tensor sector from the following condition,

$$M_T^2 = m^2 \Gamma > 0\,. \tag{5.15}$$

   This is not problematic though as the instability takes the age of the universe to develop as the mass is typically of order Hubble. However, as the sound speeds of the vector modes are also proportional to Γ,

$$C_V^2 \propto \frac{(1+r)\Gamma}{2J\xi}\,, \tag{5.16}$$

   and the coefficient of the scalar kinetic term is proportional to Γ in the $\mathscr{E} >> 1$ case (see chapter 4),

$$\mathscr{T}_S \propto \Gamma \tag{5.17}$$

   with J is still positive, the vector modes become unstable and a ghost mode is generated in the scalar sector, meaning the background solution is no longer valid.

We see that $Q = 1$ marginally misses the point of instability. Requiring that the solution does not break down before $z = 0$, we will only consider the values $Q \leq 1$.

The generation of future instabilities is not a cause for concern here. This can be seen by the nature of the instabilities generated, which is a gradient instability in the vector sector, but more importantly a ghost mode in the scalar sector in the limit $\mathscr{E} >> 1$.

As we approach the onset of the instability, the coefficient of the kinetic term for the scalar mode approaches zero. This is an indication of strong coupling which means we are entering a regime of the theory which is beyond the reach of the EFT. Therefore, the instability is generated at an energy scale beyond which the theory can describe. The upshot of this means we need to know the full UV completion to describe what is happening around the point of the instability, i.e. into the future, and is therefore not a concern for our model. Furthermore, the time of generation of the instability is sensitive to the functional form chosen for α_2' as in (4.51). Therefore, it is postulated that changing the functional form can push the instability further into the future. In this work we are mainly concerned with finding a proof of principle example and finding the observational signatures of a stable model in the present universe.

5.1.3 Varying $\Omega_{\kappa 0}$

The evolution of the universe is also sensitive to the value of $\Omega_{\kappa 0}$. As can be seen from (5.4), shifting the value of $\Omega_{\kappa 0}$, under the condition that $\Omega_{\kappa 0} + \Omega_{m0} + \Omega_{DE0} = 1$, effectively shifts the value of Ω_{DE0}, whilst keeping Ω_{m0} fixed. Fixing $Q = 1$, we plot the Hubble rate and the equation of state in Fig. 5.3. Notably, a higher value of $\Omega_{\kappa 0}$ pushes the time the instability occurs further into the future. The fractional deviation in the Hubble rate increases for higher values of $\Omega_{\kappa 0}$. For a value of $\Omega_{\kappa 0} = 6 \times 10^{-3}$, the deviation is around 4% at $z \approx 0.8$. There are two effects one can see here. For a fixed value of $\Omega_{\kappa 0}$, decreasing Q pushes the time the instability is generated into the future. Furthermore, for a fixed Q increasing $\Omega_{\kappa 0}$ also pushes the time the instability is generated into the future.

In this section, we have outlined a case study of the cosmological evolution in the minimal model of GMG. We find that the expansion history of the Universe can be matched for values of $Q \leq 1$. For a value of $Q = 1$, we can describe the evolution up to a redshift of $z \approx -0.2$ before a gradient instability is generated in the vector sector. Decreasing the value of Q or increasing $\Omega_{\kappa 0}$, pushes the time the instability is generated further into the future. The equation of state undergoes a bounce from $w < -1$ to $w = -1$ and has a dynamical dark energy–like effect which could be constrained using observations.

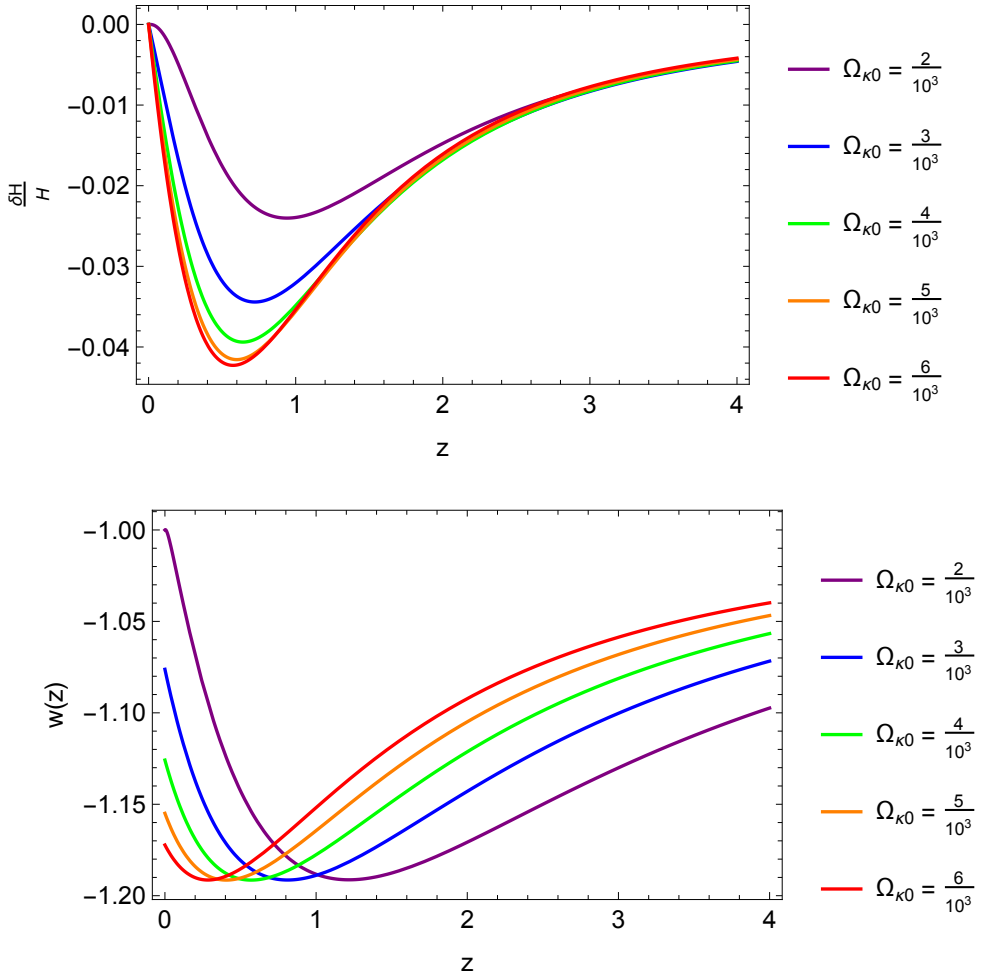

Figure 5.3: For different values of $\Omega_{\kappa 0}$, top panel shows fractional deviation in the Hubble rate in GMG compared to ΛCDM, $\frac{\delta h}{h} = \frac{h - h_{\Lambda\text{CDM}}}{h_{\Lambda\text{CDM}}}$, and the bottom panel shows the equation of state.

5.2 Linear Perturbations

In this section we outline the study of linear perturbations and the derivation of the Poisson's equation to determine the effect of GMG on the growth of structure.

5.2.1 Set up

Only the linear scalar perturbations are relevant for the derivation of the Poisson's equation, so we decompose the g-metric as:

$$g_{\mu\nu} dx^\mu dx^\nu = -(1+2\phi) dt^2 + a\,\partial_i B\, dt\, dx^i + a^2 \left(\Omega_{ij} + h_{ij}\right) dx^i dx^j, \tag{5.18}$$

with h_{ij} decomposed as

$$h_{ij} = 2\psi\,\Omega_{ij} + \left(D_i D_j - \frac{1}{3}\Omega_{ij} D_l D^l\right) S\,. \tag{5.19}$$

In this set up, D_l is the covariant derivative compatible with the 3-metric Ω_{ij}. Spatial indices are raised and lowered with Ω^{ij}. Perturbations to the matter sector are introduced via $\rho(t,x^i) = \rho(t) + \delta\rho(t,x^i)$ and $u^\mu = (1-\phi, \partial^i v)$, where v is the longitudinal component of the velocity perturbation, this leads to the following form for $T^\mu_{\ \nu}$:

$$\begin{aligned} T^0_{\ 0} &= -(\delta\rho + \rho)\,, \\ T^0_{\ i} &= a\rho(\partial_i B + a\partial_i v)\,, \\ T^i_{\ 0} &= -\rho\partial^i v\,, \\ T^i_{\ j} &= 0\,. \end{aligned} \tag{5.20}$$

We exhaust the gauge freedom by fixing the unitary gauge, $\delta\phi^a = 0$, thus the fiducial metric $f_{\mu\nu}$ remains unperturbed. Using the metric decomposition (5.18), along with Eqs.(4.6) and (5.20), we calculate the perturbed Einstein's equations. Schematically, we end up with 4 coupled Einstein's equations denoted by $\mathscr{E}^{00}, \mathscr{E}^{0i}, \mathscr{E}^{tr}, \mathscr{E}^{tl}$, where "tr" and "tl" denote the trace and traceless parts of the (ij) equation, respectively.

The unitary gauge that we are using leaves the metric and matter perturbations intact. In order to compare with GR, it is useful to define gauge invariant variables that can be constructed out of the available fields. We start with the coordinate transformation

$$x^\mu \to x^\mu + \delta x^\mu, \tag{5.21}$$

where $\delta x^\mu = (\delta x^0, \Omega^{ij}\partial_j \delta x)$ is of order of perturbations. Under (5.21) the metric and matter perturbations transform as,

$$\begin{aligned} \phi &\to \phi + \delta\dot{x}^0\,, \\ B &\to B + a\,\delta\dot{x} - \frac{1}{a}\delta x^0\,, \\ \psi &\to \psi + \frac{1}{3} D_i D^i \delta x + H\,\delta x^0\,, \\ S &\to S + 2\delta x\,, \\ \delta\rho &\to \delta\rho + \dot{\rho}\,\delta x^0\,, \\ v &\to v - \delta\dot{x}\,. \end{aligned} \tag{5.22}$$

With these transformations, we can construct the gauge-invariant variables that are analogues of the Newtonian gauge in GR:

$$\begin{aligned}
\Phi &= \phi - \partial_t \zeta\,, \\
\Psi &= \psi - H\zeta - \frac{1}{6} D^i D_i S\,, \\
\tilde{\delta\rho} &= \delta\rho - \dot{\rho}\,\zeta\,, \\
\tilde{v} &= v + \frac{1}{2}\dot{S}, \qquad (5.23)
\end{aligned}$$

where

$$\zeta \equiv -aB + \frac{1}{2}a^2\dot{S}. \qquad (5.24)$$

We also define a convenient combination for density contrast

$$\Delta \equiv \frac{\tilde{\delta\rho}}{\rho} - 3a^2 H\tilde{v}\,, \qquad (5.25)$$

and then substitute (5.23) and (5.25) into the equations of motion (3.6)[2] and expand all perturbation variables in scalar harmonics,

$$\begin{aligned}
\Psi &= \int d^3k\, \Psi_{|\vec{k}|}\, Y(\vec{k},\vec{x}) \\
S &= \int d^3k\, S_{|\vec{k}|}\, Y(\vec{k},\vec{x}) \\
&\vdots \qquad (5.26)
\end{aligned}$$

where the scalar harmonics satisfy $D^i D_i Y \to -k^2 Y$. We also impose (4.12), (4.15) and (5.13) to yield the perturbed Einstein equations with one covariant and one contravariant index outlined below. For the $0i$ equation, we take out the overall covariant derivative D_i. For the traceless part of the ij equation, we remove the overall $D^i D_j - \frac{\delta^i_j}{3} D_l D^l$ operator.

[2]Note here that due to the f metric being non-dynamical, we only have the g metric equations.

The equations of motion are given by

$$
\begin{aligned}
\mathscr{E}^{00} &= k^2 m^2 J\xi S + 6m^2 aHJr\xi B - \frac{4(k^2+3\kappa)\Psi}{a^2} + a^2 H\left(\frac{6\tilde{v}\rho}{M_p^2} - 3m^2 Jr\xi\dot{S}\right) \\
&\quad + 2\left(\frac{\Delta\rho}{M_p^2} + 6H^2\Phi - 3m^2 J\xi\Psi - 6H\dot{\Psi}\right), \\
\mathscr{E}^{0i} &= -2m^2 aJr^2\xi B - \frac{a^2(r+1)2\tilde{v}\rho}{M_p^2} + m^2 a^2(r+1)J(r-1)\xi\dot{S} - 4(r+1)(H\Phi - \dot{\Psi}), \\
\mathscr{E}^{tr} &= -4\frac{(k^2+6\kappa)\Phi + (k^2+3\kappa)\Psi)}{a^2} \\
&\quad + 3m^2 a\left[Jr\xi(2\dot{B} - \sqrt{\kappa}(r-1)\dot{S}) + 2B\left[H(2\Gamma + J\xi(3r-2)) + \xi((r-1)\dot{J} + J\dot{r})\right]\right] \\
&\quad + 2\left[k^2 m^2\Gamma S + 3\sqrt{\kappa}m^2 r(r-1)J\xi B + 3m^2(r-2)J\xi\Phi - \frac{6\rho\Phi}{M_p^2} - 6m^2\Gamma\Psi + 6H(3H\Phi + \dot{\Phi} - 3\dot{\Psi})\right] \\
&\quad - 3m^2 a^2\left[\left[\xi((r-1)\dot{J} + J\dot{r}) + 2H(\Gamma + J\xi(2r-1))\right]\dot{S} + rJ\xi\ddot{S}\right] - 12\ddot{\Psi}, \\
\mathscr{E}^{tl} &= m^2 a^2 S\Gamma - 2(\Phi + \Psi).
\end{aligned}
\tag{5.27}
$$

The conservation of the energy-momentum tensor, $\nabla_\mu T^\mu_{\ \nu} = 0$ yields the Euler $\mathscr{E}^{eu}$ and continuity $\mathscr{E}^{co}$ equations for the matter fluid,

$$
\begin{aligned}
\mathscr{E}^{eu} &= \left[2(k^2+3\kappa) + \frac{3a^2\rho}{M_p^2} - 3a^2(4H^2 + m^2 J\xi(r-1))\right]\tilde{v} - 2(3a^2 H\tilde{v} + \dot{\Delta} + 3\dot{\Psi}), \\
\mathscr{E}^{co} &= \Phi + a^2(2H\tilde{v} + \dot{\tilde{v}}).
\end{aligned}
\tag{5.28}
$$

5.2.2 Linear perturbation analysis

Looking at the form of the traceless equation $\mathscr{E}^{tl}$, we see that S acts as a source of anisotropic stress. In GR, the equation for the anisoptropic stress vanishes, ie: $\Phi + \Psi = 0$. Whilst in GMG, we have

$$
\Phi + \Psi = \frac{1}{2}m^2 a^2\Gamma S. \tag{5.29}
$$

This reveals that the dynamical scalar degree of freedom S could mediate a fifth force which would alter the structure of the Poisson's equation. Our goal is to investigate if S affects structure formation, and what scales the modifications to gravity appear at due

to the presence of this extra mode. To do this, we first derive the equation of motion for S. We start by solving the matter equations for $\dot{\tilde{v}}$ and $\dot{\Delta}$,

$$\dot{\tilde{v}} = -\frac{2a^2H\tilde{v}+\Phi}{a^2}, \qquad \dot{\Delta} = 3H\Phi + \tilde{v}\left[k^2+3\kappa+\frac{3}{2}m^2a^2(1-r)J\xi+\frac{3a^2\rho}{2M_p^2}\right]-3\dot{\Psi}, \tag{5.30}$$

and substitute it into the equations of motion to reduce the system to the 4 Einstein's equations. We next solve the constraint equations $\mathscr{E}^{00}$ and $\mathscr{E}^{0i}$ for the non-dynamical degrees of freedom Φ and B,

$$\Phi = \frac{1}{12M_p^2a^2H^2}\Big[-4(k^2+3\kappa)M_p^2r\Psi - 3a^4H(2\tilde{v}\rho+m^2M_p^2J\xi\dot{S})+$$
$$a^2\Big(k^2m^2Jr\xi S+2r\rho\Delta-6m^2M_p^2J\xi r\Psi+12M_p^2H\dot{\Psi}\Big)\Big]$$

$$B = \frac{r+1}{6m^2M_p^2a^3HJr\xi}\Big[-a^2(m^2M_p^2J\xi(k^2S-6\Psi)+2\rho\Delta)+4(k^2+3\kappa)M_p^2\Psi+3m^2M_p^2a^4HJ\xi\dot{S}\Big]. \tag{5.31}$$

Upon substituting (5.31) and the time derivatives $(\dot{\Phi},\dot{B})$ into $\mathscr{E}^{tr}$ and $\mathscr{E}^{tl}$, we end up with two equations $\mathscr{E}^{tr}$ and $\mathscr{E}^{tl}$ in terms of $(\Psi,S,\tilde{v})$ and their time derivatives. We then solve $\mathscr{E}^{tr}$ for $\Psi(S,\dot{S},\ddot{S},\tilde{v},\Delta)$ and replace into $\mathscr{E}^{tl}$ as well as the time derivative $\dot{\Psi}$. Upon doing this, we obtain a second order differential equation for S sourced by matter perturbations $(\Delta,\tilde{v})$.

$$\mathscr{A}\ddot{S}+H_0\mathscr{B}\dot{S}+H_0^2\mathscr{C}S+\mathscr{D}\Delta+H_0\mathscr{F}\tilde{v}=0. \tag{5.32}$$

The dimensionless coefficients $(\mathscr{A},\mathscr{B},\mathscr{C},\mathscr{D},\mathscr{F})$ are functions of (k,z) and various background quantities relating to the GMG theory. They are too complicated to present here, but they will be discussed in certain limits later in the chapter. It is pertinent to note that no assumptions have been made at this stage so this equation is the most general equation one can write down for the scalar S.

In order to gain an analytic understanding of the system, we adopt the minimal model (4.51) once more, in which we expand each of the background GMG quantities around their dRGT values as below:

$$J = \frac{Q}{10000}J_1+\mathscr{O}\left(\frac{Q}{10000}\right)^2,$$
$$\Gamma = \Gamma_0+\frac{Q}{10000}\Gamma_1+\mathscr{O}\left(\frac{Q}{10000}\right)^2,$$
$$r = \frac{aH}{\sqrt{\kappa}}+\frac{Q}{10000}r_1+\mathscr{O}\left(\frac{Q}{10000}\right)^2,$$

where the leading order terms J_1 and Γ_0 are not necessary for this discussion and can be found in Chapter 4 in equations (4.59) and (4.55) respectively.

A peculiar feature of the scalar terms in the UV is the appearance of a new energy scale H/J in addition to the scale of expansion H. For small departures from dRGT we have $J < 1$. Depending on the relation to these scales, the subhorizon modes $k \ll aH$ can have two distinct behaviours. We define the following dimensionless parameter, as in chapter 4, to distinguish between the cases [197]

$$\mathscr{E} \equiv \frac{k^2 J}{a^2 H^2}\,. \tag{5.33}$$

There are three qualitatively distinct limits:

1. $1 \ll \mathscr{E} \ll \frac{k^2}{a^2H^2}$: subhorizon modes with momenta larger than the new scale H/J. For these modes, the variation of the mass parameters due to GMG affect the UV behaviour. These cases are captured by first performing the subhorizon (UV) expansion, then the dRGT expansion.

2. $\mathscr{E} \ll 1 \ll \frac{k^2}{a^2H^2}$: subhorizon modes with wavelengths larger than the new scale. The leading order terms in the UV expansion for these modes are identical to dRGT, although the deviation due to GMG does not lead to infinite strong coupling. These cases correspond to first carrying out the dRGT expansion, then the subhorizon expansion.

3. $\frac{k^2}{a^2H^2} \ll 1$: superhorizon modes. There is no ambiguity for this case, and it corresponds to taking the superhorizon limit.

For varying values of Q, and for the parameters given in Eq. (5.6), we plot $\mathscr{E}(k)$ for $z = 10$ and $z = 0$. The result is shown in Fig. (5.4). $\mathscr{E}$ being larger for a specified value of k at $z = 0$ is expected as $\mathscr{E} \propto J$: at later times the departure from the early dRGT (or ΛCDM) behaviour, controlled by J, increases.

This feature is also seen in Fig.5.2, deviations away from ΛCDM occur at late times, whilst at early times ΛCDM is recovered. At $z = 10$, larger values of Q favour a larger $\mathscr{E}$ however at $z = 0$ this is not the case: the $Q = 1$ line coincides with the $Q = 1/4$, whilst $Q = 1/2$ gives the largest value of $\mathscr{E}$. This feature corresponds to the bounce of the effective equation of state observed in Fig.5.2.

With this information, we investigate the coefficients in (5.32) and derive which terms are dominant in the quasi-static approximation (QSA) [193], as these terms will become relevant when deriving the Poisson's equation. The quasi-static approximation amounts

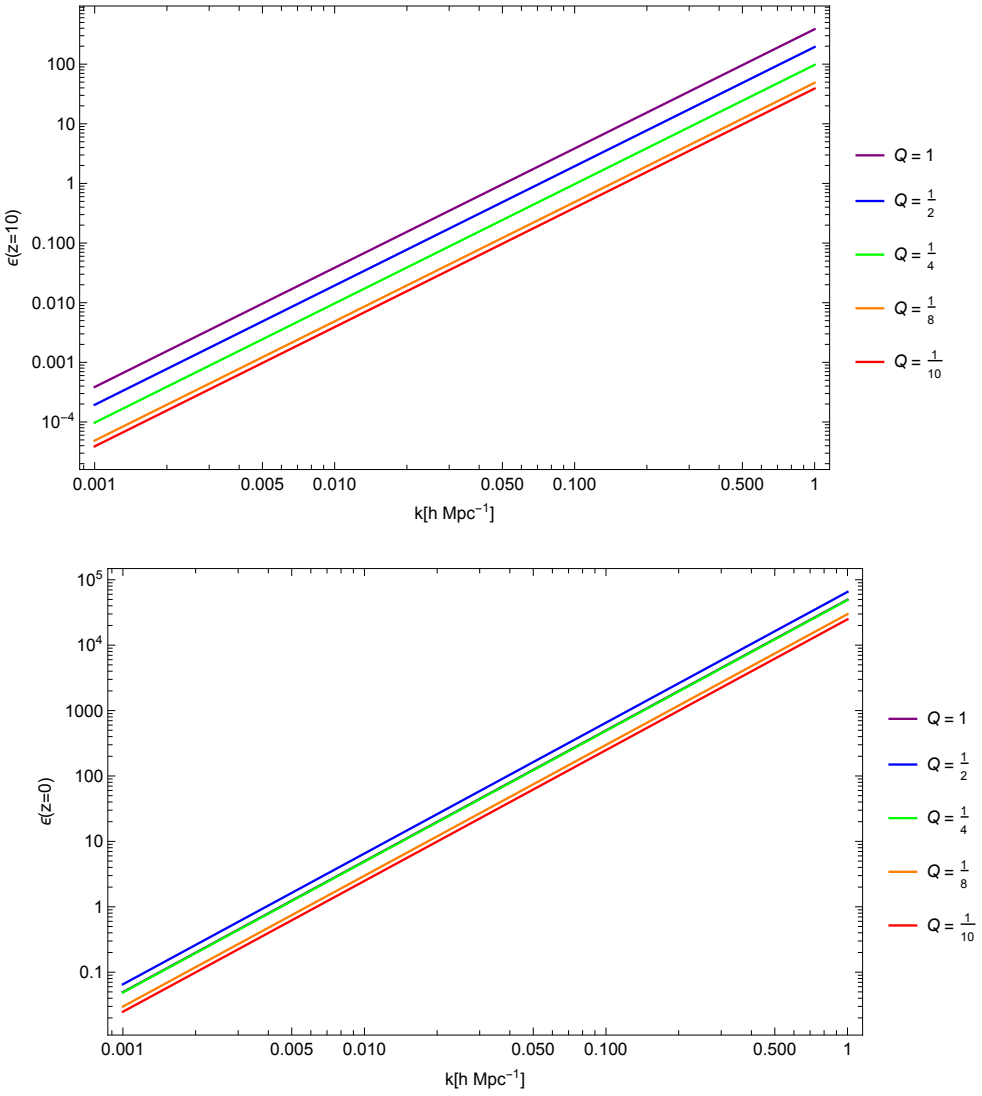

Figure 5.4: Bottom panel shows $\mathscr{E}$ evaluated at $z = 0$, whilst the top panel is $z = 10$.

to assuming $\dot{\beta} \sim H\beta \ll \partial_i \beta$ for any perturbation β, i.e. we neglect time derivatives with respect to spatial derivatives. In terms of harmonic modes, it is an expansion for large $k/(aH)$. In Fig.5.5, we present a plot of each coefficient at $z = 0$ to justify this approximation.

In Fig.5.5, the 3 regimes can be clearly identified. From right to left: regime 1 is $\mathscr{E} \gg 1$, regime 2 (the intermediate regime) is the subhorizon limit with $\mathscr{E} \ll 1$ and regime 3 is the superhorizon limit. In Appendix D, we give explicit expressions of the analytic approximations of these functions in each of the 3 regimes. We now apply the QSA to (5.32) as the Poisson's equation is defined in this limit.

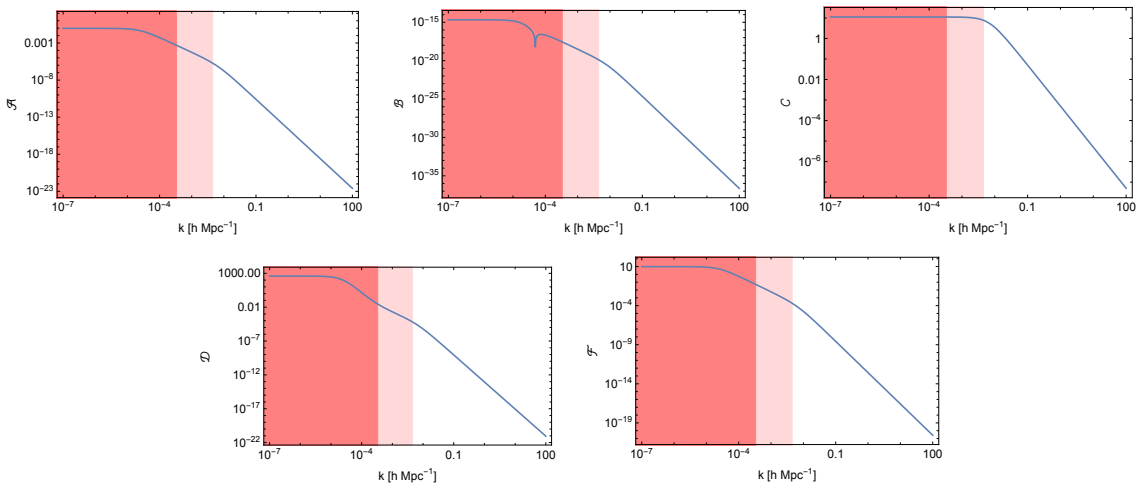

Figure 5.5: Coefficients in (5.32) at $z = 0$ as a function of k. The left hand side is large scales, whilst the right hand side is small scales. The dark shaded region corresponds super horizon modes with $k < \frac{h}{3000}\text{Mpc}^{-1}$. The light shaded region corresponds to modes in the region $\frac{h}{3000}\text{Mpc}^{-1} < k < k_*$, where k_* is the wave number corresponding to $\mathscr{E}|_{z=0} = 1$. The whole shaded region corresponds to $\mathscr{E} < 1$, whilst the area with no shading corresponds to modes with $k > k_*$ which represents $\mathscr{E} > 1$.

The QSA is valid on scales $10^{-2}\,h\,\text{Mpc}^{-1} \lesssim k$ while the linear theory is applicable up to $k \lesssim 0.1\,h\,\text{Mpc}^{-1}$, so we consider the regime in which $\mathscr{E} \gg 1$, which corresponds to the non-shaded area of Fig. 5.5.

5.2.3 Poisson's Equation

In the regime of interest, given by $\mathscr{E} \gg 1$, we calculate the following ratios of the coefficients in (5.32) to determine which are the dominant terms in the QSA. We are in essence, comparing the time derivative terms $(\ddot{S}, \dot{S})$ to the non- time derivative term S. Observing that $\tilde{v} \sim \dot{\Delta}/k^2$ from the Euler equation (5.28), we are also comparing it to the Δ term:

$$\left(\frac{H^2}{H_0^2}\right)\frac{\mathscr{A}}{\mathscr{C}} \sim \frac{a^2H^2}{k^2}\mathscr{O}(J), \qquad \left(\frac{H}{H_0}\right)\frac{\mathscr{B}}{\mathscr{C}} \sim \frac{a^2H^2}{k^2}\mathscr{O}(J), \qquad \left(\frac{H_0H}{k^2}\right)\frac{\mathscr{F}}{\mathscr{D}} \sim \frac{a^2H^2}{k^2}. \tag{5.34}$$

From (A.7), we see that in this regime, $(\ddot{S}, \dot{S}, \tilde{v})$ can be neglected as their coefficients are suppressed with respect to (S, Δ) by a^2H^2/k^2. In this approximation the master equation (5.32) reduces to the algebraic equation,

$$H_0^2\mathscr{C}S + \mathscr{D}\Delta = 0, \tag{5.35}$$

for which the solution for $S(\Delta)$ at leading order in k is,

$$
\begin{aligned}
S = -\frac{\mathscr{D}}{H_0^2\mathscr{C}}\Delta = \left[2a^2J\xi r^2(J\xi-2\Gamma)\rho\right]\frac{\Delta}{k^2}\times \\
\Big\{2\kappa M_p^2 J\xi r(2(r-1)\Gamma+J(r+2)\xi)-2\sqrt{\kappa}M_p^2 aJ\xi r(H(4(r+1)\Gamma+J\xi(r-4))-2J\dot{\xi}) \\
+a^2\Big[4M_p^2H^2\big(2(r+1)\Gamma^2+J\xi(r-4)\Gamma-2J^2\xi^2(r-1)\big) \\
-4M_p^2H\xi(\Gamma(2(r+1)\dot{J}+J\dot{r})-J(\xi(J\dot{r}-\dot{J}(r-2))+r\dot{\Gamma})) \\
+\xi\big(m^2M_p^2J^3(2-3r)r\xi^2+2J^2\xi r(m^2M_p^2(3r-1)\Gamma+\rho) \\
+2M_p^2(r+1)\dot{J}^2\xi-2J(r(\Gamma\rho+M_p^2\xi\ddot{J})-M_p^2\xi\dot{J}\dot{r})\big)\Big]\Big\}^{-1}.
\end{aligned}
\tag{5.36}
$$

Manipulating the equations of motion of linear perturbations, we can derive a Poisson's equation for the Newtonian potential sourced by the matter perturbations. We solve $(\mathscr{E}^{00},\mathscr{E}^{0i},\mathscr{E}^{\rm tr},\mathscr{E}^{\rm tl})$ for $(B,\dot{B},\Psi,\Phi)$. After applying the QSA limit, the equation takes the form:

$$
\Phi=\frac{1}{4}m^2a^2(2\Gamma-J\xi)S+\frac{1}{8rk^2}\left[3m^2a^4(m^2J^2r\xi^2+H^2(4\Gamma-2J\xi))S+8ra^2\left(m^2\frac{3}{4}\kappa J\xi S-\frac{\Delta\rho}{2M_p^2}\right)\right].
\tag{5.37}
$$

Substituting (5.36) into (5.37) we obtain the Poisson's equation for the Newtonian potential $\Phi(\Delta)$ in the QSA.

$$
\Phi=-\frac{\Delta\rho}{(k^2/a^2)}G(z),
\tag{5.38}
$$

where $G(z)$ is the scale independent effective Newton's constant, whose value in GR is given by $G_{GR}=\frac{1}{2}M_p^2$. The full Poisson's equation is too complicated to present, so we perform the dRGT expansion after substituting the solution for S. Upon substitution, and taking the leading order in dRGT expansion [3], we obtain

$$
\Phi=-\frac{\Delta\rho}{2M_p^2(k^2/a^2)}\left(1+\frac{m^2J_1\xi a}{2\sqrt{\kappa}H}\right).
\tag{5.39}
$$

The term in the brackets is the extra factor with respect to GR. Note that in dRGT we have $J_1=0$, so the Poisson's equation is the same as in GR. This is not the case in GMG.

[3] The dRGT expansion is used to obtain a analytic understanding of the system and is not a truly accurate representation of the underlying physics, therefore in the subsequent analysis we give all results without performing the dRGT expansion but still working in the UV limit of the theory to make contact with the QSA.

5.2.4 Phenomenology

In this section we study the phenomenology of the theory. Our result will determine whether the fifth force is in effect, ultimately allowing us to determine if there is a need for a screening mechanism on local scales to recover GR. Fig. (5.6) shows a comparison of

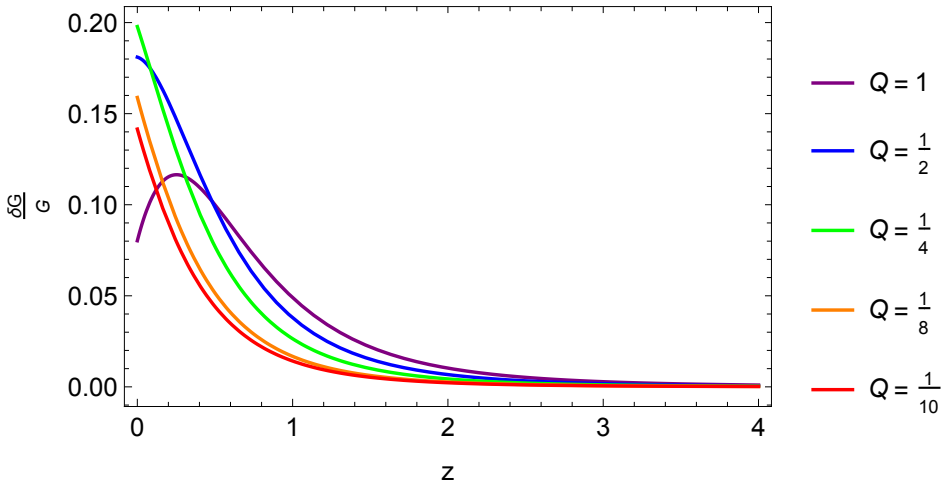

Figure 5.6: $\frac{\delta G}{G}$ as a function of redshift for varying values of Q, where $\delta G \equiv G(z) - G_{GR}$.

the effective Newton's constant in our model with respect to GR, for varying values of Q. The largest deviation at $z = 0$, which is around a 20% enhancement, is shown by the $Q = \frac{1}{4}$ curve. The smallest deviation at $z = 0$, around an 8% enhancement, is the $Q = 1$ curve. This result matches the one in Fig. (5.2), the reason why $Q = 1$ has the lowest deviation in the effective Newton's constant is because the equation of state has already undergone the turn back to $w = -1$. This implies that this branch of the theory is closer to ΛCDM at $z = 0$ than other values of Q, so this result is consistent with earlier results found in the background section.

A feature of modified gravity models which alters the effective Newton's constant is the modification to the growth rate of matter perturbations. The equation which governs the evolution of the linear matter overdensity, $\delta_m = \Delta/\rho$,

$$\ddot{\delta}_m + 2H\dot{\delta}_m - G\rho\delta_m = 0, \tag{5.40}$$

is dependent on two effects. The background expansion $H(z)$ and the effective Newton's constant G. As has been seen in earlier section, GMG modifies both of these so one expects the growth rate to be altered with respect to the ΛCDM case. We take (5.40) and

convert to redshift using the following relations;

$$\frac{d}{dt} = -(1+z)H\frac{d}{dz}, \qquad \frac{d^2}{dt^2} = (1+z)^2H^2\frac{d^2}{dz^2} + \left[(1+z)^2H\frac{dH}{dz} + (1+z)H^2\right]\frac{d}{dz}. \tag{5.41}$$

Using (5.41) in (5.40) we obtain,

$$\delta_m'' + \left[\frac{H'}{H} - \frac{1}{1+z}\right]\delta_m' - \frac{G\rho}{(1+z)^2H^2}\delta_m = 0, \tag{5.42}$$

where a prime denotes a derivative with respect to redshift. We solve (5.42) with the initial conditions,

$$\delta_m(z_i) = \frac{1}{1+z_i}, \qquad \delta_m'(z_i) = -\frac{1}{(1+z_i)^2}, \tag{5.43}$$

which are the same initial conditions as ΛCDM. This is an accurate approximation as GMG mimics the expansion history of ΛCDM at early times. We solve for $\delta_m(z)$ and compare with the solution in ΛCDM, the result is shown in Fig. (5.7). In this case, the

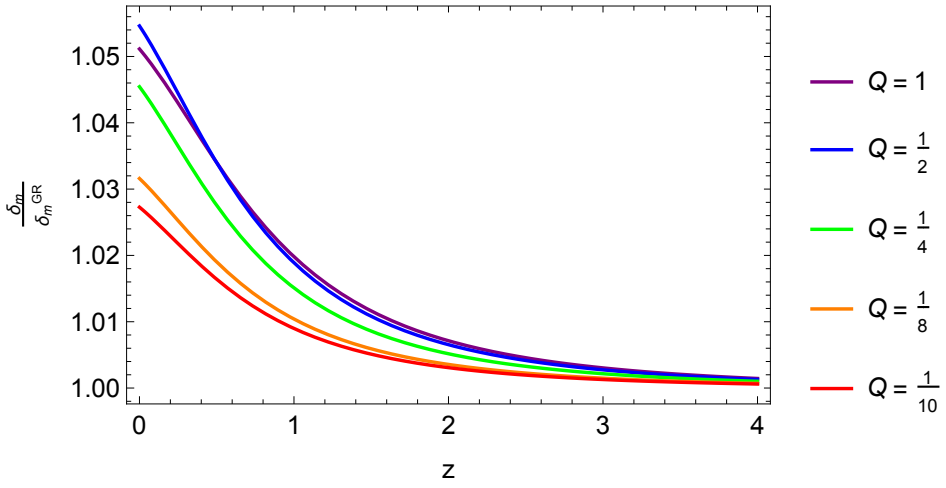

Figure 5.7: Ratio of the growth rate in GMG to the growth rate in ΛCDM as a function of redshift.

highest deviation comes from $Q = \frac{1}{2}$ at around the 5% level with respect to the ΛCDM case. To determine the strongest contribution to the growth rate, from the change in the background expansion caused by $H(z)$ or the modification to the Newton's constant, we isolate the $Q = 1$ case and solve Eq. (5.42) independently for 3 cases. In Fig. (5.8), we show a comparison of the full GMG growth function to ΛCDM, along with two cases where one of $H(z)$ and G are modified. The main result of Fig. (5.8) is that the strongest

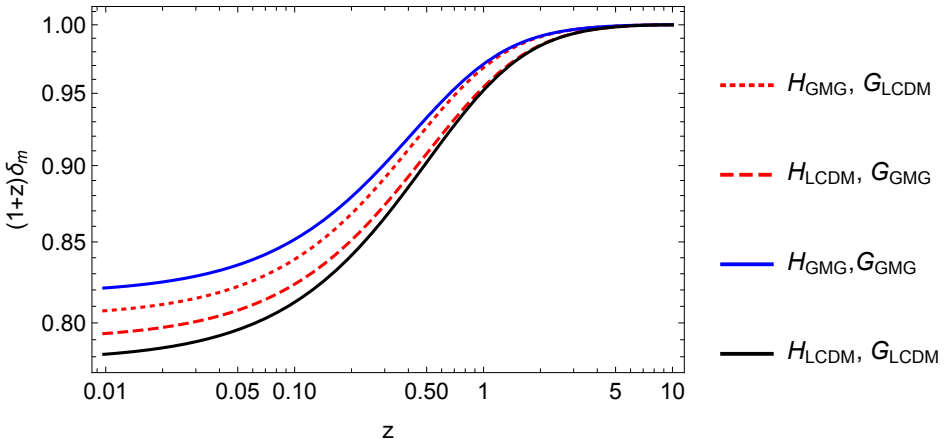

Figure 5.8: Growth rate comparison, as a function of redshift, between competing effects in GMG. The black curve shows the result in ΛCDM. The dashed curve shows result using the Hubble rate in ΛCDM and the GMG Newton's constant, whilst the dotted curve shows the opposite scenario. The solid blue curve shows the solution using both quantities in GMG.

modification to ΛCDM occurs when both the effects of the background expansion and the modification to the Newton's constant are included. However, the change in background expansion with respect to ΛCDM has a larger effect on the growth rate than the modified Newton's constant. This is again consistent with the results of Fig.(5.2), whereby $Q = \frac{1}{2}$ has a larger deviation from ΛCDM at the background level in H than the case $Q = 1$. At early times GMG matches the growth rate of ΛCDM, however at late times there is a discernible deviation from ΛCDM.

5.2.5 Gravitational wave propagation

To study the propagation of gravitational waves, we first quote the equation of motion for the tensor modes [4]

$$\ddot{h_{ij}} + 3H\dot{h}_{ij} + \left[(1+z)^2(k^2 - 2\kappa) + M_T^2\right] h_{ij} = 0, \tag{5.44}$$

where the only modification with respect to ΛCDM is that the tensor modes acquire a time dependent mass, $M_T = m\sqrt{\Gamma}$, which is also the same modification as dRGT [200]. We plot the tensor mass M_T for varying values of Q shown in FIG. 5.9. For lower values of Q, the tensors acquire a higher mass at any given redshift around an order of magnitude

[4] For the derivation of the quadratic action for the tensors, see Chapter 4.

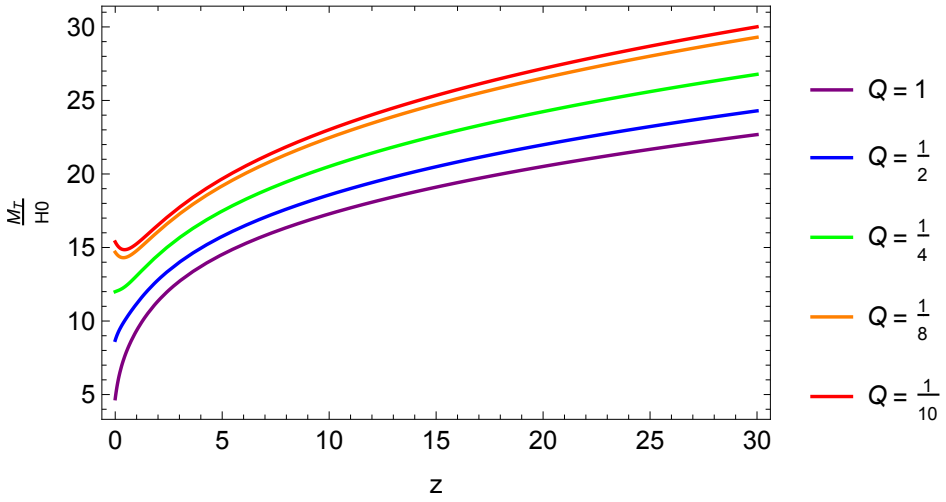

Figure 5.9: Mass of the tensor modes, normalised to H_0 for varying Q.

higher than H_0. This is due to the normalisation of μ. When we fix μ, imposing that the Hubble rate at $z = 0$ matches the value in ΛCDM, lower values of Q lead to a higher values of μ, therefore the mass of the modes increases towards lower values of Q. Additionally, the mass of the tensor modes increases as redshift increases. This feature is due to the behaviour of r, which appears in the functional form for Γ (4.26), which is an increasing function in redshift.

The modification to the mass modifies the speed of gravitational waves. However, the modification is small as $M_T \sim \mathcal{O}(10)H_0 \sim \mathcal{O}(10)10^{-33}$eV and is well within the bound on the speed of gravity from the detected binary neutron star merger [201]. For instance, the bound from LIGO on the mass of the tensor modes is,

$$M_T < 10^{-22}\text{eV}. \tag{5.45}$$

The friction term for the propagation of gravitational waves is unmodified with respect to the ΛCDM case, which leads to the luminosity distance of gravitational waves in GMG being unmodified with respect to that of light[5].

[5]Modified gravity models with non-minimal coupling or higher order covariant actions such as the Horndeski theory [47] can produce a modified friction term [153, 202–204] which can invoke a time dependent Newton's constant for gravitational waves and modify the gravitational wave luminosity distance. So it is possible that GMG with non-minimal coupling [205] could alter the GW luminosity distance with respect to that of light

5.3 Conclusions

In this chapter we studied the background cosmology and linear scalar perturbations in the Generalised Massive Gravity theory. For simplicity, we considered a minimal model where all these functions vanish except α_2, which slowly varies around its dRGT value and α_4, which was chosen to be a non-zero constant compatible with the stability conditions found in chapter 4. Controlling the variation of α_2 with the parameter $q = 10^{-4}Q$, we studied the evolution of cosmological solutions in this model. The background is FLRW with an effective fluid corresponding to the mass term, with an equation of state satisfying $w(z) \leq -1$ throughout the evolution. At early times, this effective fluid starts off like a cosmological constant, gradually decreasing. Eventually, it starts to increase again until it reaches $w = -1$ where we lose perturbative control. The time of crossing of the phantom divide[6] can be controlled by the q parameter. We find that for values of $q \lesssim 10^{-4}$, the crossing can be moved to the future. We also find that increasing the amount of negative curvature today has the same effect. The time dependent equation of state modifies the expansion rate by $\mathcal{O}(10^{-2})$ with respect to ΛCDM, with the maximum deviation at redshifts $z < 1$, depending on the value of q.

We also studied the evolution of linear perturbations. We found that the growth function for matter perturbation is modified at $\mathcal{O}(10^{-2})$ with respect to ΛCDM at low z. The non-zero anisotropic stress indicates the presence of a fifth force which contributes to gravitational interactions and increases the effective Newton's constant. This strengthening of gravity contributes to the matter growth, although the modified background evolution $H(z)$ contributes about twice the amount than the former. In the tensor sector, we find that the only modification to gravitational wave propagation arises in the tensor modes picking up a time dependent mass, which increases with redshift and with lower values of Q.

[6] Crossing of the phantom divide defined as the equation of state crossing $w = -1$

CHAPTER 6

CONCLUSIONS

In this thesis we have studied the cosmology of extended theories of massive gravity, namely the bigravity theory and the generalised massive gravity theory. In particular, we have studied the viability of the aforementioned theories as alternatives to general relativity in the context of cosmology. However as we have seen, modifying general relativity is not easy. Finding a stable theory of massive gravity that brings wanted effects, such as late time acceleration, without introducing pathologies is a non-trivial exercise. Nevertheless in this thesis we have identified a stable model of massive gravity, namely the generalised massive gravity, which could be a candidate for dark energy.

In chapter 2 we outlined the history of the construction of dRGT massive gravity, from the linear theory of Fierz-Pauli to the full non-linear theory. We found that stable massive gravity cosmologies have been hard to find, which led to the construction of many extended theories of massive gravity attempting to resolve the issues plagued by massive cosmologies in dRGT. In particular, the lack of stable flat/ closed FLRW solutions [116] posed a serious question over the viability of massive gravity as a possible solution for dark energy. However it was found that open FLRW solutions were allowed [114] at the background level, but when analysing the perturbations the self-accelerating branch was shown to have infinite strong coupling [119]. The upshot of this result being that normal perturbation theory techniques can no longer be applied.

In chapter 3 we studied the cosmology of the bigravity theory, where there are two dynamical metric tensors which propagate 7 degrees of freedom. We then discussed cosmological solutions in bigravity that exist in the literature, of which there are many

branches. To find a stable cosmology, we studied the low energy limit model which assumes $m^2 M_g^2 \gg \rho$. The effect of this is to push a gradient instability [171] generated in models where $m \sim H_0$ to early times [169, 191]. The viability of this model was studied as a candidate for dark energy. We identified the effective cosmological constant that appears in the Friedmann equation, which in turn causes a late-time acceleration of the universe. Analysis of the linear perturbations allowed us to identify the modified Poisson's equation which showed modifications at scales $k > 0.1\text{Mpc}/h$, where linear perturbation theory is no longer applicable. The Poisson's equation is modified by the extra scalar mode present, that needs to be screened by the Vainshtein mechanism. We derived the non-linear equations for the extra scalar mode and identified the Vainshtein radius. Then, imposing that we can describe the evolution of the scale factor back to the last scattering surface, we found that the early time solution does not exist if we require a working Vainshtein mechanism to satisfy observations. There are two ways to circumvent this apparent no-go theorem for bigravity cosmologies. One is to impose a hierachy between the two Planck scales [184] making the theory indistinguishable from GR. This brings the theory in-line with observations. The second is to postulate the presence of a Vainshtein-like mechanism [189, 190] to screen the effect of the instability at early times to recover GR.

In chapter 4 we introduced the Generalised Massive Gravity theory which was first studied in [106]. The theory promotes the mass parameters of dRGT to functions of the Lorentz invariant combination $\phi^a \phi_a$. This choice means the Stückelberg constraint equation is modified with respect to dRGT. We derived the quadratic action for cosmological perturbations for the tensor, vector and scalar modes. From the quadratic action, we identified the no-ghost and no-gradient instability conditions, as well as the tensor mass, as a function of the model parameters. Due to the modification of the Stückelberg constraint equation, the kinetic terms for the vectors and scalars were non-vanishing. This indicates that the modes are not infinitely strongly coupled, which is an advantage over dRGT massive gravity. We identified a region of parameter space that was compatible with the stability conditions, as well as imposing that the model admits a self-accelerating solution from the effective cosmological constant. From this we concluded that at the level of the quadratic action, GMG is stable and could be a viable dark energy model.

In chapter 5 we studied generalised massive gravity in more detail, focusing on the phenomenology and effect on large scale structure. We found a modified background expansion rate with respect to ΛCDM and a dynamical equation of state of dark energy. For a particular choice of the α functions we found that the Hubble rate today is modified

at the percent level with respect to ΛCDM, whilst the equation of state exhibits a bounce away from $w = -1$ to the phantom regime, showing a maximum deviation from ΛCDM at around the 20 percent level. The solution then breaks down as w crosses -1, which is caused by a gradient instability that is generated in the vector sector. The time the instability is generated can be pushed into the future by considering values of $Q < 1$, where Q is a parameter which controls the deviation away from dRGT. In addition, the time of the instability is sensitive to the value of $\Omega_{\kappa 0}$. Increasing the value of $\Omega_{\kappa 0}$ also pushes the time the instability is generated into the future.

We then performed a linear study of the scalar perturbations. This study revealed the presence of anisotropic stress which modified the Poisson's equation, via a modification to the effective Newton's constant. We found the modifications to the Newton's constant are enhanced at late times, with a maximum enhancement of 20 percent. We then compared the growth rate of matter perturbations with that of ΛCDM and found that the growth rate is enhanced at late times at around the percent level. We finished chapter 5 by discussing the propagation of gravitational waves. The tensor modes acquired a time dependent mass $\sim H_0$ which make this model distinguishable from scalar-tensor theories which also predict similar effects on LSS. The linear study reveals the presence of a fifth force, which needs to be screened at solar system scales via the Vainshtein mechanism. GMG theory is known to admit a Vainshtein mechanism similarly to dRGT [106] in the decoupling limit. In order to determine the details of the screening it is necessary to study non-linear perturbations and identify the Vainshtein radius. This is left for future work.

A second motivation for investigating the non-linear behaviour is provided by the dRGT limit of our model. The evolution in the asymptotic past coincides with the self-accelerating branch of dRGT. These solutions have exactly vanishing kinetic terms, controlled by the function J, leading to an infinitely strong coupling in the vector and scalar sectors. The solutions in GMG however never have vanishing J although as we go back in the evolution, they do decrease. Whether these modes are strongly coupled depends on the evolution of the non-linear terms and how they depend on J. Unlike in dRGT, this is not trivial. The non-linear study will allow us to determine the fate of the perturbative expansion, and provide the scale associated with this strong coupling if it exists. It should be noted that this issue has been observed in the context of the minimal theory, where only the $\alpha_2(t)$ function varies rapidly. However, generalised massive gravity is a theory with four arbitrary functions, and by using a very limited set of parameters, we have only scratched its surface. In general, we expect that using a slowly varying

function we can keep the strong coupling scale finite without affecting the past evolution of the Universe. This is to be explored in a future publication [206].

Moreover, GMG has been extended to a general theory class in Ref. [205], including non-minimal couplings. Finally, relaxing the dRGT constraint to be valid only within the range of the effective field theory, we expect that disformal couplings to matter can be allowed [207]. A natural next step is to exploit the full freedom of this theory class, determining new ways to achieve self acceleration and finding other applications in cosmology.

The main conclusion of this thesis is that whilst some models of massive gravity are plauged with pathologies, and have been ruled out on theoretical consistency or observational grounds, there are still models which are interesting for cosmology. It is important to continue analysis of the healthy models, combating them with all the observational data which we have at our disposal to really understand their viability. At the end of the day, if the models indeed do get ruled out, we will have learnt more about the robustness of General Relativity and maybe future observations will give an idea of where to look next.

APPENDIX A

VAINSHTEIN MECHANISM IN THE CUBIC GALILEON MODEL

As discussed in chapter 2, the nature of the non-linearities in massive gravity allow a working Vainshtein mechanism. This mechanism allows the recovery of GR on local scales, but allows the effect of the 5th force due to the extra degrees of freedom to manifest on cosmological scales, driving the accelerated expansion of the universe. To illustrate the Vainshtein mechanism, we take for simplicity the cubic galileon which arises in the decoupling limit of massive gravity [90, 101] and in the boundary effective action of DGP [49, 208]. The action for the cubic galileon takes the form,

$$S = \int d^4x - \frac{1}{2}\left(\partial\phi\right)^2 - \frac{1}{\Lambda_3^3}\left(\partial\phi\right)^2\Box\phi + \frac{1}{M_p}\phi T, \tag{A.1}$$

where the non-linear term is suppressed by the scale $\Lambda_3^3 = m^2 M_p$. Replacing $\phi \to \bar{\phi} + \delta\phi$, where $\bar{\phi}$ is the background field value and $\delta\phi$ the perturbation to the field, expanding the action to linear order and varying with respect to $\delta\phi$ we obtain the equation of motion,

$$\Box\bar{\phi} + \frac{1}{\Lambda_3^3}\left[2\partial^\mu\left(\partial_\mu\bar{\phi}\Box\bar{\phi}\right) - \Box\left(\partial\bar{\phi}\right)^2\right] + \frac{T}{M_p} = 0. \tag{A.2}$$

We then consider a static and spherically symmetric source, so the 4 gradient operator reduces to the del operator in spherical coordinates. The equation of motion becomes,

$$\nabla^2\bar{\phi} + \frac{1}{\Lambda_3^3}\left[2\nabla\left(\nabla\bar{\phi}\nabla^2\bar{\phi}\right) - \nabla^2\left(\left(\nabla\bar{\phi}\right)^2\right]\right] + \frac{T}{M_p} = 0. \tag{A.3}$$

Factoring out a del operator, using a static matter source described by $T = -M\delta^3(r)$ and using vector identities the equation can be rewritten as,

$$\nabla.\hat{r}\left[\bar{\phi}'(r) + \frac{4}{\Lambda_3^3 r}\bar{\phi}'(r)^2\right] = \frac{M}{M_p}\delta^3(r), \tag{A.4}$$

where $\hat{r}$ is a unit vector in the radial direction. Integrating this equation once over the 3-dimensional volume we obtain,

$$4\pi r^2\left(\phi'(r) + \frac{4}{\Lambda_3^3 r}\bar{\phi}'(r)^2\right) = \frac{M}{M_p}. \tag{A.5}$$

Reducing the order of the equation with $u(r) = \bar{\phi}'(r)$ we can solve the resulting quadratic equation for $u(r)$ and replace back $\phi'(r)$,

$$\bar{\phi}'(r) = -\frac{r\Lambda_3^3}{8} + \frac{\Lambda_3^3}{\sqrt{\pi r}}\sqrt{\pi r^3 + 4R_V^3}, \tag{A.6}$$

where we have defined the Vainshtein radius as $R_V^3 \equiv \left(\frac{M}{\Lambda_3^3 M_p}\right)$ and taken the positive solution. Letting $\alpha = r/R_V$ we can examine the behaviour for different regimes in r. For small α, so $r \ll R_v$ the solution becomes,

$$\bar{\phi}'(r) \sim \Lambda_3^{\frac{3}{2}}\sqrt{\frac{M}{16\pi M_p r}} \sim \frac{1}{\sqrt{r}}, \tag{A.7}$$

whilst for large α, or $r \gg R_V$ the solution is,

$$\bar{\phi}'(r) \sim \frac{M}{4\pi M_p r^2} \sim \frac{1}{r^2}. \tag{A.8}$$

Equations (A.7) and (A.8) perfectly show the essence of the Vainshtein mechanism. At large distances, the field becomes GR like with the usual $1/r^2$ profile. Whilst at shorter distances, the force exerted by the scalar is much weaker than GR and is suppressed.

APPENDIX B

VARIATION OF THE DRGT MASS TERM

In this appendix we compute the variation of the mass term for dRGT with a dynamical reference metric in order to derive the equations of motion for bigravity as outlined in section 3.1. The mass term takes the form,

$$\mathscr{L}_{mass} = m^2 M_p^2 \sqrt{-g} \sum_{n=0}^{4} \alpha_n \mathscr{U}_n(\mathscr{K}), \tag{B.1}$$

$\mathscr{U}_n$ are the dRGT potential terms.

$$\begin{aligned}
\mathscr{U}_0(\mathscr{K}) &= 1, \\
\mathscr{U}_1(\mathscr{K}) &= [\mathscr{K}], \\
\mathscr{U}_2(\mathscr{K}) &= \frac{1}{2!}([\mathscr{K}]^2 - [\mathscr{K}^2]), \\
\mathscr{U}_3(\mathscr{K}) &= \frac{1}{3!}([\mathscr{K}]^3 - 3[\mathscr{K}][\mathscr{K}^2] + 2[\mathscr{K}^3]), \\
\mathscr{U}_4(\mathscr{K}) &= \frac{1}{4!}([\mathscr{K}]^4 - 6[\mathscr{K}]^2[\mathscr{K}^2] + 8[\mathscr{K}][\mathscr{K}^3] + 3[\mathscr{K}^2]^2 - 6[\mathscr{K}^4]),
\end{aligned} \tag{B.2}$$

and in this case α_n are free parameters. The $\mathscr{K}$ tensor is,

$$\mathscr{K}^{\mu}_{\ \nu} = \delta^{\mu}_{\ \nu} - X^{\mu}_{\ \nu}, \tag{B.3}$$

and we define $X^{\mu}_{\ \nu}$ to be,

$$X^{\mu}_{\ \nu} = \left(\sqrt{g^{-1}f}\right)^{\mu}_{\ \nu}, \tag{B.4}$$

which implies

$$X^{\mu\lambda}X_{\lambda\nu} = g^{\mu\lambda}f_{\lambda\nu}. \tag{B.5}$$

The tricky part here is the variation of the trace of the square root tensor, we compute the variation as follows,

$$\delta[X^n] = \frac{n}{2}(X^n)^{\alpha}_{\ \mu}\left(g_{\alpha\nu}\delta g^{\mu\nu} - f_{\alpha\nu}\delta f^{\mu\nu}\right), \tag{B.6}$$

which is valid for any power $n \geq 1$. In the above we made use of $\delta f_{\mu\nu} = -f_{\mu\alpha}f_{\nu\beta}\delta f^{\alpha\beta}$. The variation of the interaction terms can be written in the following form:

$$\begin{aligned}
\delta\mathscr{U}_1 &= -\frac{1}{2}X^{\alpha}_{\ \mu}\left(g_{\alpha\nu}\delta g^{\mu\nu} - f_{\alpha\nu}\delta f^{\mu\nu}\right),\\
\delta\mathscr{U}_2 &= \left[\left(-\frac{3}{2}+\frac{1}{2}[X]\right)X - \frac{1}{2}X^2\right]^{\alpha}_{\ \mu}\left(g_{\alpha\nu}\delta g^{\mu\nu} - f_{\alpha\nu}\delta f^{\mu\nu}\right),\\
\delta\mathscr{U}_3 &= \left[\left(-\frac{3}{2}+[X]-\frac{1}{4}[X]^2+\frac{1}{4}[X]^2\right)X + \left(-1+\frac{1}{2}[X]\right)X^2 - \frac{1}{2}X^3\right]^{\alpha}_{\ \mu}\left(g_{\alpha\nu}\delta g^{\mu\nu} - f_{\alpha\nu}\delta f^{\mu\nu}\right),\\
\delta\mathscr{U}_4 &= \left[\left(-\frac{1}{2}+\frac{1}{2}[X]-\frac{1}{4}[X]^2+\frac{1}{12}[X]^3+\frac{1}{4}[X^2]-\frac{1}{4}[X][X^2]+\frac{1}{6}[X^3]\right)X\right.\\
&\qquad \left. +\left(-\frac{1}{2}+\frac{1}{2}[X]-\frac{1}{4}[X]^2+\frac{1}{4}[X^2]\right)X^2 + \left(-\frac{1}{2}+\frac{1}{2}[X]\right)X^3 - \frac{1}{2}X^4\right]^{\alpha}_{\ \mu}\left(g_{\alpha\nu}\delta g^{\mu\nu} - f_{\alpha\nu}\delta f^{\mu\nu}\right).
\end{aligned} \tag{B.7}$$

APPENDIX C

ALGORITHM FOR CALCULATING THE SQUARE ROOT MATRIX

For a generic metric g and f, which are non diagonal, to calculate the square root tensor we first define,

$$X = g^{-1} f. \tag{C.1}$$

We use ϵ as a parameter which controls the order of perturbations. The zeroth order part of X is diagonal,

$$X^{\epsilon=0} = g^{-1} f\big|_{\epsilon=0}, \tag{C.2}$$

so we can trivially take the square root as the square root of the components,

$$\sqrt{X}^{\epsilon=0} = \sqrt{g^{-1} f}\big|_{\epsilon=0}. \tag{C.3}$$

To calculate the first order part, we introduce a trial 4 x 4 matrix $\tilde{X}$ with 16 independent components and write the square root of X as,

$$\sqrt{X}^{\epsilon=1} = \sqrt{X}^{\epsilon=0} + \epsilon \tilde{X}. \tag{C.4}$$

We then solve the first order equation for the 16 components,

$$X - \left(\sqrt{X}^{\epsilon=1}\right).\left(\sqrt{X}^{\epsilon=1}\right) = 0, \tag{C.5}$$

and substitute into (C.4) to obtain the expression for the square root under perturbative expansion. To extend to second order, we write

$$\sqrt{X}^{\epsilon=2} = \sqrt{X}^{\epsilon=1} + \epsilon^2 \tilde{X}, \tag{C.6}$$

and again solve the equation,

$$X - \left(\sqrt{X}^{\epsilon=2}\right).\left(\sqrt{X}^{\epsilon=2}\right) = 0, \tag{C.7}$$

for the components of the matrix $\tilde{X}$ and substitute into (C.6) to obtain the desired expression. This algorithm can then be extended to arbitary order. As a sanity check, once we have reached the order we require, we calculate,

$$X - \left(\sqrt{X}^{\epsilon=n}\right).\left(\sqrt{X}^{\epsilon=n}\right) = \mathcal{O}(n+1), \tag{C.8}$$

and if the right hand side satisfies the relation in (C.8) then we have successfully calculated the square root.

APPENDIX D

FUNCTIONS IN THE EQUATION OF MOTION FOR S

In this appendix we present exact expressions of the coefficients in the equation of motion for S, given by 5.32, in the three different regimes for the parameter $\mathscr{E}$ as outlined in section 5.2.

D.0.0.1 Case 1: $\mathscr{E} \gg 1$

$$\mathscr{A} = \frac{9\kappa m^2 M_p^2 \Gamma_0 a^2}{2k^4}, \quad H_0\mathscr{B} = \frac{9\kappa m^2 M_p^2 a^2(\dot{\Gamma}_0 + 5H\Gamma_0)}{2k^4}, \quad H_0^2\mathscr{C} = \frac{3\sqrt{\kappa} m^2 M_p^2 \Gamma_0^2 aH}{J_1 \xi k^2}, \quad \mathscr{D} = \frac{3m^2\Gamma_0 a^2 \rho}{2k^4},$$

$$H_0\mathscr{F} = -\frac{27\sqrt{\kappa} m^2 \Gamma_0^2 a^5 H^2 \rho}{J_1 \xi k^6}. \tag{D.1}$$

D.0.0.2 Case 2: $\mathscr{E} \ll 1$

$$\mathscr{A} = \frac{3J_1\sqrt{\kappa}\xi a m^2 M_p^2}{4Hk^2}$$

$$H_0\mathscr{B} = \frac{3m^2\xi\left[2J_1\kappa^{3/2}M_p^2 + 2\kappa M_p^2 a(\dot{J}_1 + 5J_1 H) + \sqrt{\kappa}a^2(2\dot{J}_1 M_p^2 H + 8J_1 M_p^2 H^2 + J_1\rho\right]}{8aH^2k^2}$$

$$H_0^2\mathscr{C} = \frac{1}{2}m^2 M_p^2 \Gamma_0, \qquad \mathscr{D} = \frac{J_1\xi m^2 a\rho}{4\sqrt{\kappa}Hk^2}, \qquad H_0\mathscr{F} = \frac{3J_1\xi m^2 a^3\rho}{4\sqrt{\kappa}k^2}. \tag{D.2}$$

D.0.0.3 Case 3: $k \to 0$

$$\mathscr{A} = \frac{J_1 m^2 M_p^2 a\xi}{4\sqrt{\kappa}H}, \quad H_0\mathscr{B} = \frac{m^2\xi\left[2J_1\kappa M_p^2 + 2\sqrt{\kappa}M_p^2 a(\dot{J}_1 + 5J_1 H) + a^2(2\dot{J}_1 M_p^2 H + 8J_1 H^2 M_p^2 + J_1\rho)\right]}{8\sqrt{\kappa}aH^2}$$

$$\mathscr{D} = \left[2J_1\kappa^2 M_p^2 + 2\kappa^{3/2} M_p^2 a(\dot{J}_1 + 3HJ_1) + J_1\sqrt{\kappa}a^3 H\rho + J_1 a^4 H^2\rho + \kappa a^2(2\dot{J}_1 M_p^2 H + 4J_1 M_p^2 H^2 + J_1\rho) \right] \times \frac{m^2\xi\rho}{24\kappa^{5/2} M_p^2 a H^3}$$

(D.3)
$$H_0^2\mathscr{C} = \frac{1}{2}m^2 M_p^2 \Gamma_0, \quad H_0\mathscr{F} = \frac{J_1\xi m^2 a^3\rho}{4\kappa^{3/2}}.$$

BIBLIOGRAPHY

[1] C. Pitrou, X. Roy, and O. Umeh, "xPand: An algorithm for perturbing homogeneous cosmologies," *Class. Quant. Grav.*, vol. 30, p. 165002, 2013.

[2] N. Aghanim *et al.*, "Planck 2018 results. VI. Cosmological parameters," *Astron. Astrophys.*, vol. 641, p. A6, 2020.

[3] B. Abbott *et al.*, "Observation of Gravitational Waves from a Binary Black Hole Merger," *Phys. Rev. Lett.*, vol. 116, no. 6, p. 061102, 2016.

[4] D. G. York *et al.*, "The Sloan Digital Sky Survey: Technical Summary," *Astron. J.*, vol. 120, pp. 1579–1587, 2000.

[5] R. Laureijs *et al.*, "Euclid Definition Study Report," arXiv: 1110.3193.

[6] G. F. R. Ellis, R. Maartens, and M. A. H. MacCallum, *Relativistic Cosmology*. Cambridge University Press, 2012.

[7] S. Weinberg, *The Quantum Theory of Fields*, vol. 1. Cambridge University Press, 1995.

[8] P. Peter and J.-P. Uzan, *Primordial Cosmology*. Oxford Graduate Texts, Oxford University Press, 2 2013.

[9] D. Baumann, "Inflation," in *Theoretical Advanced Study Institute in Elementary Particle Physics: Physics of the Large and the Small*, pp. 523–686, 2011.

[10] L. Kofman, A. D. Linde, and A. A. Starobinsky, "Towards the theory of reheating after inflation," *Phys. Rev. D*, vol. 56, pp. 3258–3295, 1997.

[11] A. G. Riess *et al.*, "Observational evidence from supernovae for an accelerating universe and a cosmological constant," *Astron. J.*, vol. 116, pp. 1009–1038, 1998.

[12] S. Perlmutter *et al.*, "Measurements of Omega and Lambda from 42 high redshift supernovae," *Astrophys. J.*, vol. 517, pp. 565–586, 1999.

[13] A. Einstein, "The Foundation of the General Theory of Relativity," *Annalen Phys.*, vol. 49, no. 7, pp. 769–822, 1916.

[14] C. M. Will, "The Confrontation between General Relativity and Experiment," *Living Rev. Rel.*, vol. 17, p. 4, 2014.

[15] R. M. Wald, *General relativity*.
Chicago, IL: Chicago Univ. Press, 1984.

[16] S. M. Carroll, *Spacetime and Geometry: An Introduction to General Relativity*.
Cambridge University Press, 2019.

[17] D. Fixsen, "The Temperature of the Cosmic Microwave Background," *Astrophys. J.*, vol. 707, pp. 916–920, 2009.

[18] M. Colless, "First results from the 2dF galaxy redshift survey," *Phil. Trans. Roy. Soc. Lond. A*, vol. 357, p. 105, 1999.

[19] P. Ntelis *et al.*, "Exploring cosmic homogeneity with the BOSS DR12 galaxy sample," *JCAP*, vol. 06, p. 019, 2017.

[20] G. Efstathiou, "A Lockdown Perspective on the Hubble Tension (with comments from the SH0ES team)," arXiv:2007.10716 [astro-ph.CO].

[21] A. G. Riess, L. Macri, S. Casertano, H. Lampeitl, H. C. Ferguson, A. V. Filippenko, S. W. Jha, W. Li, and R. Chornock, "A 3% Solution: Determination of the Hubble Constant with the Hubble Space Telescope and Wide Field Camera 3," *Astrophys. J.*, vol. 730, p. 119, 2011.
[Erratum: Astrophys.J. 732, 129 (2011)].

[22] A. G. Riess *et al.*, "A 2.4% Determination of the Local Value of the Hubble Constant," *Astrophys. J.*, vol. 826, no. 1, p. 56, 2016.

[23] A. G. Riess, S. Casertano, W. Yuan, L. M. Macri, and D. Scolnic, "Large Magellanic Cloud Cepheid Standards Provide a 1% Foundation for the Determination of the Hubble Constant and Stronger Evidence for Physics beyond ΛCDM," *Astrophys. J.*, vol. 876, no. 1, p. 85, 2019.

[24] H. Desmond, B. Jain, and J. Sakstein, "Local resolution of the Hubble tension: The impact of screened fifth forces on the cosmic distance ladder," *Phys. Rev. D*, vol. 100, no. 4, p. 043537, 2019.

[Erratum: Phys.Rev.D 101, 069904 (2020), Erratum: Phys.Rev.D 101, 129901 (2020)].

[25] K. Freese, "Status of Dark Matter in the Universe," *Int. J. Mod. Phys.*, vol. 1, no. 06, pp. 325–355, 2017.

[26] T. Clifton, P. G. Ferreira, A. Padilla, and C. Skordis, "Modified Gravity and Cosmology," *Phys. Rept.*, vol. 513, pp. 1–189, 2012.

[27] J. F. Koksma and T. Prokopec, "The Cosmological Constant and Lorentz Invariance of the Vacuum State," *arXiv e-prints*, p. arXiv:1105.6296, May 2011.

[28] A. Padilla, "Lectures on the Cosmological Constant Problem," arXiv:1502.05296 [hep-th].

[29] F. Simpson, "Scattering of dark matter and dark energy," *Phys. Rev. D*, vol. 82, p. 083505, 2010.

[30] A. Pourtsidou and T. Tram, "Reconciling CMB and structure growth measurements with dark energy interactions," *Phys. Rev. D*, vol. 94, no. 4, p. 043518, 2016.

[31] M. Bordag, G. Klimchitskaya, U. Mohideen, and V. Mostepanenko, *Advances in the Casimir effect*, vol. 145.
Oxford University Press, 2009.

[32] G. Lemaitre, "The expanding universe," *Gen. Rel. Grav.*, vol. 29, pp. 641–680, 1997.

[33] R. C. Tolman, "Effect of inhomogeneity on cosmological models," *Proceedings of the National Academy of Sciences*, vol. 20, no. 3, pp. 169–176, 1934.

[34] H. Bondi, "Spherically symmetrical models in general relativity," *Mon. Not. Roy. Astron. Soc.*, vol. 107, pp. 410–425, 1947.

[35] D. Lovelock, "The Einstein tensor and its generalizations," *J. Math. Phys.*, vol. 12, pp. 498–501, 1971.

[36] D. Lovelock, "The four-dimensionality of space and the einstein tensor," *J. Math. Phys.*, vol. 13, pp. 874–876, 1972.

[37] E. P. Verlinde, "Emergent Gravity and the Dark Universe," *SciPost Phys.*, vol. 2, no. 3, p. 016, 2017.

[38] A. Tamosiunas, D. Bacon, K. Koyama, and R. C. Nichol, "Testing Emergent Gravity on Galaxy Cluster Scales," *JCAP*, vol. 05, p. 053, 2019.

[39] P. Horava, "Quantum Gravity at a Lifshitz Point," *Phys. Rev. D*, vol. 79, p. 084008, 2009.

[40] B. P. Abbott *et al.*, "Gravitational Waves and Gamma-rays from a Binary Neutron Star Merger: GW170817 and GRB 170817A," *Astrophys. J.*, vol. 848, no. 2, p. L13, 2017.

[41] B. Abbott *et al.*, "Multi-messenger Observations of a Binary Neutron Star Merger," *Astrophys. J. Lett.*, vol. 848, no. 2, p. L12, 2017.

[42] A. Emir Gümrükçüoğlu, M. Saravani, and T. P. Sotiriou, "Hořava gravity after GW170817," *Phys. Rev. D*, vol. 97, no. 2, p. 024032, 2018.

[43] E. Belgacem, Y. Dirian, S. Foffa, and M. Maggiore, "Nonlocal gravity. Conceptual aspects and cosmological predictions," *JCAP*, vol. 03, p. 002, 2018.

[44] G. Dvali, G. Gabadadze, and M. Porrati, "4-D gravity on a brane in 5-D Minkowski space," *Phys. Lett. B*, vol. 485, pp. 208–214, 2000.

[45] R. Maartens and K. Koyama, "Brane-World Gravity," *Living Rev. Rel.*, vol. 13, p. 5, 2010.

[46] K. S. Stelle, "Classical Gravity with Higher Derivatives," *Gen. Rel. Grav.*, vol. 9, pp. 353–371, 1978.

[47] G. W. Horndeski, "Second-order scalar-tensor field equations in a four-dimensional space," *Int. J. Theor. Phys.*, vol. 10, pp. 363–384, 1974.

[48] M. Ostrogradsky, "Mémoires sur les équations différentielles, relatives au problème des isopérimètres," *Mem. Acad. St. Petersbourg*, vol. 6, no. 4, pp. 385–517, 1850.

[49] A. Nicolis, R. Rattazzi, and E. Trincherini, "The Galileon as a local modification of gravity," *Phys. Rev. D*, vol. 79, p. 064036, 2009.

[50] J. M. Ezquiaga and M. Zumalacárregui, "Dark Energy After GW170817: Dead Ends and the Road Ahead," *Phys. Rev. Lett.*, vol. 119, no. 25, p. 251304, 2017.

[51] C. de Rham and S. Melville, "Gravitational Rainbows: LIGO and Dark Energy at its Cutoff," *Phys. Rev. Lett.*, vol. 121, no. 22, p. 221101, 2018.

[52] M. Hull, K. Koyama, and G. Tasinato, "A Higgs Mechanism for Vector Galileons," *JHEP*, vol. 03, p. 154, 2015.

[53] M. Hull, K. Koyama, and G. Tasinato, "Covariantized vector Galileons," *Phys. Rev. D*, vol. 93, no. 6, p. 064012, 2016.

[54] S. F. Hassan and R. A. Rosen, "Bimetric Gravity from Ghost-free Massive Gravity," *JHEP*, vol. 02, p. 126, 2012.

[55] K. Koyama, "Cosmological Tests of Modified Gravity," *Rept. Prog. Phys.*, vol. 79, no. 4, p. 046902, 2016.

[56] L. Heisenberg, "A systematic approach to generalisations of General Relativity and their cosmological implications," *Phys. Rept.*, vol. 796, pp. 1–113, 2019.

[57] T. E. Collett, L. J. Oldham, R. J. Smith, M. W. Auger, K. B. Westfall, D. Bacon, R. C. Nichol, K. L. Masters, K. Koyama, and R. van den Bosch, "A precise extragalactic test of General Relativity," *Science*, vol. 360, p. 1342, 2018.

[58] A. Joyce, B. Jain, J. Khoury, and M. Trodden, "Beyond the Cosmological Standard Model," *Phys. Rept.*, vol. 568, pp. 1–98, 2015.

[59] F. Sbisà, "Classical and quantum ghosts," *Eur. J. Phys.*, vol. 36, p. 015009, 2015.

[60] J. M. Cline, S. Jeon, and G. D. Moore, "The Phantom menaced: Constraints on low-energy effective ghosts," *Phys. Rev. D*, vol. 70, p. 043543, 2004.

[61] K. Hinterbichler and J. Khoury, "Symmetron Fields: Screening Long-Range Forces Through Local Symmetry Restoration," *Phys. Rev. Lett.*, vol. 104, p. 231301, 2010.

[62] J. Khoury and A. Weltman, "Chameleon cosmology," *Phys. Rev. D*, vol. 69, p. 044026, 2004.

[63] J. Khoury and A. Weltman, "Chameleon fields: Awaiting surprises for tests of gravity in space," *Phys. Rev. Lett.*, vol. 93, p. 171104, 2004.

[64] C. Burrage and J. Sakstein, "Tests of Chameleon Gravity," *Living Rev. Rel.*, vol. 21, no. 1, p. 1, 2018.

[65] J. Wang, L. Hui, and J. Khoury, "No-Go Theorems for Generalized Chameleon Field Theories," *Phys. Rev. Lett.*, vol. 109, p. 241301, 2012.

[66] T. Damour and A. M. Polyakov, "The String dilaton and a least coupling principle," *Nucl. Phys. B*, vol. 423, pp. 532–558, 1994.

[67] E. Babichev, V. Mukhanov, and A. Vikman, "k-Essence, superluminal propagation, causality and emergent geometry," *JHEP*, vol. 02, p. 101, 2008.

[68] V. F. Mukhanov, H. A. Feldman, and R. H. Brandenberger, "Theory of cosmological perturbations. Part 1. Classical perturbations. Part 2. Quantum theory of perturbations. Part 3. Extensions," *Phys. Rept.*, vol. 215, pp. 203–333, 1992.

[69] S. Weinberg, *Gravitation and Cosmology: Principles and Applications of the General Theory of Relativity*.
New York, NY: Wiley, 1972.

[70] W. Hu and I. Sawicki, "A Parameterized Post-Friedmann Framework for Modified Gravity," *Phys. Rev. D*, vol. 76, p. 104043, 2007.

[71] T. Baker, P. G. Ferreira, and C. Skordis, "The Parameterized Post-Friedmann framework for theories of modified gravity: concepts, formalism and examples," *Phys. Rev. D*, vol. 87, no. 2, p. 024015, 2013.

[72] T. Baker, P. G. Ferreira, C. Skordis, and J. Zuntz, "Towards a fully consistent parameterization of modified gravity," *Phys. Rev. D*, vol. 84, p. 124018, 2011.

[73] C. M. Will and K. Nordtvedt, Jr., "Conservation Laws and Preferred Frames in Relativistic Gravity. I. Preferred-Frame Theories and an Extended PPN Formalism," *Astrophys. J.*, vol. 177, p. 757, 1972.

[74] H. Kodama and M. Sasaki, "Cosmological Perturbation Theory," *Prog. Theor. Phys. Suppl.*, vol. 78, pp. 1–166, 1984.

[75] S. W. Hawking, "Perturbations of an expanding universe," *Astrophys. J.*, vol. 145, pp. 544–554, 1966.

[76] M. Trenti and P. Hut, "Gravitational N-body Simulations," 6 2008.

[77] B. Wright, "Modelling non-linear structure formation with modified gravity and massive neutrinos," 2019.

[78] E. Bertschinger, "On the Growth of Perturbations as a Test of Dark Energy," *Astrophys. J.*, vol. 648, pp. 797–806, 2006.

[79] J. M. Bardeen, "Gauge Invariant Cosmological Perturbations," *Phys. Rev. D*, vol. 22, pp. 1882–1905, 1980.

[80] P. A. Zyla *et al.*, "Review of Particle Physics," *PTEP*, vol. 2020, no. 8, p. 083C01, 2020.

[81] M. Tanabashi *et al.*, "Review of Particle Physics," *Phys. Rev. D*, vol. 98, no. 3, p. 030001, 2018.

[82] M. Fierz and W. Pauli, "On relativistic wave equations for particles of arbitrary spin in an electromagnetic field," *Proc. Roy. Soc. Lond.*, vol. A173, pp. 211–232, 1939.

[83] H. van Dam and M. Veltman, "Massive and mass-less yang-mills and gravitational fields," *Nuclear Physics B*, vol. 22, no. 2, pp. 397 – 411, 1970.

[84] V. I. Zakharov, "Linearized gravitation theory and the graviton mass," *JETP Lett.*, vol. 12, p. 312, 1970.
[Pisma Zh. Eksp. Teor. Fiz.12,447(1970)].

[85] D. G. Boulware and S. Deser, "Can gravitation have a finite range?," *Phys. Rev. D*, vol. 6, pp. 3368–3382, Dec 1972.

[86] N. Arkani-Hamed, H. Georgi, and M. D. Schwartz, "Effective field theory for massive gravitons and gravity in theory space," *Annals Phys.*, vol. 305, pp. 96–118, 2003.

[87] C. de Rham, G. Gabadadze, and A. J. Tolley, "Resummation of Massive Gravity," *Phys. Rev. Lett.*, vol. 106, p. 231101, 2011.

[88] C. de Rham and G. Gabadadze, "Generalization of the Fierz-Pauli Action," *Phys. Rev. D*, vol. 82, p. 044020, 2010.

[89] C. Burrage, N. Kaloper, and A. Padilla, "Strong Coupling and Bounds on the Spin-2 Mass in Massive Gravity," *Phys. Rev. Lett.*, vol. 111, no. 2, p. 021802, 2013.

[90] K. Hinterbichler, "Theoretical Aspects of Massive Gravity," *Rev. Mod. Phys.*, vol. 84, pp. 671–710, 2012.

[91] F. Sbisà, "Modified Theories of Gravity," arXiv: 1406.3384.

[92] L. Perivolaropoulos, "PPN Parameter gamma and Solar System Constraints of Massive Brans-Dicke Theories," *Phys. Rev. D*, vol. 81, p. 047501, 2010.

[93] E. C. G. Stueckelberg, "Theory of the radiation of photons of small arbitrary mass," *Helv. Phys. Acta*, vol. 30, pp. 209–215, 1957.

[94] A. I. Vainshtein, "To the problem of nonvanishing gravitation mass," *Physics Letters B*, vol. 39, pp. 393–394, May 1972.

[95] K. Schwarzschild, "On the gravitational field of a sphere of incompressible fluid according to Einstein's theory," *Sitzungsber. Preuss. Akad. Wiss. Berlin (Math. Phys.)*, vol. 1916, pp. 424–434, 1916.

[96] K. Schwarzschild, "On the gravitational field of a mass point according to Einstein's theory," *Sitzungsber. Preuss. Akad. Wiss. Berlin (Math. Phys.)*, vol. 1916, pp. 189–196, 1916.

[97] M. Porrati, "Fully covariant van Dam-Veltman-Zakharov discontinuity, and absence thereof," *Phys. Lett. B*, vol. 534, pp. 209–215, 2002.

[98] C. Deffayet, G. R. Dvali, G. Gabadadze, and A. I. Vainshtein, "Nonperturbative continuity in graviton mass versus perturbative discontinuity," *Phys. Rev. D*, vol. 65, p. 044026, 2002.

[99] M. Mirbabayi, "A Proof Of Ghost Freedom In de Rham-Gabadadze-Tolley Massive Gravity," *Phys. Rev. D*, vol. 86, p. 084006, 2012.

[100] J. Bonifacio and J. Noller, "Strong coupling scales in minimal massive gravity," *Phys. Rev. D*, vol. 92, no. 10, p. 104001, 2015.

[101] C. de Rham, "Massive Gravity," *Living Rev. Rel.*, vol. 17, p. 7, 2014.

[102] M. D. Schwartz, "Constructing gravitational dimensions," *Phys. Rev. D*, vol. 68, p. 024029, 2003.

[103] P. Creminelli, A. Nicolis, M. Papucci, and E. Trincherini, "Ghosts in massive gravity," *JHEP*, vol. 09, p. 003, 2005.

[104] C. de Rham and G. Gabadadze, "Selftuned Massive Spin-2," *Phys. Lett. B*, vol. 693, pp. 334–338, 2010.

[105] S. F. Hassan and R. A. Rosen, "On Non-Linear Actions for Massive Gravity," *JHEP*, vol. 07, p. 009, 2011.

[106] C. de Rham, M. Fasiello, and A. J. Tolley, "Stable FLRW solutions in Generalized Massive Gravity," *Int. J. Mod. Phys.*, vol. D23, no. 13, p. 1443006, 2014.

[107] L. Alberte, A. H. Chamseddine, and V. Mukhanov, "Massive Gravity: Resolving the Puzzles," *JHEP*, vol. 12, p. 023, 2010.

[108] L. Alberte, A. H. Chamseddine, and V. Mukhanov, "Massive Gravity: Exorcising the Ghost," *JHEP*, vol. 04, p. 004, 2011.

[109] J. Kluson, "Remark About Hamiltonian Formulation of Non-Linear Massive Gravity in Stuckelberg Formalism," *Phys. Rev. D*, vol. 86, p. 124005, 2012.

[110] J. Kluson, "Non-Linear Massive Gravity with Additional Primary Constraint and Absence of Ghosts," *Phys. Rev. D*, vol. 86, p. 044024, 2012.

[111] J. Kluson, "Comments About Hamiltonian Formulation of Non-Linear Massive Gravity with Stuckelberg Fields," *JHEP*, vol. 06, p. 170, 2012.

[112] E. Babichev and C. Deffayet, "An introduction to the Vainshtein mechanism," *Class. Quant. Grav.*, vol. 30, p. 184001, 2013.

[113] C. de Rham, G. Gabadadze, L. Heisenberg, and D. Pirtskhalava, "Cosmic Acceleration and the Helicity-0 Graviton," *Phys. Rev. D*, vol. 83, p. 103516, 2011.

[114] A. E. Gumrukcuoglu, C. Lin, and S. Mukohyama, "Open FRW universes and self-acceleration from nonlinear massive gravity," *JCAP*, vol. 11, p. 030, 2011.

[115] A. De Felice, A. E. Gümrükçüoğlu, C. Lin, and S. Mukohyama, "On the cosmology of massive gravity," *Class. Quant. Grav.*, vol. 30, p. 184004, 2013.

[116] G. D'Amico, C. de Rham, S. Dubovsky, G. Gabadadze, D. Pirtskhalava, and A. J. Tolley, "Massive Cosmologies," *Phys. Rev.*, vol. D84, p. 124046, 2011.

[117] S. H. Pereira, E. L. Mendona, A. Pinho S. S., and J. F. Jesus, "Cosmological bounds on open FLRW solutions of massive gravity," *Rev. Mex. Astron. Astrofis.*, vol. 52, no. 1, pp. 125–131, 2016.

[118] A. De Felice, A. E. Gumrukcuoglu, and S. Mukohyama, "Massive gravity: nonlinear instability of the homogeneous and isotropic universe," *Phys. Rev. Lett.*, vol. 109, p. 171101, 2012.

[119] A. E. Gumrukcuoglu, C. Lin, and S. Mukohyama, "Cosmological perturbations of self-accelerating universe in nonlinear massive gravity," *JCAP*, vol. 1203, p. 006, 2012.

[120] S. F. Hassan, R. A. Rosen, and A. Schmidt-May, "Ghost-free Massive Gravity with a General Reference Metric," *JHEP*, vol. 02, p. 026, 2012.

[121] D. Langlois and A. Naruko, "Cosmological solutions of massive gravity on de Sitter," *Class. Quant. Grav.*, vol. 29, p. 202001, 2012.

[122] A. Higuchi, "Forbidden Mass Range for Spin-2 Field Theory in De Sitter Space-time," *Nucl. Phys.*, vol. B282, pp. 397–436, 1987.

[123] M. Fasiello and A. J. Tolley, "Cosmological perturbations in Massive Gravity and the Higuchi bound," *JCAP*, vol. 1211, p. 035, 2012.

[124] M. Fasiello and A. J. Tolley, "Cosmological Stability Bound in Massive Gravity and Bigravity," *JCAP*, vol. 12, p. 002, 2013.

[125] P. Martin-Moruno and M. Visser, "Is there vacuum when there is mass? Vacuum and non-vacuum solutions for massive gravity," *Class. Quant. Grav.*, vol. 30, p. 155021, 2013.

[126] A. E. Gumrukcuoglu, C. Lin, and S. Mukohyama, "Anisotropic Friedmann-Robertson-Walker universe from nonlinear massive gravity," *Phys. Lett. B*, vol. 717, pp. 295–298, 2012.

[127] K. Koyama, G. Niz, and G. Tasinato, "Analytic solutions in non-linear massive gravity," *Phys. Rev. Lett.*, vol. 107, p. 131101, 2011.

[128] K. Koyama, G. Niz, and G. Tasinato, "Strong interactions and exact solutions in non-linear massive gravity," *Phys. Rev. D*, vol. 84, p. 064033, 2011.

[129] P. Gratia, W. Hu, and M. Wyman, "Self-accelerating Massive Gravity: Exact solutions for any isotropic matter distribution," *Phys. Rev. D*, vol. 86, p. 061504, 2012.

[130] M. Wyman, W. Hu, and P. Gratia, "Self-accelerating Massive Gravity: Time for Field Fluctuations," *Phys. Rev. D*, vol. 87, no. 8, p. 084046, 2013.

[131] N. Khosravi, G. Niz, K. Koyama, and G. Tasinato, "Stability of the Self-accelerating Universe in Massive Gravity," *JCAP*, vol. 08, p. 044, 2013.

[132] Q.-G. Huang, Y.-S. Piao, and S.-Y. Zhou, "Mass-Varying Massive Gravity," *Phys. Rev.*, vol. D86, p. 124014, 2012.

[133] A. E. Gumrukcuoglu, K. Hinterbichler, C. Lin, S. Mukohyama, and M. Trodden, "Cosmological Perturbations in Extended Massive Gravity," *Phys. Rev.*, vol. D88, no. 2, p. 024023, 2013.

[134] G. D'Amico, G. Gabadadze, L. Hui, and D. Pirtskhalava, "Quasidilaton: Theory and cosmology," *Phys. Rev. D*, vol. 87, p. 064037, 2013.

[135] G. D'Amico, G. Gabadadze, L. Hui, and D. Pirtskhalava, "On Cosmological Perturbations of Quasidilaton," *Class. Quant. Grav.*, vol. 30, p. 184005, 2013.

[136] S. Anselmi, D. López Nacir, and G. D. Starkman, "Extreme parameter sensitivity in quasidilaton massive gravity," *Phys. Rev. D*, vol. 92, no. 8, p. 084033, 2015.

[137] A. De Felice and S. Mukohyama, "Towards consistent extension of quasidilaton massive gravity," *Phys. Lett. B*, vol. 728, pp. 622–625, 2014.

[138] G. Gabadadze, R. Kimura, and D. Pirtskhalava, "Self-acceleration with Quasidilaton," *Phys. Rev. D*, vol. 90, no. 2, p. 024029, 2014.

[139] T. Kahniashvili, A. Kar, G. Lavrelashvili, N. Agarwal, L. Heisenberg, and A. Kosowsky, "Cosmic expansion in extended quasidilaton massive gravity," *Phys. Rev. D*, vol. 91, no. 4, p. 041301, 2015.
[Erratum: Phys.Rev.D 100, 089902 (2019)].

[140] H. Motohashi and W. Hu, "Stability of cosmological solutions in extended quasidilaton massive gravity," *Phys. Rev. D*, vol. 90, no. 10, p. 104008, 2014.

[141] A. E. Gumrukcuoglu, K. Koyama, and S. Mukohyama, "Stable cosmology in ghost-free quasidilaton theory," *Phys. Rev. D*, vol. 96, no. 4, p. 044041, 2017.

[142] J. Klusoň, "Consistent Extension of Quasidilaton Massive Gravity," *J. Grav.*, vol. 2014, p. 413835, 2014.

[143] S. Anselmi, S. Kumar, D. López Nacir, and G. D. Starkman, "Failures of homogeneous and isotropic cosmologies in extended quasidilaton massive gravity," *Phys. Rev. D*, vol. 96, no. 8, p. 084001, 2017.

[144] A. De Felice and S. Mukohyama, "Minimal theory of massive gravity," *Phys. Lett. B*, vol. 752, pp. 302–305, 2016.

[145] A. De Felice and S. Mukohyama, "Phenomenology in minimal theory of massive gravity," *JCAP*, vol. 04, p. 028, 2016.

[146] A. De Felice, S. Mukohyama, and M. Oliosi, "Minimal theory of quasidilaton massive gravity," *Phys. Rev. D*, vol. 96, no. 2, p. 024032, 2017.

[147] A. De Felice, S. Mukohyama, and M. Oliosi, "Horndeski extension of the minimal theory of quasidilaton massive gravity," *Phys. Rev. D*, vol. 96, no. 10, p. 104036, 2017.

[148] A. De Felice, S. Mukohyama, and M. Oliosi, "Phenomenology of minimal theory of quasidilaton massive gravity," *Phys. Rev. D*, vol. 99, no. 4, p. 044055, 2019.

[149] R. Hagala, A. De Felice, D. F. Mota, and S. Mukohyama, "Nonlinear Dynamics of the Minimal Theory of Massive Gravity," 11 2020.

[150] T. Fujita, S. Kuroyanagi, S. Mizuno, and S. Mukohyama, "Blue-tilted Primordial Gravitational Waves from Massive Gravity," *Phys. Lett. B*, vol. 789, pp. 215–219, 2019.

[151] L. Iacconi, M. Fasiello, H. Assadullahi, E. Dimastrogiovanni, and D. Wands, "Interferometer Constraints on the Inflationary Field Content," *JCAP*, vol. 03, p. 031, 2020.

[152] M. Biagetti, E. Dimastrogiovanni, and M. Fasiello, "Possible signatures of the inflationary particle content: spin-2 fields," *JCAP*, vol. 10, p. 038, 2017.

[153] E. Belgacem *et al.*, "Testing modified gravity at cosmological distances with LISA standard sirens," *JCAP*, vol. 07, p. 024, 2019.

[154] V. A. Rubakov, "Lorentz-violating graviton masses: Getting around ghosts, low strong coupling scale and VDVZ discontinuity," 7 2004.

[155] S. L. Dubovsky, "Phases of massive gravity," *JHEP*, vol. 10, p. 076, 2004.

[156] Z. Berezhiani, D. Comelli, F. Nesti, and L. Pilo, "Spontaneous Lorentz Breaking and Massive Gravity," *Phys. Rev. Lett.*, vol. 99, p. 131101, 2007.

[157] Z. Berezhiani, D. Comelli, F. Nesti, and L. Pilo, "Exact Spherically Symmetric Solutions in Massive Gravity," *JHEP*, vol. 07, p. 130, 2008.

[158] C. Lin, "SO(3) massive gravity," *Phys. Lett. B*, vol. 727, pp. 31–36, 2013.

[159] C. de Rham, L. Heisenberg, and R. H. Ribeiro, "Quantum Corrections in Massive Gravity," *Phys. Rev. D*, vol. 88, p. 084058, 2013.

[160] C. de Rham, J. T. Deskins, A. J. Tolley, and S.-Y. Zhou, "Graviton Mass Bounds," *Rev. Mod. Phys.*, vol. 89, no. 2, p. 025004, 2017.

[161] J. G. Williams, S. G. Turyshev, and D. H. Boggs, "Progress in lunar laser ranging tests of relativistic gravity," *Phys. Rev. Lett.*, vol. 93, p. 261101, 2004.

[162] K. Hinterbichler, "Cosmology of massive gravity and its extensions," arXiv:1701.02873 [astro-ph.CO].

[163] M. Kenna-Allison, A. E. Gumrukcuoglu, and K. Koyama, "Viability of bigravity cosmology," *Phys. Rev.*, vol. D99, no. 10, p. 104032, 2019.

[164] C. de Rham, L. Heisenberg, and R. H. Ribeiro, "On couplings to matter in massive (bi-)gravity," *Class. Quant. Grav.*, vol. 32, p. 035022, 2015.

[165] K. Aoki and K.-i. Maeda, "Cosmology in ghost-free bigravity theory with twin matter fluids: The origin of dark matter," *Phys. Rev. D*, vol. 89, no. 6, p. 064051, 2014.

[166] K. Aoki and S. Mukohyama, "Massive gravitons as dark matter and gravitational waves," *Phys. Rev. D*, vol. 94, no. 2, p. 024001, 2016.

[167] K. Aoki and K.-i. Maeda, "Dark matter in ghost-free bigravity theory: From a galaxy scale to the universe," *Phys. Rev. D*, vol. 90, p. 124089, 2014.

[168] K. Aoki, K.-i. Maeda, Y. Misonoh, and H. Okawa, "Massive Graviton Geons," *Phys. Rev. D*, vol. 97, no. 4, p. 044005, 2018.

[169] A. De Felice, A. E. Gumrukcuoglu, S. Mukohyama, N. Tanahashi, and T. Tanaka, "Viable cosmology in bimetric theory," *JCAP*, vol. 1406, p. 037, 2014.

[170] D. Comelli, M. Crisostomi, and L. Pilo, "Perturbations in Massive Gravity Cosmology," *JHEP*, vol. 06, p. 085, 2012.

[171] D. Comelli, M. Crisostomi, and L. Pilo, "FRW Cosmological Perturbations in Massive Bigravity," *Phys. Rev.*, vol. D90, p. 084003, 2014.

[172] P. Bull *et al.*, "Beyond ΛCDM: Problems, solutions, and the road ahead," *Phys. Dark Univ.*, vol. 12, pp. 56–99, 2016.

[173] A. Schmidt-May and M. von Strauss, "Recent developments in bimetric theory," *J. Phys. A*, vol. 49, no. 18, p. 183001, 2016.

[174] M. von Strauss, A. Schmidt-May, J. Enander, E. Mortsell, and S. F. Hassan, "Cosmological Solutions in Bimetric Gravity and their Observational Tests," *JCAP*, vol. 03, p. 042, 2012.

[175] F. Koennig, A. Patil, and L. Amendola, "Viable cosmological solutions in massive bimetric gravity," *JCAP*, vol. 03, p. 029, 2014.

[176] D. Comelli, M. Crisostomi, F. Nesti, and L. Pilo, "FRW Cosmology in Ghost Free Massive Gravity," *JHEP*, vol. 03, p. 067, 2012.
[Erratum: JHEP 06, 020 (2012)].

[177] A. Caravano, M. Lüben, and J. Weller, "Combining cosmological and local bounds on bimetric theory," arXiv:2101.08791 [gr-qc].

[178] M. Lüben, A. Schmidt-May, and J. Weller, "Physical parameter space of bimetric theory and SN1a constraints," *JCAP*, vol. 09, p. 024, 2020.

[179] F. Koennig, Y. Akrami, L. Amendola, M. Motta, and A. R. Solomon, "Stable and unstable cosmological models in bimetric massive gravity," *Phys. Rev.*, vol. D90, p. 124014, 2014.

[180] G. Cusin, R. Durrer, P. Guarato, and M. Motta, "Gravitational waves in bigravity cosmology," *JCAP*, vol. 1505, no. 05, p. 030, 2015.

[181] F. Könnig, "Higuchi Ghosts and Gradient Instabilities in Bimetric Gravity," *Phys. Rev. D*, vol. 91, p. 104019, 2015.

[182] M. Lagos and P. G. Ferreira, "Cosmological perturbations in massive bigravity," *JCAP*, vol. 1412, p. 026, 2014.

[183] F. Konnig and L. Amendola, "Instability in a minimal bimetric gravity model," *Phys. Rev.*, vol. D90, p. 044030, 2014.

[184] Y. Akrami, S. F. Hassan, F. Könnig, A. Schmidt-May, and A. R. Solomon, "Bimetric gravity is cosmologically viable," *Phys. Lett.*, vol. B748, pp. 37–44, 2015.

[185] M. Lüben, A. Schmidt-May, and J. Smirnov, "Vainshtein Screening in Bimetric Cosmology," *Phys. Rev. D*, vol. 102, p. 123529, 2020.

[186] M. Högås and E. Mörtsell, "Observational constraints on bimetric gravity," arXiv:2101.08795 [gr-qc].

[187] M. Kocic, F. Torsello, M. Högås, and E. Mörtsell, "Initial data and first evolutions of dust clouds in bimetric relativity," *Class. Quant. Grav.*, vol. 37, no. 16, p. 165010, 2020.

[188] M. Högås, F. Torsello, and E. Mörtsell, "On the stability of bimetric structure formation," *JCAP*, vol. 04, p. 046, 2020.

[189] E. Mortsell and J. Enander, "Scalar instabilities in bimetric gravity: The Vainshtein mechanism and structure formation," *JCAP*, vol. 10, p. 044, 2015.

[190] K. Aoki, K.-i. Maeda, and R. Namba, "Stability of the Early Universe in Bigravity Theory," *Phys. Rev.*, vol. D92, no. 4, p. 044054, 2015.

[191] A. De Felice, T. Nakamura, and T. Tanaka, "Possible existence of viable models of bi-gravity with detectable graviton oscillations by gravitational wave detectors," *PTEP*, vol. 2014, p. 043E01, 2014.

[192] M. Fasiello and R. H. Ribeiro, "Mild bounds on bigravity from primordial gravitational waves," *JCAP*, vol. 1507, no. 07, p. 027, 2015.

[193] I. Sawicki and E. Bellini, "Limits of quasistatic approximation in modified-gravity cosmologies," *Phys. Rev.*, vol. D92, no. 8, p. 084061, 2015.

[194] P. Brax, C. Burrage, and A.-C. Davis, "Laboratory Tests of the Galileon," *JCAP*, vol. 1109, p. 020, 2011.

[195] J. Sakstein, B. Jain, J. S. Heyl, and L. Hui, "Tests of Gravity Theories Using Supermassive Black Holes," *Astrophys. J.*, vol. 844, no. 1, p. L14, 2017.

[196] C. De Rham, L. Keltner, and A. J. Tolley, "Generalized galileon duality," *Phys. Rev.*, vol. D90, no. 2, p. 024050, 2014.

[197] M. Kenna-Allison, A. E. Gümrükçüoglu, and K. Koyama, "Stable cosmology in generalized massive gravity," *Phys. Rev. D*, vol. 101, no. 8, p. 084014, 2020.

[198] G. D. Moore and A. E. Nelson, "Lower bound on the propagation speed of gravity from gravitational cherenkov radiation," *Journal of High Energy Physics*, vol. 2001, p. 023–023, Sep 2001.

[199] M. Kenna-Allison, A. E. Gümrükçüoglu, and K. Koyama, "Cosmic acceleration and growth of structure in massive gravity," *Phys. Rev. D*, vol. 102, no. 10, p. 103524, 2020.

[200] A. E. Gumrukcuoglu, S. Kuroyanagi, C. Lin, S. Mukohyama, and N. Tanahashi, "Gravitational wave signal from massive gravity," *Class. Quant. Grav.*, vol. 29, p. 235026, 2012.

[201] B. Abbott *et al.*, "GW170817: Observation of Gravitational Waves from a Binary Neutron Star Inspiral," *Phys. Rev. Lett.*, vol. 119, no. 16, p. 161101, 2017.

[202] N. B. Hogg, M. Martinelli, and S. Nesseris, "Constraints on the distance duality relation with standard sirens," 7 2020.

[203] E. Belgacem, Y. Dirian, S. Foffa, and M. Maggiore, "Modified gravitational-wave propagation and standard sirens," *Phys. Rev. D*, vol. 98, no. 2, p. 023510, 2018.

[204] E. Belgacem, Y. Dirian, S. Foffa, and M. Maggiore, "Gravitational-wave luminosity distance in modified gravity theories," *Phys. Rev. D*, vol. 97, no. 10, p. 104066, 2018.

[205] A. E. Gumrukcuoglu, R. Kimura, and K. Koyama, "Massive gravity with nonminimal coupling," *Phys. Rev. D*, vol. 101, no. 12, p. 124021, 2020.

[206] M. Kenna-Allison, A. E. Gumrukcuoglu, R. Kimura, and K. Koyama In preparation.

[207] A. E. Gümrükçüoglu and K. Koyama, "Generalizing the matter coupling in massive gravity: A search for new interactions," *Phys. Rev. D*, vol. 99, no. 8, p. 084004, 2019.

[208] A. Nicolis and R. Rattazzi, "Classical and quantum consistency of the DGP model," *JHEP*, vol. 06, p. 059, 2004.